



# City Research Online

## City St George's, University of London

**Citation:** Brammall, C. F. (1984). A study of photo anodes and oxygen evolution. (Unpublished Doctoral thesis, The City University)

This is the accepted version of the paper.

This version of the publication may differ from the final published version. To cite this item please consult the publisher's version.

**Permanent repository link:** <https://openaccess.city.ac.uk/id/eprint/34279/>

**Copyright and Reuse:** Copyright and Moral Rights remain with the author(s) and/or copyright holders. Copies of full items can be used for personal research or study, educational, or not-for-profit purposes without prior permission or charge, unless otherwise indicated, provided that the authors, title and full bibliographic details are credited, a hyperlink and/or URL is given for the original metadata page and the content is not changed in any way. For full details of reuse please refer to [City Research Online policy](#).

DECLARATION

A STUDY OF PHOTO ANODES AND OXYGEN EVOLUTION

A thesis submitted for the

degree of

Doctor of Philosophy

by

CHRISTOPHER FRANCIS BRAMMALL

at

Chemistry Department

The City University

London

This work was carried out under the  
supervision of Prof. A.C.C. Tseung

Submitted January 1984

DEDICATION

To my family and friends whose support has seen me through this work.

"So enormous is the energy wealth of universe and so great is the memory and intellectual wisdom of continuous man in respect to his previous experiences, and so fundamentally has he inter-tooled his advantages, that it is completely clear that all men may now be successful in living in a progressively satisfactory enjoyment of total earth."

R. Buckminster Fuller

# C O N T E N T S

	<u>Page</u>
<u>CHAPTER ONE</u>	
INTRODUCTION	21
1.1 THE IMPORTANCE OF SOLAR ENERGY CONVERSION	22
1.2 MEANS OF SOLAR ENERGY CONVERSION	26
1.3 THE ELECTROCHEMICAL BEHAVIOUR OF SEMI-CONDUCTING ELECTRODES UNDER ILLUMINATION	28
1.4 OXYGEN EVOLUTION	33
1.5 CONCLUSIONS	36
<u>CHAPTER TWO</u>	
THE ELECTROCHEMICAL BEHAVIOUR OF SEMI-CONDUCTING ELECTRODES UNDER ILLUMINATION - A BRIEF REVIEW	37
2.1 INTRODUCTION	38
2.2 THE BASIC CRITERIA FOR A SEMI- CONDUCTOR TO BE USABLE IN A PHOTO- ELECTROCHEMICAL DEVICE	40
2.3 MATERIALS SUITABLE FOR PHOTO- ELECTROCHEMICAL DEVICES	45
2.4 THE THEORY OF PHOTO ELECTROCHEMICAL PROCESSES	49
2.4.1 The overall process	50
2.4.2 Charge transfer at illuminated semi- conductors	55

	<u>Page</u>	
2.4.3	Charge transport in the semi-conductor	58
2.4.4	The mechanism of the evolution of oxygen on illuminated semi-conductors	59
2.5	APPLICATIONS AND TRENDS ON PHOTO ELECTROCHEMISTRY	60
2.5.1	Photoelectrochemical devices	60
2.5.2	Voltage generation with regenerative photo cells	62
2.5.3	Photoelectrosynthesis	66
2.5.4	Improvement of photoelectrochemical performance	67
2.6	CONCLUSIONS	70

### CHAPTER THREE

	THE CHOICE OF MATERIAL FOR A TEST ELECTRODE	72
--	---	----

### CHAPTER FOUR

	THE PHOTOELECTROCHEMICAL BEHAVIOUR OF FLAME OXIDISED IRON METALS	78
4.1	INTRODUCTION	79

	<u>Page</u>	
4.2	THE STRUCTURE OF THERMALLY OXIDISED IRON	82
4.3	ELECTRODE PREPARATION	83
4.4	ELECTROCHEMICAL EXPERIMENTAL SET UP	84
4.5	REFERENCE ELECTRODE - THE DYNAMIC HYDROGEN ELECTRODE	88
4.6	STEADY STATE ELECTROCHEMICAL PERFORMANCE	89
4.7	PHOTO CURRENT TRANSIENT BEHAVIOUR UNDER VARYING CONDITIONS OF ILLUMINATION	92
4.8	DISCUSSION OF THE OXY-HYDROXY INTERMEDIATE MODEL	103
4.9	A REVIEW OF THE EVIDENCE IN THE PHOTOELECTROCHEMICAL LITERATURE FOR THE OXY-HYDROXY INTERMEDIATE MODEL	113
4.10	CONCLUSIONS	119
 <u>CHAPTER FIVE</u>		
	THE STEADY STATE ELECTROCHEMICAL BEHAVIOUR OF TRANSITION METAL SILICATES	122
5.1	INTRODUCTION	123
5.2	LITERATURE REVIEW OF TRANSITION METAL SILICATES	124

	<u>Page</u>	
5.2.1	Cobalt silicate	124
5.2.2	Nickel silicate	126
5.2.3	Iron silicate	127
5.3	THE PREPARATION OF TRANSITION METAL SILICATES	128
5.3.1	Solid state sintering	129
5.3.2	Co-precipitation from a sodium silicate solution	130
5.3.3	Gelling method with tetra ethyl ortho silicate	131
5.4	CHARACTERISATION OF THE ELECTRODE MATERIALS	132
5.4.1	Conductivity measurements	132
5.4.2	X-ray analysis	135
5.4.3	Surface area measurements	136
5.5	STEADY STATE ELECTROCHEMICAL MEASUREMENTS	138
5.5.1	Fabrication of electrodes	138
5.5.2	General electrochemical testing	140
5.5.3	Steady state polarisation curves	143
5.6	STEADY STATE ELECTROCHEMICAL PERFORMANCE	148
5.6.1	Steady state electrochemical performance of cobalt silicate	148
5.6.2	The steady state electrochemical behaviour of iron silicate	152

	<u>Page</u>	
5.6.3	The long term electrochemical testing of cobalt silicate	155
5.7	CONCLUSIONS AND SUGGESTIONS FOR FURTHER WORK	159
 <u>CHAPTER SIX</u>		
6.1	A MECHANISTIC STUDY OF THE EVOLUTION OF OXYGEN ON COBALT SILICATE	161
6.1	CYCLIC VOLTAMMETRY	162
6.1.1	The measurement of the electron transfer rate constant using cyclic voltammetry	164
6.1.2	Additional diagnostic tests of the cyclic voltammetry results	167
6.1.3	Conclusions of the cyclic voltammetry experiments	172
6.2	POTENTIOSTATIC PULSE INVESTIGATIONS OF TEFLON BONDED COBALT SILICATE ELECTRODES	172
6.2.1	Introduction	172
6.2.2	Experimental procedure	175
6.2.3	Potentiostatic pulse results and their interpretation	179
6.3	CONCLUSIONS	187



INDEX OF FIGURES

Page

CHAPTER SEVEN

Page

7.0	CONCLUSIONS AND SUGGESTIONS FOR FURTHER WORK	189
7.1	CONCLUSIONS	190
7.2	POSSIBLE FURTHER INVESTIGATIONS INTO PHOTOELECTROCHEMISTRY	191
7.3	FURTHER INVESTIGATIVE WORK INTO THE PROPERTIES OF COBALT SILICATE with a redox electrolyte under illumination with an applied potential.	192
7.3	Current/voltage curves for photoelectrolysis and a photovoltaic device.	34
7.1	Energy conversion efficiency vs band gap.	84
7.2	Energy diagram of a N-type semiconductor in contact with a redox electrolyte.	31
7.3	Energy diagram of a N-type semiconductor in contact with a counter electrode.	36

## INDEX OF FIGURES

		<u>Page</u>
1.1	Stylised view of a N-type semi-conductor in contact with a redox electrolyte under illumination.	30
1.2	Stylised view of a N-type semi-conductor in contact with a redox electrolyte under illumination with an applied potential.	32
1.3	Current/voltage curves for photoelectrolysis and a photovoltaic device.	34
2.1	Energy conversion efficiency vs band gap.	44
2.2	Energy diagram of a N-type semi-conductor in contact with a redox electrolyte.	51
2.3	Energy diagram of a N-type semi-conductor in contact with a counter electrode.	54

	<u>Page</u>
2.4	Energy diagrams of N-type semi-conductors in contact with metal counter electrodes under the conditions necessary for the photoelectrolysis of water. 56
2.5	A photoelectrochemical storage cell. 65
4.1	Diagram of an experimental cell. 85
4.2	Schematic circuit diagram for potentiostatic measurements. 87
4.3	Voltage/current curve for a flame oxidised Iron electrode in 5M KOH with and without illumination with a 150 watt spotlight. 90
4.4	Voltage/current curves for a flame oxidised Iron electrode in 5M KOH electrolyte under varying levels of illumination. 91
4.5	Current transients of a flame oxidised Iron electrode under illumination. 94
4.6	Schematic circuit for cyclic voltammetry. 98

		<u>Page</u>
4.7	Current voltammograms of flame oxidised Iron in 5M KOH showing the effect of illumination.	99
4.8	Current transients of flame oxidised Iron at different voltages.	100
4.9	Comparison of photo current transients under various levels of illumination.	105
4.10	Effect of voltage on flame oxidised Iron photo current transients.	106
4.11	Effect of voltage on flame oxidised Iron photo current transients at high illumination levels.	108
4.12	Effect of voltage on flame oxidised Iron photo current transients at reduced illumination levels.	109
4.13	Voltage/current curves for flame oxidised Titanium in 5M KOH under illumination by a 1600 Watt Xenon	111

		<u>Page</u>
	lamp and under darkness.	111
4.14	Photo current transients of flame oxidised Titanium in 5M KOH at varying voltages.	112
4.15	Quasi-Fermi levels in an illuminated space charge layer at steady state in the presence of a charge transfer reaction by minority carriers at the surface.	114
4.16	Energy correlation between band edges and the Fermi energies of electrode reactions in aqueous solution at pH 7 for $TiO_2$ .	115
5.1	Powder conductivity measurement cell.	133
5.2	Diagram of an experimental cell.	141
5.3	Schematic circuit diagram for potentiostatic measurements.	144

	<u>Page</u>	<u>Page</u>
5.4	Schematic circuit for measurement of ohmic overpotential using the interruptor method.	145
5.5	Typical traces for determining ohmic overpotential.	147
5.6	IR corrected potentiostatic current/voltage curves of a Teflon bonded Cobalt Silicate electrode (14.7 mg loading) in 5M KOH at various temperatures.	149
5.7	Effect of loading at various temperatures showing the IR corrected voltage for a current of 1 amp.	151
5.8	Current/voltage curve (IR corrected) for $Fe_2 Si O_4$ before (1) and after (2) 168 hours polarisation at 1 amp, 5M KOH electrolyte at 25°C.	154
5.9	Long term test cell.	156

		<u>Page</u>
5.10	Long term performance of cobalt silicate	157
6.1	Cyclic voltammogram of a Teflon bonded cobalt silicate electrode (17.3mg loading) in 5M KOH at 25 <sup>0</sup> C at a scan rate of 20mV/sec.	163
6.2	Plot of peak current vs voltage scan rate for a Teflon bonded cobalt silicate electrode (17.3mg loading) in 5M KOH at 25 <sup>0</sup> C).	170
6.3	Plot of peak current vs square route of voltage scan for a Teflon bonded Cobalt Silicate electrode (17.3mg loading) in 5M KOH at 25 <sup>0</sup> C.	171
6.4	Double layer charging trace for a Teflon bonded Cobalt Silicate electrode in 5M KOH at 25 <sup>0</sup> C in a N <sub>2</sub> atmosphere.	176

## INDEX OF TABLES

6.5	Schematic circuit diagram for potentiostatic pulse measurements.	178
6.6	Schematic circuit diagram for galvanostatic pulse measurements.	180
6.7	Tafel plot for a Teflon bonded Cobalt Silicate (17.4 mg loading) electrode in 5M KOH at 25 <sup>o</sup> C.	182
6.8	Comparison of V/i curves obtained for a Teflon bonded Cobalt Silicate electrode (17.4 mg loading) in 5M KOH at 25 <sup>o</sup> C by steady state and pulse measurements.	185
	Ve D.H.C. in 5M KOH for 24 hours.	182
8.1	Electron transfer rate constant calculated at various voltages scan rates.	186
8.2	Diagnostic tests for reaction control using cyclic voltammetry results.	189



## INDEX OF TABLES

	<u>Page</u>
2.1 Publications using titanium dioxide as a photo anode.	46
2.2 Publications using materials other than titanium dioxide as a photo anode.	47
2.3 Publications using materials as a photo cathode.	48
4.1 Intensities of various lattice spacings of flame oxidised iron before and after polarization at +1000mV Vs D.H.E. in 5MKOH for 24 hours.	102
6.1 Electron transfer rate constant calculated at various voltage scan rates.	166
6.2 Diagnostic tests for reaction control using cyclic voltammetry results.	168

## ACKNOWLEDGEMENTS

I would like to express my sincere thanks to my Supervisor, Prof. A.C.C. Tseung for his interest, support, suggestions and encouragement during the course of this work.

I would like to thank all my colleagues in the Electrochemical Research Group for their suggestions and discussions - all contributed, but a special mention must be made of [REDACTED] [REDACTED] for explaining so well the ins and outs of semiconductor physics to a confused chemist!

I would like to thank the academic and technical staff of the Chemistry Department for all their assistance.

I would like to thank my brother [REDACTED] for the excellent illustrations in this thesis.

I would like to thank [REDACTED] [REDACTED] for typing it.

Finally I would like to sincerely thank the S.R.C. and the N.R.D.C. for their financial support during this work.

C.F. Brammall  
Department of Chemistry,  
The City University,  
Northampton Square,  
London, E.C.1

## DECLARATION

I grant the University Librarian the power of discretion to allow this thesis to be copied in whole or in part without reference to myself. This is done on the understanding that any such copy will be a single copy for study purposes only and will be subject to the normal conditions of acknowledgement.

The importance of this to the general field of photo-electrochemistry has been considered.

using the oxy-hydroxyl intermediate theory as its basic premise, the anodic electrochemical behaviour of certain transition metal silicates has been studied.

Samples of cobalt, iron and nickel silicates were made by thermal sintering methods and characterized by conductivity measurements and X-ray analysis. Nickel silicate could not be made in a suitably conducting form to be fabricated into an electrode. Iron silicate was found to show a decrease in polarization resistance when polarized anodically. Cobalt silicate was found to have a reasonable performance for the evolution of oxygen. A mechanistic study of cobalt silicate as an electrocatalyst for the evolution

ABSTRACT

The anodic photoelectrochemical behaviour of flame oxidised iron has been investigated. The transient photo current behaviour has been explained in terms of the creation and subsequent reduction of an oxy-hydroxy intermediate on the electrode's surface. This has been supported by the results gained by voltammetry and X-ray analysis. The importance of this to the general field of photo-electrochemistry has been considered.

Using the oxy-hydroxy intermediate theory as its basic premise, the anodic electrochemical behaviour of certain transition metal silicates has been studied.

Samples of cobalt , iron and nickel silicates were made by thermal sintering methods and characterised by conductivity measurements and X-ray analysis. Nickel silicate could not be made in a suitably conducting form to be fabricated into an electrode. Iron silicate was found to slowly corrode when polarised anodically. Cobalt silicate was found to have a reasonable performance for the evolution of oxygen. A mechanistic study of cobalt silicate as an electro catalyst for the evolution

of oxygen using cyclic voltammetry and potentiostatic pulse techniques has shown that the formation of an oxy-hydroxy intermediate is the essential step in the reaction mechanism.

Unfortunately, the anodic photoelectrochemical behaviour of cobalt silicate has not been studied due to experimental limitations. However, there are grounds to suggest that due to band gap limitations, it will have a poor photoelectrochemical performance.

#### INTRODUCTION

## 1.1 The Importance of solar energy conversion

Today's society is becoming increasingly a society based on the wide spread usage of energy. This energy has to be available in various convenient forms and is the life blood of a modern technological civilisation. At present, the main sources of this energy are oil, coal and gas. These have the advantages of being easily obtained and converted into convenient forms of energy such as electricity, but have the disadvantages of being in a finite supply and they pollute the environment. The need to find alternatives to these is brought home in a consideration of the possible sources of energy available and the availability of it.

### CHAPTER ONE

#### INTRODUCTION

These sources can be identified as follows:

- 1) Natural products such as wood.
- 2) Fossil fuels.
- 3) Solar radiation, hydraulic, wind, waves.
- 4) Tidal.
- 5) Geothermal.
- 6) Nuclear fission.
- 7) Nuclear fusion.

## 1.1 The importance of solar energy conversion

Today's society is becoming increasingly a society based on the wide spread usage of energy. This energy has to be available in various convenient forms and is the life blood of a modern technological civilisation. At present, the main sources of this energy are oil, coal and gas. These have the advantages of being easily obtained and converted into convenient forms of energy such as electricity but have the disadvantages of being in a finite supply and they pollute the environment. The need to find alternatives to these is brought home in a consideration of the possible sources of energy available and the availability of it.<sup>(1)</sup>

These sources can be identified as follows:-

- 1) Natural products such as wood.
- 2) Fossil fuels.
- 3) Solar radiation, hydraulic, wind, waves.
- 4) Tidal.
- 5) Geothermal.
- 6) Nuclear fission.
- 7) Nuclear fusion.

The availability and amount of energy from these sources is open to great speculation but a rough outline would be as follows:-

- 1) Natural Products- This is potentially a large store of energy since  $\sim 0.1\%$  of the solar energy falling on the earth is converted by photosynthesis to vegetable matter. However, the problems of converting this  $\sim 3 \times 10^{21}$  J are considerable and a large proportion must be considered unavailable.
- 2) Fossil fuels- The world's total recoverable reserves are estimated at  $\sim 3 \times 10^{22}$  J. Geographical, economic and political factors make the full availability of these reserves doubtful.
- 3) Solar energy- Total received at the Earth's surface  $\sim 4 \times 10^{24}$  J/year. This is converted to other energy forms which could be utilised:-
  - a) Hydraulic -  $\sim 35 \times 10^{18}$  J/year of which less than 50% is available most of the year.



b) Wind - total available  $\sim 6 \times 10^{21}$  J/year.

c) Ocean Thermal gradients -  $\sim 6 \times 10^{18}$

J/year but many sites are far from land.

d) Waves - combination of wind and  
gravitational forces.

It is difficult to assess the energy available,  
and only sites near to land are useful.

4) Geothermal - to a depth of 10km about  
 $\sim 4 \times 10^{22}$  J available of which  $10^{18}$  J is usable.

5) Nuclear Fission - a full evaluation is  
limited by political and economic factors.  
However, about  $6.7 \times 10^{22}$  J are realisable.

6) Nuclear Fusion - Deuterium and Tritium are  
effectively in infinite supply if they can  
be extracted from the oceans -  $> 10^{28}$  J.

The present world energy consumption is somewhat  
less than  $3 \times 10^{20}$  J/year and is increasing.

This leads to several conclusions:-

- 1) Fossil fuels will run out in about 160 years at current rate of consumption.
- 2) No single alternative technology will provide for all our requirements. However, a combination of several with the greatest emphasis on solar energy is the most desirable.
- 3) Fusion is the only source which could provide a large percentage of our needs and be in unlimited supply. However, controlled nuclear fusion has yet to be demonstrated.
- 4) Most energy supplies have some form of environmental hazards attached to them. The most extreme of these must be nuclear fission, which has made people unwilling to move to an economy totally based on nuclear fission.

From these statements the importance of solar power generation can be seen, as it must play an important part in the provision of energy in the period of the run down of fossil fuel supplies and development of cheap fusion power.

## 1.2 Means of solar energy conversion

Although there are many means of solar energy conversion, they can be separated out into 4 basic categories:-

- 1) Thermal convertors- these vary from the black radiators of a simple space heating system to ocean thermal energy convertors.
- 2) Electrical convertors- these convert sunlight to electricity and include such devices as thermo electric, thermionic and photo voltaic cells.
- 3) Chemical convertors- these include the biological, photo chemical and photo electrochemical systems. The usual route is the use of a light assisted chemical reaction to produce a suitable fuel. For example the electro chemical photolysis of water which produces hydrogen.
- 4) Indirect methods- these are the solar influenced natural forces such as wind and waves which can be harnessed to produce energy.

The problems of solar energy conversion are multi-faceted and wide varying but could be simplified into the following:-

- 1) Conversion of diffuse low grade energy into concentrated, high grade energy for immediate or future use.
- 2) The variability of the solar energy supply from day to night and season to season. This inevitably means some form of energy storage system must be incorporated.
- 3) Technological and economic constraints due to scale and efficiency.

The general, but no universally accepted route for large scale solar energy use revolves around the production of hydrogen either directly from the chemical photolysis of water, or indirectly by solar produced electricity being used for water electrolysis. As hydrogen can be used as a simple source of energy by being burnt for heat, used as a fuel in an engine or converted into electricity in a fuel cell and is easily stored, it is on the way to solving the first two problems. It is the 3rd area where the blocks on the

development of wide scale usage of solar energy lie. Much research effort has been put into the search for an efficient, cheap photo voltaic device or a simple photo chemical system to make solar energy viable. In recent years one area of research has been into the electrochemical photolysis of water and related processes. It is these processes which are at the heart of the work carried out.

### 1.3 The electro chemical behaviour of semi-conducting electrodes under illumination

Since it was first reported by Fujishima Honda and Kukuchi in 1972<sup>(2)</sup> the electrochemical photolysis of water and related subjects have received great attention. This wide field is best described as the electrochemical behaviour of semi-conducting electrodes under illumination. While this will be expanded on later, it will be useful to outline the basic process now.

When a N type semi-conductor is immersed in an electrolyte and is irradiated, the absorption of light means that the electrons become excited. At the energy level and local position where the electron has absorbed the quanta a hole is left and the excited

electron is transferred to a higher energy state. In a metallic conductor, the mean free energy of the electrons cannot be changed a great deal because too many electrons with energies near the Fermi level are present and these equalise out the average value. However in a semi-conductor, although the electrons are excited in a similar way and they lose some of their excess energy, there is a barrier for the equalising of the energies, as in the metallic case, caused by the slow transition from band to band. This results in the slow recombination of holes (that is slow in relation to that of energy exchange between electronic and vibrational quantum states in the same energy band of electrons). This is shown in Figure 1.1. When a potential is applied the potential difference between the interior of the semi-conductor and the bulk of the electrolyte consists of 2 factors, one of which is the potential difference in the space charge layer due to the separation of charge - i.e. the electrons and positive holes and the other being the potential difference in the double layer where ionic charges are accumulated in the electrolyte solution. The space charge layer is characterised by the properties of the bulk semi-conductor, while the double layer with the solution is characterised by the nature of both the electrolyte and the interaction

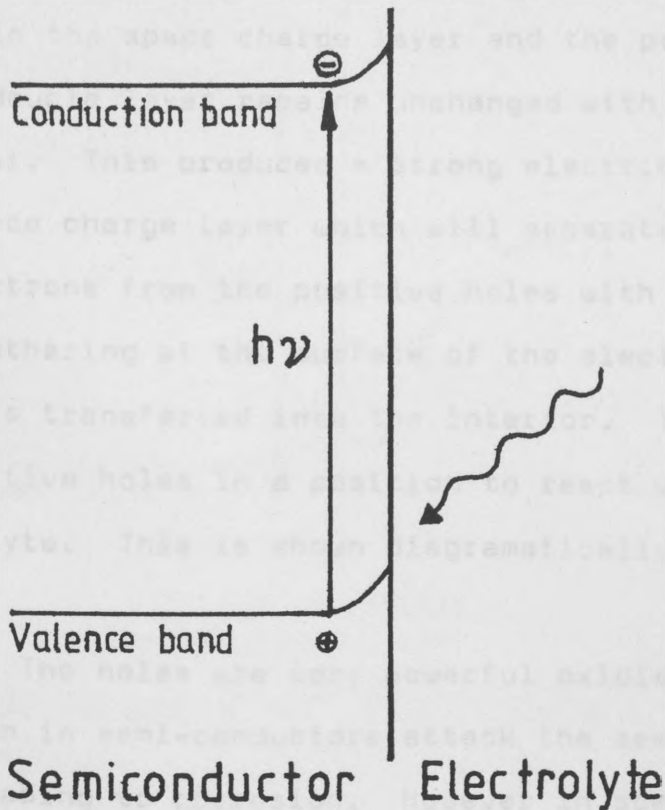


**Fig 1.1**

Stylised view of a N type semiconductor in contact with a redox electrolyte under illumination.

of the semi-conductor surface and the solution. When polarised anodically, almost all the change in potential occurs in the space charge layer and the potential drop in the double layer remains unchanged with the external potential. This produces a strong electric field in the space charge layer which will separate even more the electrons from the positive holes with the positive holes gathering at the surface of the electrode and the electrons transferred into the interior. This leaves the positive holes in a position to react with the electrolyte. This is shown diagrammatically in Figure 12

The holes are very powerful oxidising agents and often in semi-conductors attack the semi-conductor bonds leading to corrosion. However in some semi-conductors the bonds are strong enough to resist this and the holes attack the electrolyte and liberate oxygen.

In electrochemical terms this exhibits itself as the evolution of oxygen at a potential more cathodic than would be expected. If the conditions are such that this potential is moved far enough cathodically then the evolution of oxygen can occur at the same potential as the evolution of hydrogen. So if a suitable electrode is connected to the semi-conductor, the



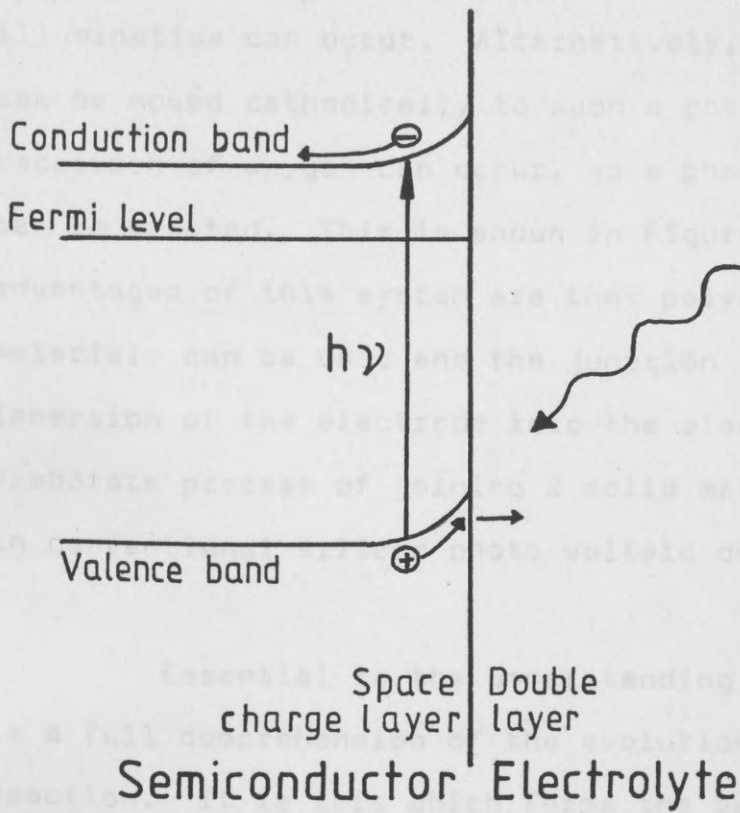


**Fig 1.2**

Stylised view of a N type semiconductor in contact with a redox electrolyte under illumination with an applied potential.

splitting of water into hydrogen and oxygen by illumination can occur. Alternatively, the potential can be moved cathodically to such a potential that the reduction of oxygen can occur, so a photo voltaic device can be created. This is shown in Figure 1.3. The advantages of this system are that polycrystalline materials can be used and the junction is created by the immersion of the electrode into the electrolyte not the elaborate process of joining 2 solid materials necessary in conventional silicon photo voltaic devices.

Essential to the understanding of this process is a full comprehension of the evolution of oxygen reaction. It is this which forms the basis of the study carried out.

#### 1.4 Oxygen Evolution

Besides the importance of studying oxygen evolution in relation to the behaviour of semi-conducting electrodes under illumination, a consideration of the position of oxygen evolution in water electrolysis is in order.

An efficient electrode for the evolution of oxygen is a vital part in a water electrolysis cell.

Fig 1.3

Current/voltage curves for photoelectrolysis

and a photo voltaic device

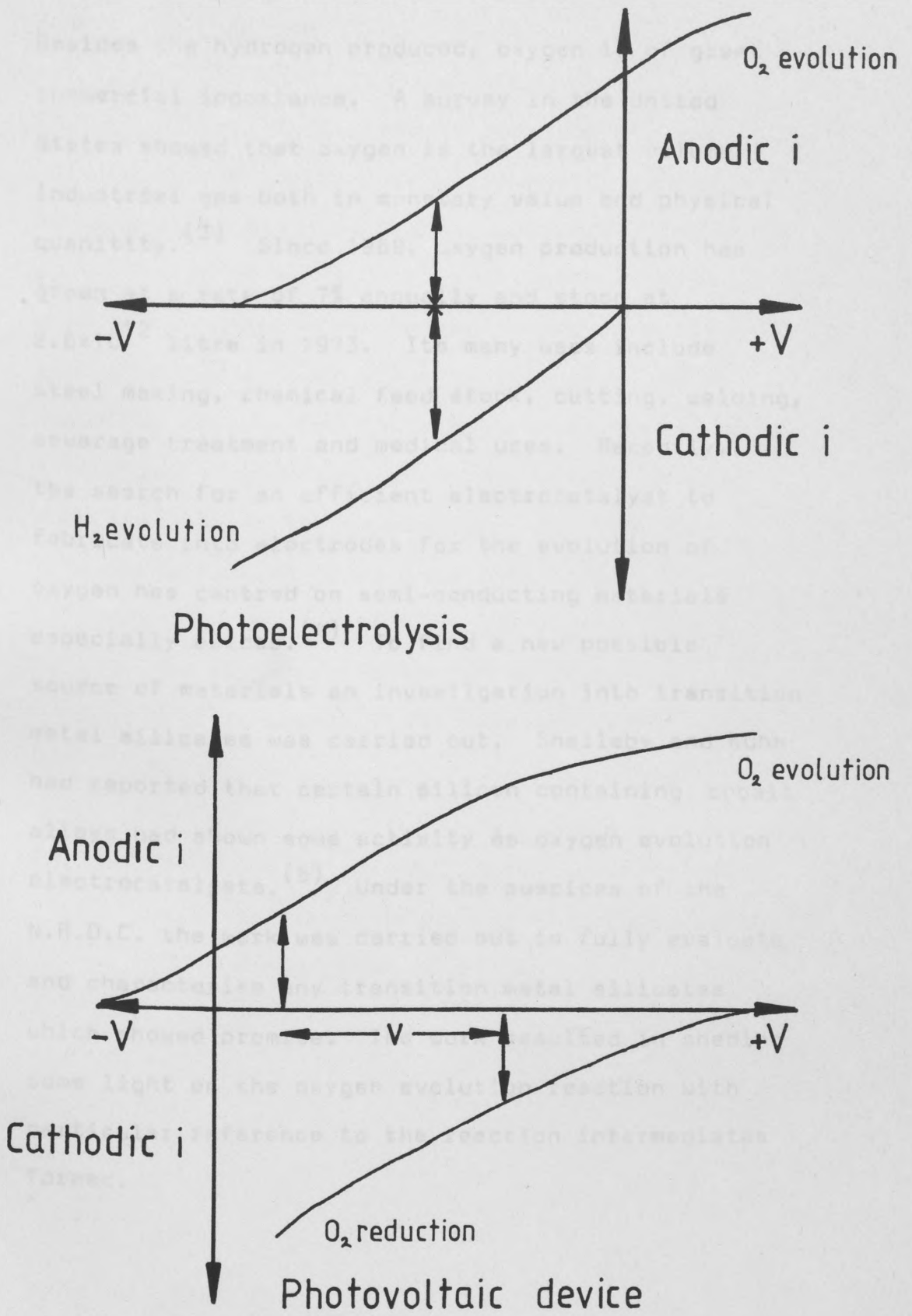


Fig 1.3

Current/voltage curves for photoelectrolysis and a photovoltaic device.

Besides the hydrogen produced, oxygen is of great commercial importance. A survey in the United States showed that oxygen is the largest volume industrial gas both in monetary value and physical quantity.<sup>(3)</sup> Since 1969, oxygen production has grown at a rate of 7% annually and stood at  $2.6 \times 10^{12}$  litre in 1973. Its many uses include steel making, chemical feed stock, cutting, welding, sewerage treatment and medical uses. Recently, the search for an efficient electrocatalyst to fabricate into electrodes for the evolution of oxygen has centred on semi-conducting materials especially oxides.<sup>(4)</sup> To find a new possible source of materials an investigation into transition metal silicates was carried out. Shallaby and Kuhn had reported that certain silicon containing cobalt alloys had shown some activity as oxygen evolution electrocatalysts.<sup>(5)</sup> Under the auspices of the N.R.D.C. the work was carried out to fully evaluate and characterise any transition metal silicates which showed promise. The work resulted in shedding some light on the oxygen evolution reaction with particular reference to the reaction intermediates formed.

## 1.5 Conclusions

To meet future energy requirements the development of large scale solar energy convertors to produce hydrogen is highly desirable. The evolution of oxygen at a more cathodic voltage than its standard electrode potential on certain semi-conductors under illumination, provides the basis for devices for the direct or indirect production of hydrogen. Central to this is an understanding of the oxygen evolution reaction. This investigation falls into 2 distinct parts:

- 1) The study of the evolution of oxygen on illuminated flame oxidised iron electrodes.
- 2) The study of several transition metal silicates as conventional electrocatalysts for the evolution of oxygen.

Since the work of Becquerel in 1839 it has been known that the irradiation of an electrode in an electrochemical cell can induce the flow of current in the external circuit. (6)

Consequently there is an oxidation - reduction process occurring. CHAPTER TWO

THE ELECTROCHEMICAL BEHAVIOUR OF SEMI-CONDUCTING ELECTRODES UNDER ILLUMINATION - A BRIEF REVIEW

out, as was mentioned in Section 1, semi-conductors give the most efficient photocurrents for a given light intensity.

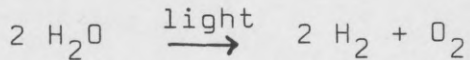
The basis of our understanding of the various processes occurring at a semi-conducting electrode under illumination stems from the work of H. Lohmeyer and his colleagues carried out in the late 1950's and early 1960's. This was fully reviewed in 1961 and it contains many of the basic features of semi-conductor electrochemistry. (6) This work contains observations of the electrochemical behaviour of semi-conducting electrodes under illumination, but the significant process which was

## 2.1 Introduction

Since the work of Becquerel in 1839 it has been known that the irradiation of an electrode in an electrochemical cell could induce the flow of current in the external circuit.<sup>(6)</sup> Consequently there is an oxidation - reduction process occurring, and the possibility of using the products of these processes as fuels exists. Becquerel and subsequent workers (e.g. Pleskov and Rotenberg<sup>(7)</sup>) worked with metal electrodes, but, as was mentioned in Section 1, semi-conductors give the most efficient photocurrents for a given light density.

The basis of our understanding of the various processes occurring at a semi-conducting electrode under illumination stems from the work of H. Gerischer and his colleagues carried out in the late 1950's and early 1960's. This was fully reviewed in 1961 and it contains many of the basic features of semi-conductor electrochemistry<sup>(8)</sup>. This work contains observations of the electrochemical behaviour of semi-conducting electrodes under illumination, but the significant process which was

occurring was the corrosion of the semi-conductor, as opposed to the evolution of oxygen. However, in the early 1970's Fujishima and Honda published work on a photoelectrochemical cell based on titanium dioxide (2,9). Titanium dioxide did not corrode and so the process



could occur in a cell with an illuminated titanium dioxide anode and a suitable cathode. In 1975 Gerischer outlined the principles for a light to electrical energy conversion device using a semiconductor based photoelectrochemical cell (10). From these beginnings a large research effort began in scientific institutions around the world and the trickle of publications in the mid 1970's became a torrent by the end of the decade. Journals such as "Electrochemical Acta" and "The Journal of the Electrochemical Society" now carry the order of 1-2 papers an issue on the subject of photoelectrochemistry and most major conferences on electrochemistry or solar power contain a section devoted to the same subject.

It is this explosion of information which must be considered as the limiting factor of this review. It is not the purpose of this review to



to encompass all that has been published on photoelectrochemistry. Rather its purpose is to collate pertinent information, so the nature of the work reported in this thesis can be seen against the background of the general field of photoelectrochemistry. The areas to be covered are:

- 1) Basic criteria for a photoelectrochemical device.
- 2) Materials available.
- 3) Theory of photo electrochemistry.
- 4) Uses and trends of photo electrochemistry.

It should be noted that to prevent repetition, information about the photoelectrochemical behaviour of iron oxide and related subjects will be covered in Chapter 4 in greater detail.

## 2.2 The basic criteria for a semi-conductor to be usable in a photoelectrochemical device

In Section 1.3 a simple outline of the mechanism of the photo assisted evolution of oxygen

was given. The following criteria, quoted by Atkaitis and Rouh, sum up the basic requirements for a semi-conductor material to be suitable for use as a photo anode for the photoelectrochemical decomposition of water<sup>(11)</sup>:-

- 1) The position of valance and conduction band edges should straddle the aqueous  $H^+/H_2$  and  $H_2O/O_2$  redox couples.
- 2) The band gap should be low enough ( $\approx 1.8$  to  $2.2\text{eV}$ ) to efficiently utilize the solar spectrum.
- 3) The material should be stable under prolonged operating conditions.

The first requirement can be refined by consideration of the flat band potential. The conduction and valance bands of a semi-conductor are bent at the interface of the semi-conductor and the electrolyte. This band bending is due to the separation of charge in the space charge layer. The degree of band bending will alter with applied

potential and the potential at which there is no band bending is known as the flat band potential. The flat band potential can be determined by plotting the (differential capacitance)<sup>-2</sup> against potential, the intercept potential being the flat band potential, Bolts and Wrighton have stressed the importance of the flat band potential and have found that for several photo anodes it correlates with the onset of photo anodic currents corresponding to oxygen evolution (12).

The importance of the correct band gap has been stressed from the beginning of the study of photoelectrochemistry. Fujishima and Honda stated that as for the electrochemical decomposition of water a potential difference of more than 1.23V was required, then radiation of 1,000 nm or less would be usable for this process (2). However, the wavelength suitable for the absorption of light to carry out the process is associated with the band gap of the material. Fujishima and Honda found that the onset of the anodic photocurrent of titanium dioxide was associated with wavelengths shorter than 415 nm, and this corresponds to 3.0 eV, which is the value of the bandgap of titanium dioxide (2). When

the percentage of light available in normal solar radiation suitable for use in a titanium dioxide based photo electrochemical cell is calculated, this is slightly less than 3% (13).

So such a device would be limited to converting slightly less than 3% of the available energy at best. So if a material can be found with a lower band gap, then more of the energy available in solar radiation can be utilized. Memming has also reported that the band gap shapes the solar energy conversion efficiency of any device (14). He reported that the optimum band gap was about 1.6 eV and at that band gap an efficiency of about 30% was possible. The variation of energy conversion efficiency and band gap is shown in Figure 2.1. The values of the band gap of some common materials used in photo electrochemical devices are shown as well.

The importance of the long term stability of the electrode is self-evident, as any deterioration with time would render such a device useless. It was this aspect which has ruled out the more well known semi-conductors of germanium and silicon (8,15).

Energy conversion efficiency vs band gap.

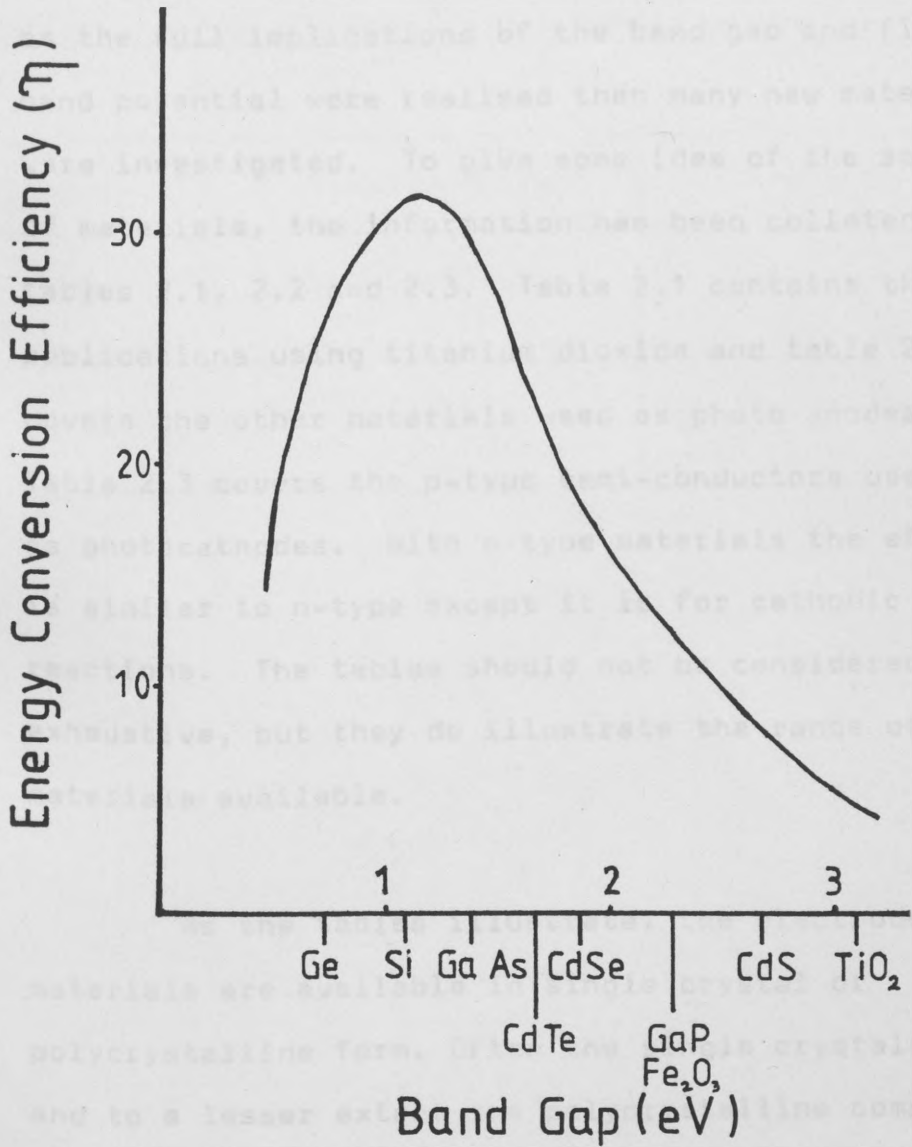


Fig. 2.1

Energy conversion efficiency vs band gap.

### 2.3 Materials suitable for photo electrochemical devices

The original investigations into photoelectrochemical devices centred on titanium dioxide. However, as the full implications of the band gap and flat band potential were realised then many new materials were investigated. To give some idea of the spread of materials, the information has been collated in tables 2.1, 2.2 and 2.3. Table 2.1 contains the publications using titanium dioxide and table 2.2 covers the other materials used as photo anodes. Table 2.3 covers the p-type semi-conductors used as photocathodes. With p-type materials the effect is similar to n-type except it is for cathodic reactions. The tables should not be considered exhaustive, but they do illustrate the range of materials available.

As the tables illustrate, the electrode materials are available in single crystal or polycrystalline form. Often the single crystals and to a lesser extent the polycrystalline compounds are non-conducting. Various methods have been used to improve the conductivity such as heating under

TABLE 2.1

Publications using materials other than titanium dioxide

as a photo anode

TABLE 2.1

Reference

Publications using titanium dioxide as a photo anode

Material	Crystalline Form	Reference
TiO <sub>2</sub>	SINGLE CRYSTAL	2,12,16→33
	POLYCRYSTALLINE	11,30, 34→46

TABLE 2.2

Publications using materials other than titanium dioxide  
as a photo anode

Material	Crystalline Form	Reference
Sn O <sub>2</sub>	polycrystalline	34
Nb <sub>2</sub> O <sub>3</sub>	polycrystalline	34
Al <sub>2</sub> O <sub>3</sub>	polycrystalline	34
Si N <sub>4</sub>	polycrystalline	34
Ga As	polycrystalline/ single crystal	34, 47→50
Ga Al As	polycrystalline	34
Cd S	polycrystalline/ single crystal	10, 48, 50→53
Cd Se	polycrystalline/ single crystal	10, 47→48, 51, 53→57
Sr Ti O <sub>3</sub>	polycrystalline/ single crystal	12, 19→20, 28, 58→60
Fe <sub>2</sub> O <sub>3</sub>	polycrystalline	61→73
W O <sub>3</sub>	polycrystalline	74→76
Mo Se <sub>2</sub>	polycrystalline	77→78
W Se <sub>2</sub>	polycrystalline	77, 79
Ga P	polycrystalline	10, 50, 80
Cd Te	polycrystalline	48, 81
Cu In S <sub>2</sub>	polycrystalline	48
Sb doped SnO <sub>2</sub>	polycrystalline	12, 82
K Ta O <sub>3</sub>	polycrystalline/ single crystal	12
Mo S <sub>2</sub>	polycrystalline	78, 83→84



TABLE 2.3Publications using materials as a photo cathode

Material	Crystalline Form	Reference
Ga P	Polycrystalline/ Single crystal	30,34,85,86
Cd Te	Single crystal	20,54,86
Zn Te	Single crystal	86
Ga As	Single crystal	86
In P	Single crystal	86
Si C	Single crystal	86
Si	Single crystal	86
Ge	Single crystal	50

a) Charge transfer.

b) Charge transport.

c) The evolution of oxygen on illuminated photo anodes.

hydrogen<sup>(20)</sup>, heating under vacuum<sup>(22)</sup> or doping<sup>(11)</sup>.

Polycrystalline electrodes were made by various methods such as solid state sintering<sup>(46)</sup>, chemical vapour deposition<sup>(72)</sup>, sputtering<sup>(75)</sup>, thermal oxidation<sup>(64)</sup> and electrolytic co-deposition<sup>(57)</sup>.

Juliao, Decker and Abramovich have even reported the use of titanium dioxide in its natural mineral form<sup>(45)</sup>.

#### 2.4 The theory of photoelectrochemical processes

The theory of photoelectrochemical processes could be considered to fall into 4 areas of interest. The first of these is that of an overall explanation of the process in terms of general semi-conductor theory. The other 3 areas could be considered as the following:-

- a) Charge transfer.
- b) Charge transport.
- c) The evolution of oxygen on illuminated photo anodes.

### 2.4.1 The overall process

The essentials of the reactions occurring on an illuminated semi-conducting electrode have been mentioned in Section 1.3. Gerischer has treated an illuminated semi-conductor in a suitable redox electrolyte as being equivalent to a Schottky barrier. In this case the redox electrolyte replaces the metal normally found in such a device. The energy diagram for such a situation is shown in Figure 2.2. Here the equilibrium situation is compared with the flat band situation in terms of the energy band scheme for the interface between an n-type semi-conductor and the redox potential  $U_0$ , causing a band bending of  $e_0 \Delta e_{s.c.} = U_0 - U_{FB}$  at equilibrium. Now if light with an energy greater than the band gap irradiates the semi-conductor surface and is absorbed in the space charge layer, then electron - hole pairs are generated. These two charge carriers will be separated due to the field in the space charge layer. If they do not recombine due to coulombic attraction or collision with other carriers, the electrons will migrate into the bulk and the holes will accumulate at the surface. These

Energy diagram of a N type semiconductor in contact with a redox electrolyte.

Key to symbols used:  $E_c$  - conduction band edge;  $E_v$  - valence band edge;  $E_f$  - Fermi level; prefix " - Flat band situation;  $U_0$  - redox potential;  $U_{FB}$  - flat band potential.

# Semiconductor

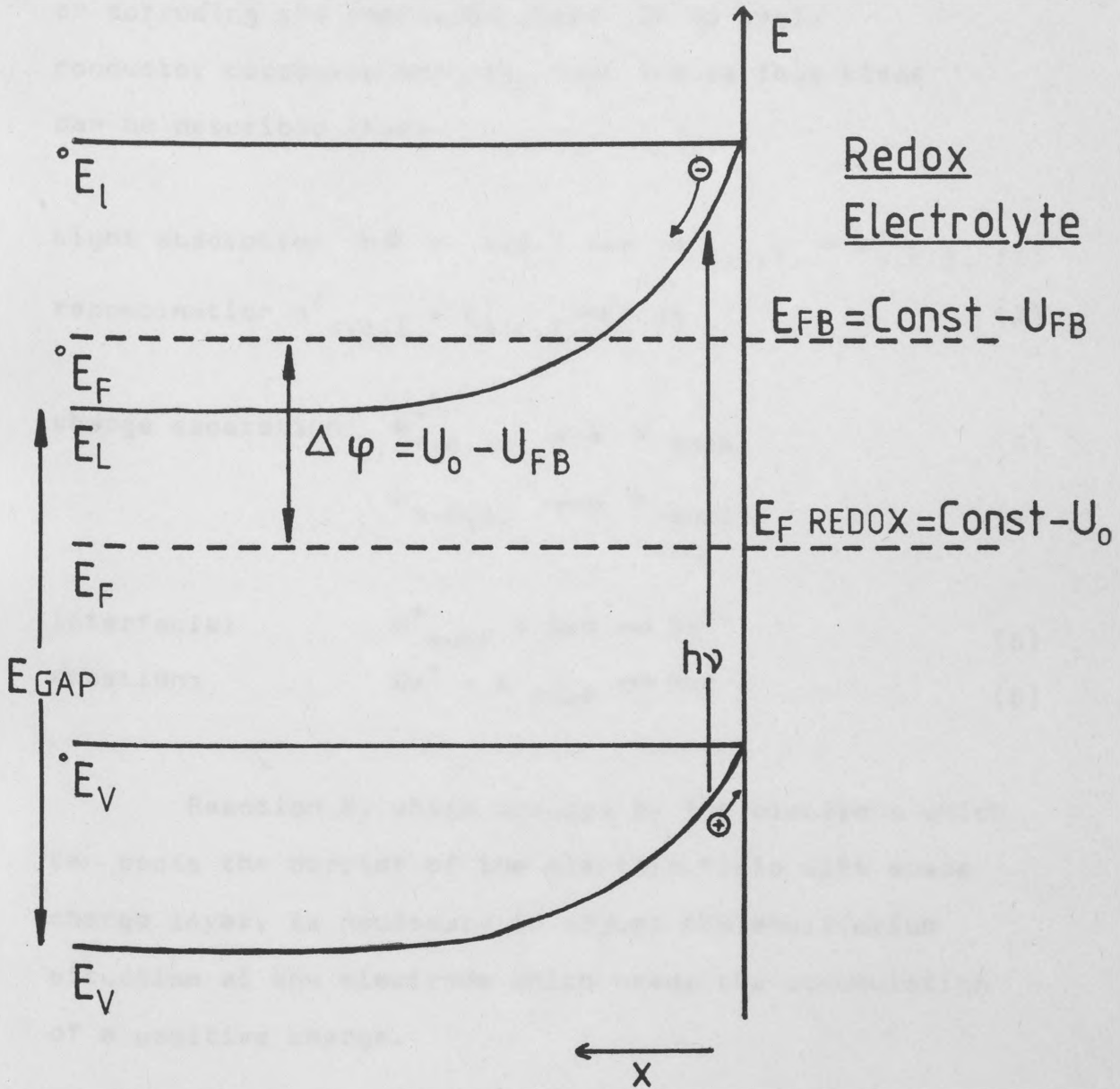
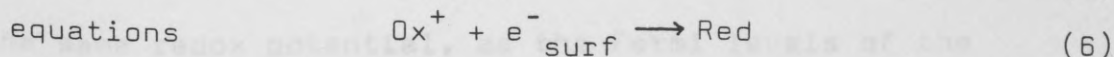
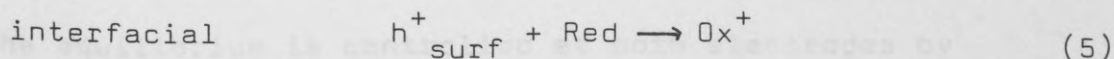
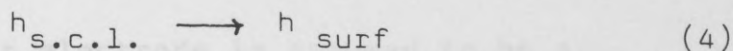
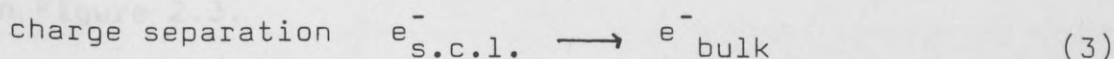
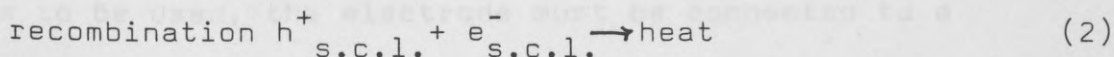
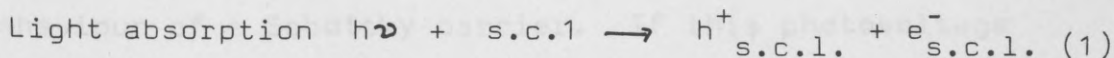


Fig 2.2

Energy diagram of a N type semiconductor in contact with a redox electrolyte.

Key to symbols used:  $E_L$ -conduction band edge;  $E_V$ -valence band edge;  $E_F$ -Fermi level; prefix °-Flat band situation;  $U_0$ -redox potential;  $U_{FB}$ -Flat band potential.

holes are then available for reaction either oxidizing the electron donors of the redox system or corroding the semi-conductor. If no semi-conductor corrosion occurs, then the various steps can be described thus:-



Reaction 6, which occurs by the electrons which can cross the barrier of the electric field with space charge layer, is necessary to adjust the equilibrium situation at the electrode which needs the accumulation of a positive charge.

Under illumination, a photo voltage is obtained. This generation of electric charge causes a deviation from the equilibrium charge distribution. This diminishes

the degree of band bending. A steady state is reached when steps 1,3 and 4 equal 2 and 6. Since the rate of steps 2 and 6 will increase with diminished band bending, the photovoltage will increase with illumination intensity. This is similar to the behaviour of a Schottky barrier. If this photovoltage is to be used, the electrode must be connected to a suitable counter electrode. This situation is shown in Figure 2.3.

If the counter electrode is assumed to be a reversible redox electrode for the redox system, then the equilibrium is controlled at both electrodes by the same redox potential, as the Fermi levels of the metal, the semi-conductor and the electrolyte are the same. The counter electrode guarantees a fast approach to equilibrium once both electrodes are in contact. As reaction 6 can now occur at the counter electrode, the imbalance caused by illumination, can be resolved by flow of electrons in the external circuit, hence the photovoltage can be used for electrical work.

Memming has extended this model to cover the photo electrolysis of water<sup>(14)</sup>. Here two redox

Key to symbols used:  $E_c$  - conduction band;  $E_v$  - valence band;  $E_f$  - Fermi level; \* - illuminated;  $U_{phot}$  - photo voltage.

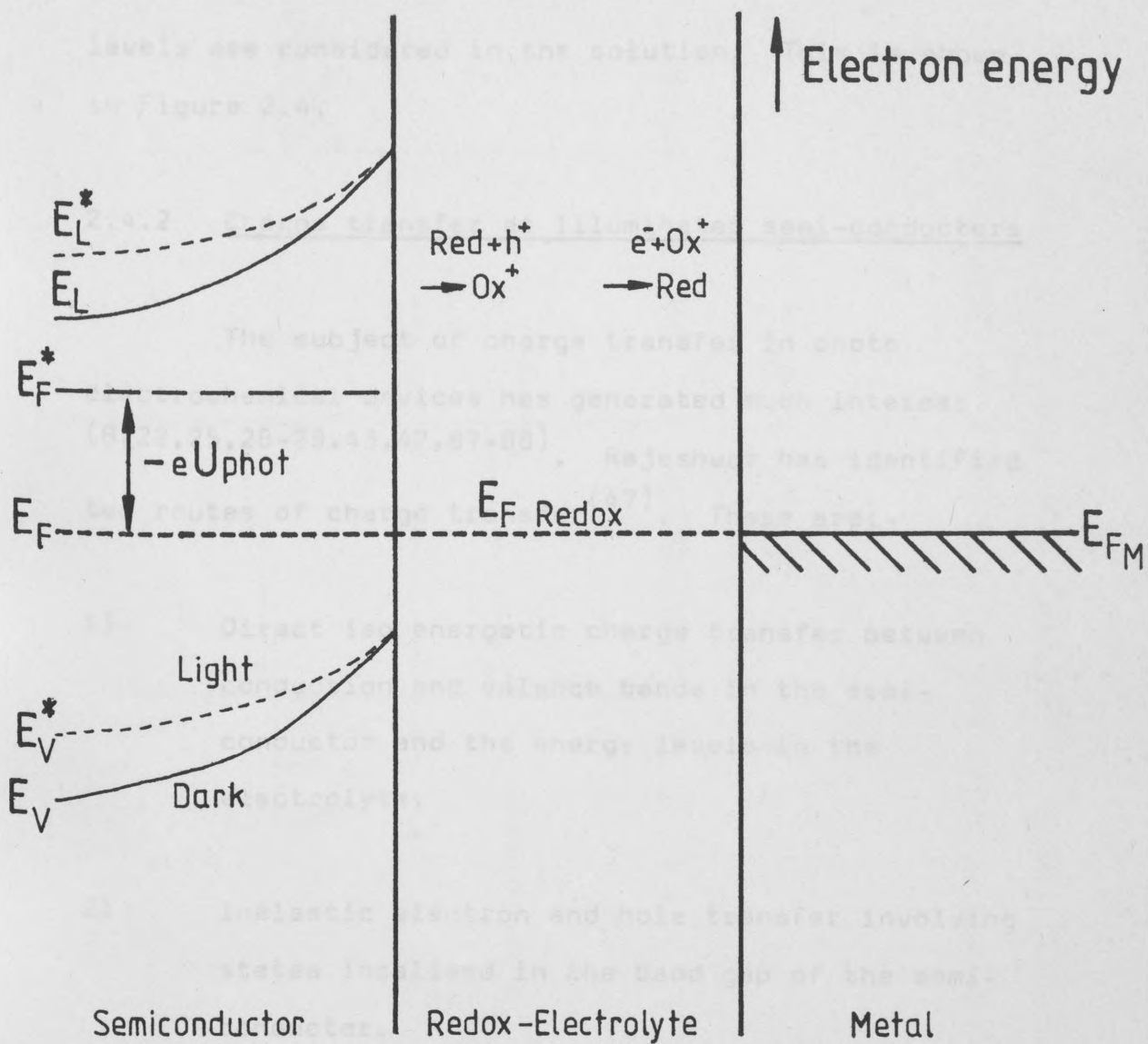


Fig. 2.3

Energy diagram of a N type semiconductor in contact with a counter electrode.

Key to symbols used:  $E_L$ -conduction band;  $E_V$ -valence band;  $E_F$ -Fermi level; \* -illuminated;  $U_{\text{phot}}$ -photo voltage.

levels are considered in the solution. This is shown in Figure 2.4.

#### 2.4.2 Charge transfer at illuminated semi-conductors

The subject of charge transfer in photo electrochemical devices has generated much interest (8,22,25,28-29,43,47,87-88). Rajeshwar has identified two routes of charge transfer<sup>(47)</sup>. These are:-

- 1) Direct iso energetic charge transfer between conduction and valence bands in the semi-conductor and the energy levels in the electrolyte.
- 2) Inelastic electron and hole transfer involving states localised in the band gap of the semi-conductor.

Although much detailed theoretical treatment has been carried out on the first route<sup>(1) (8)</sup>, Rayeshwar feels that the body of evidence lies with the second route<sup>(47)</sup>. He supports this with 2 statements:-

Fig. 2.4



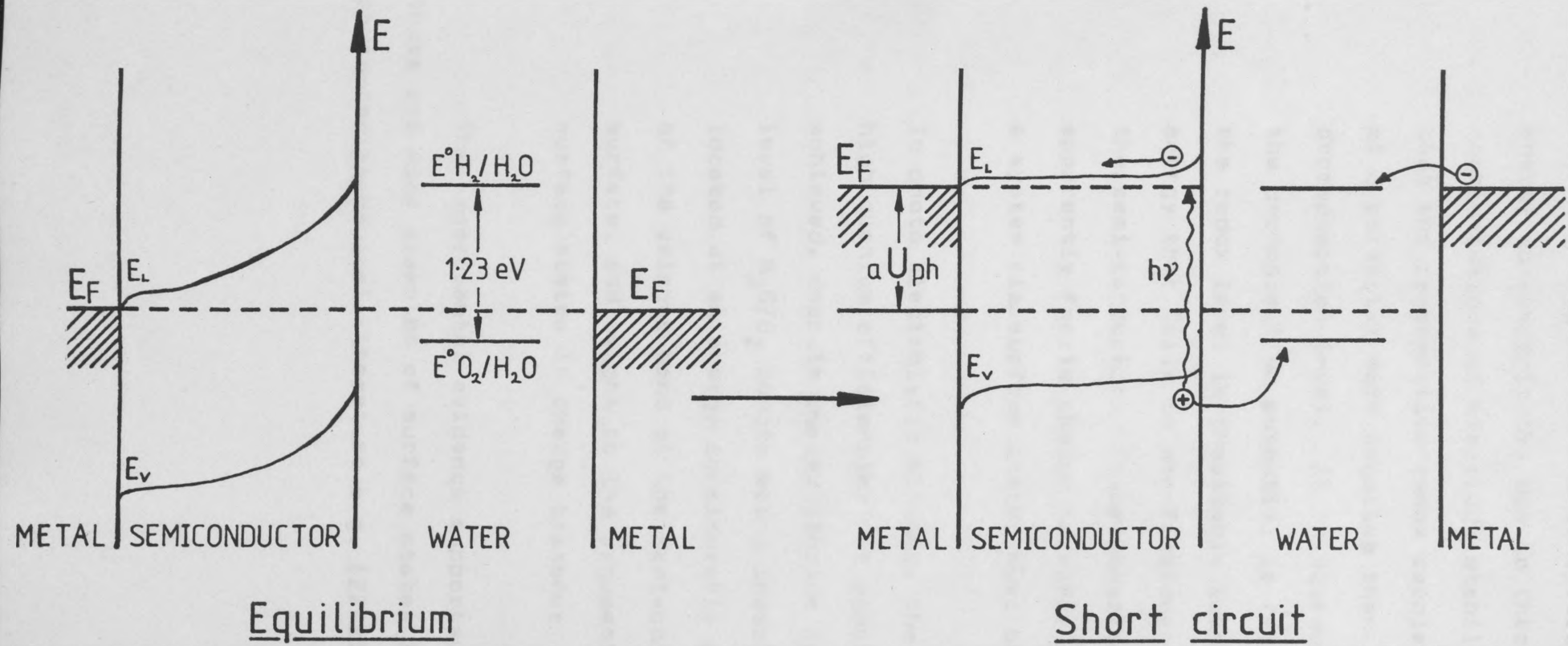


Fig 2.4

Energy diagrams of N type semiconductors in contact with metal counter electrodes under the conditions necessary for the photoelectrolysis of water.

1) Devices designed for the conversion of solar energy to electricity, due to thermodynamic considerations of electrode stability, require that the regenerative redox couple is located at a potential more negative than the decomposition level. As in aqueous systems the decomposition potential is fairly negative, the redox level is inevitably located at an energy that falls in the forbidden gap of the semi-conductor. To rationalise the apparently facile charge transfer observed, a system via surface states must be used.

2) In photo electrolytic systems, the surprisingly high quantum efficiencies for electron flow achieved, despite the equilibrium redox level of  $H_2O/O_2$  couple being invariably located at an energy considerably over the top of the valence band at the semi-conductor surface, add weight to the argument for surface states in charge transfer

The experimental evidence supports this as there are many examples of surface states in the photoelectrochemical literature e.g. (22,25,28-29,43).

Rujeshwar has formulated a model for charge transfer via surface states based on adsorbed anions on the semi-conductor<sup>(47)</sup>. These adsorbed ions are either one of the components of the redox couple or are one of the constituent ions of the supporting electrolyte. Wilson, in his study of oxygen evolution on titanium dioxide has postulated that these surface states are intermediates of the oxygen evolution reaction<sup>(29)</sup>. So a consideration of the mode of charge transfer is important when considering the mechanism of the evolution of oxygen on illuminated semi-conductors. This will be returned to and expanded on in Section 4.9 as part of the consideration of the results obtained on flame oxidized iron.

#### 2.4.3. Charge transport in the semi-conductor

Although originally studied by Gerischer back in the late 50's and early 60's<sup>(8)</sup>, the processes occurring in the space charge layer, with special reference to charge transport, has only relatively recently been studied in relation to its implications for photo electrochemical reactions. As the active species at the surface of an illuminated semi-conductor is a positive hole, the emphasis has been

on the nature of these minority carriers. The possibility of such charge transport being the limitation on an electrode's performance must not be ruled out. Ullman has used a model of the photocurrent being limited by the charge transport through the space charge layer to explain experimentally observed results on titanium dioxide<sup>(19)</sup>. Because of this the need to be able to model the behaviour expected in the space charge layer is obvious. Several models have been evaluated(19,58,89,90) but these are limited in their application, as they only hold for simplified situations such as simple redox solutions and single crystal electrodes, and as such could not be applied to polycrystalline semi-conductors. So the use of qualitative judgements and empirical observations have to be used, when deciding if these factors are affecting the performance of an electrode.

#### 2.4.4. The mechanism of the evolution of oxygen on illuminated semi-conductors

Publications on this subject have been mainly associated with the charge transfer by surface state investigations mentioned earlier. It is generally considered that the reaction intermediates of oxygen evolution are the surface states required for charge

transfer (e.g. 29). As mentioned in Section 2.4.2, this will be more fully discussed in Section 4.9.

## 2.5 Applications and trends in photoelectrochemistry

It is the potential use of photoelectrochemical devices as solar energy convertors which has spurred the great interest in them. As the complex problem of creating a junction of the semi-conductor with a metal or another semi-conductor has been elegantly solved by immersing the semi-conductor in an electrolyte, one of the greatest barriers to the exploitation of solar energy has been removed.

The applications and trends in photoelectrochemistry can be considered to be in two general areas. These are:-

- a) Photoelectrochemical devices.
- b) Improvements in photoelectrochemical performance.

### 2.5.1 Photoelectrochemical Devices

This area can be conveniently split into 3 sub-sections. These are:-

- a) Photo electrolysis.
- b) Voltage generation with regenerative photo cells.
- c) Photo electrosynthesis.

Photo electrolysis, as it is such a desirable process with its provision of hydrogen by illumination, is still very much at the centre of the study of photoelectrochemistry. However, as Memming pointed out in his recent review, there are several major barriers to overcome before a suitable device can become a technical possibility<sup>(14)</sup>. The most important of these are the energy parameters. The energetic conditions required are as follows:-

$$E_g > E_{O_2/H_2O}^0 - E_{H_2/H_2O}^0 = 1.23eV$$

$$E_c < E_{H_2/H_2O}^0, \quad E_v > E_{O_2/H_2O}^0$$

$E_g$  - Band gap

$E_c$  - Conduction band

$E_v$  - Valence band

Only 3 materials meet this criteria -

$Sr Ti O_3$ ,  $K Ta O_3$  and  $K Ta_x Nb_{1-x} O_3$  ( $x = 0.77$ ) (12,59,82). Titanium dioxide just meets the criteria, but its value of  $E_c$  is almost equal to  $E_{H_2/H_2O}^0$  so

high intensities are required (40). Also these materials have a large band gap ( $> 3.0$  eV) and only absorb in the U.V. This means that only a small portion of the solar spectrum can be utilized. One answer to this dilemma is the combination of p and n semi-conducting photo electrodes. Bhashi, McCann and Bockris have successfully done this and found that an-Sr  $TiO_3$ /p-GaP under xenon light gave a quantum efficiency of 0.7% and a nTi  $O_2$ /pGaP cell gave an efficiency of 0.1% in solar radiation conditions (20). Also there was a usable voltage associated with the cell.

However, the technological realisation of a photo electrolysis cell must be far away. As Memming states in his review, even if a suitable semi-conductor can be found, the large scale fabrication of it into a high area cell with the resultant collection of the hydrogen from a large area is fraught with difficulties. The use of a large area regenerative photo cell which only produces electrical power, which can be used in a centralised conventional water electrolyser seems a more likely route (14).

### 2.5.2 Voltage generation with regenerative photo cells

As noted above, increasingly the interest in

in photoelectrochemistry is centering on regenerative photo cells. As the process centres on one redox couple, it has not got the limitations of 2 redox couples inherent in photo electrolysis. This means that semi-conductors with lower band gaps can be used and the redox couple can be chosen to give a more stable electrode.

As with so much of photoelectrochemistry, the original suggestion for such a cell came from Gerischer<sup>(10)</sup>. Since that suggestion, a wide range of materials have been investigated. An early investigation was that of Gissler, Lensi and Pizzini<sup>(40)</sup>. They postulated a cell based on titanium dioxide using the oxygen redox couple and experimentally found the cell to be about 0.5% efficient at pH 11. Another cell using the oxygen redox couple was reported by Ang and Sammells<sup>(67)</sup>. They used a flame oxidised iron photo anode and a fuel cell type cathode. Under illumination with a 150 watt Xenon light source a photo voltage of up to 400mv and a short circuit current of  $1\text{ma}/\text{cm}^2$  was obtained.

Most work however has centred on such electrodes as cadmium sulphide and the sulphur redox couple e.g. ref. (10,48,51). One area of interest is the combination of a regenerative photo cell with a storage electrode. Manassen, Hodes and Cahen have



made cells using cadmium selenide and the sulphur redox couple<sup>(56,57)</sup>. They also incorporated a storage electrode so the cell gave power in the dark as well as when illuminated. The cell arrangement is shown in Figure 2.5. The cell made use of a reversible reaction (they used  $\text{Ag}_2\text{S} + 2\text{e}^- \rightleftharpoons 2\text{Ag} + \text{S}$ ) at the storage electrode, which could be recharged when the photo anode was illuminated, and discharged when it was dark. By suitable sizing of the loads  $L_1$  and  $L_2$  a useful voltage could be maintained all the time. They quoted performances of 0.67V and short circuit currents of up to  $12\text{ma}/\text{cm}^2$ . This is of interest as it neatly gets round the problem of all solar power convertors - that is what happens at night.

Heller and Miller have recently reviewed the situation in regenerative photoelectrochemical cells<sup>(48)</sup>. This useful review not only highlights the problem areas such as photo corrosion, surface state shunts and reflectivity of electrodes but also illustrates possible solutions - these being careful choice of redox couple, reacting surface states with strongly chemisorbed species and roughening up the surface. Using these methods

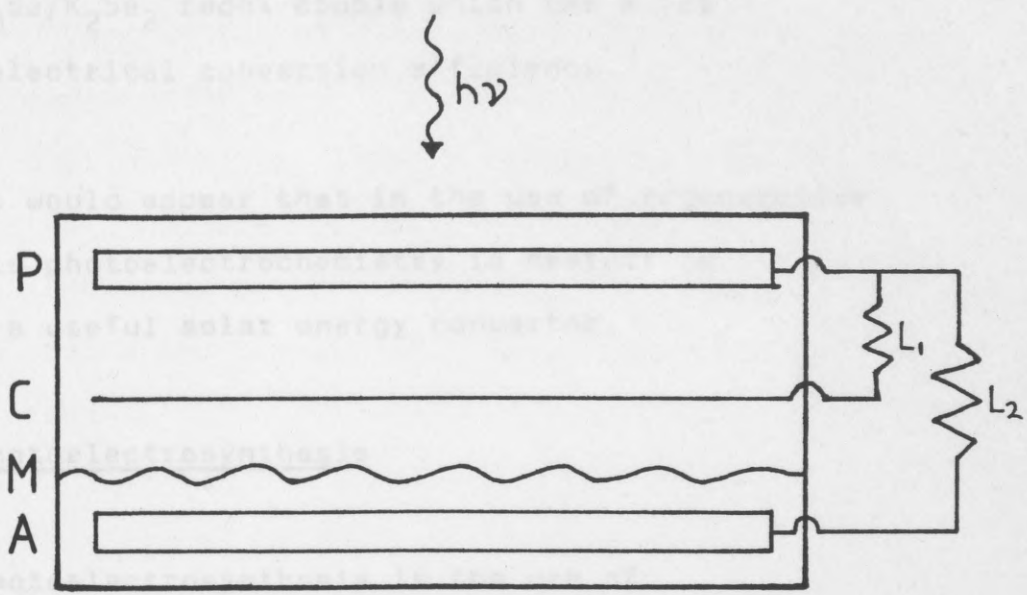


Fig. 2.5

A photoelectrochemical storage cell.

Key to symbols used:

- P - Photoanode
- C - Counter electrode
- M - Cationic membrane
- A - Storage electrode

they have produced a cell based on n Gallium Arsenide and the  $K_2Se/K_2Se_2$  redox couple which has a 12% solar to electrical conversion efficiency.

It would appear that in the use of regenerative solar cells photoelectrochemistry is nearest to achieving a useful solar energy convertor.

### 2.5.3. Photoelectrosynthesis

Photoelectrosynthesis is the use of photoelectrochemical reactions to produce a chemical product. A good example of this was reported by Kraeutler and Bard <sup>(21)</sup>. They studied the behaviour of a titanium dioxide electrode in a acetonitrile solution of tetra-n-butylammonium acetate. The reaction products were found to include ethane and as such this can be considered to be a photo-assisted version of the Kolbe reaction.

Miyake, Yoneyama and Tamura have studied titanium dioxide in solutions containing such organic compounds as methanol and iso-propanol <sup>(33)</sup>. These were oxidised by photo-assisted reactions to formaldehyde and acetone respectively. They also incorporated a p- Gallium Phosphide photo anode into the cell with a resultant improvement in performance.

A particularly novel use of photo electrochemical devices in photoelectrosynthesis was the so called mini-cells reported by Bard<sup>(37)</sup>. He deposited small amounts of platinum on to titanium dioxide particles. These could be considered as short circuited photoelectrochemical cells. When placed in various organic solutions and irradiated, they broke down the compounds present.

Various inorganic photo elctrosyntheses have been reported. Jorne has reported that tungsten trioxide electrodes photo-assist the production of Chlorine<sup>(74)</sup>. Clechet, Martelet, Martin and Olier have reported the production of hydrogen peroxide on titanium dioxide<sup>(42)</sup>, but this must be viewed as a by-product of oxygen reduction<sup>(32)</sup>.

Photoelectrosynthesis is an area that has not attracted so much attention as such subjects as regenerative solar cells. However, its use as a possible source of novel catalysts, particularly for organic solutions is of great interest.

#### 2.5.4 Improvement of photo electrochemical performance

The main area of interest for this subject has been the alteration of semi-conductors with a wide

band gap in such a way that they can utilise more of the solar spectrum.

The first attempt to achieve this was by Tomkiewicz and Woodall<sup>(54)</sup>. They sputtered thin films of wide band gap materials, hoping that the lower band gap material could generate the holes and the higher band gap material could prevent the photo-corrosion. However, even when great care was taken with the preparation of the dual layer electrodes, photo-corrosion still occurred, although it was diminished by several orders of magnitude.

Two other mechanisms have been investigated to see if visible light response could be obtained on a wide band gap semi-conductor. These are doping and the use of dye sensitizers.

Doping has met with some success. Monnier and Augustynski reported that doping polycrystalline titanium dioxide electrodes with nickel, chromium or zinc led to a decrease in quantum efficiency, but also a shift in photo response in the direction of visible light<sup>(35)</sup>. Alkaitis and Rauh found similar results with titanium dioxide doped with chromium<sup>(11)</sup>. They explained this in terms of the 3d transition metal ion additives acting as intergap sensitizers as well as traps. The  $3d^N$  levels seem to have acted

as localised levels and therefore could act as bulk carrier recombination centres. Matsumoto, Kurimoto, Amagasaki and Sato found that titanium dioxide doped with cobalt also gave similar properties of diminished quantum efficiency in association with increased visible light response<sup>(46)</sup>.

They attributed this to a newly formed d-band caused by the interaction of the interstitial Ti or Co ion in the titanium dioxide lattice. This new d-band forms underneath the conduction band, and so effectively lowers the apparent band gap.

The use of dye sensitizers in electron transfer processes in semi-conductor materials has been known for some time. However, the use of such sensitizers in photoelectrochemistry is not so widespread. Typical of such a use is the work reported by Fleischauer and Allen<sup>(44)</sup>. Using thin film titanium dioxide electrodes and rhodamine B as the sensitizer, the photo response was extended to the 500-630 nm region. Apparently this was not at the expense of the quantum efficiency. Schumacher, Wilson and Harris have also studied the same system<sup>(30)</sup>. They found the observed photo response increased by a factor of 8 with doping. They also investigated

response can be fine tuned.

the nature of the bond between the dye and semiconductor.

## 2.6 Conclusions

The study of photoelectrochemistry is now one which is rich and multi-faceted. The diverse paths of research are all joined in the search for a photoelectrochemical device which will enable cheap solar energy convertors to be produced. At the moment that still seems far in the future, but the advancement of knowledge since Fujishima and Honda's paper in Nature in 1972 has been so rapid that such a device may not be so far away as we think.

From this survey of the state of the art in photoelectrochemistry two things became obvious:-

- 1) The ultimate control on the efficiency of photo electrochemical devices is the nature of the charge transfer process. If this can be more fully understood, then a suitable material can be found . When that material is recognised, then other factors in its overall efficiency such as width of spectral response can be fine tuned.

- 2) A great deal of the work reported on photoelectrochemistry had been empirical in its choice of materials and had been approached from a photo chemistry or a semi-conductor property point of view. Not much attempt has been made to view the problems of photoelectrochemistry from a kinetic electrochemical point of view.

### CHAPTER THREE

It is the proposal of this research to investigate the nature of charge transfer in photoelectrochemistry from a kinetic electrochemical point of view. Firstly this will involve the choice of a suitable test material and it is this choice which is the basis of the next chapter.



If the experimental work carried out in the literature reported in Chapter 7 is taken as a guide, the following five basic principles can be suggested as a set of guidelines for the choice of a suitable test material, assuming, obviously, that the material exhibits a photo electrochemical effect. These are, not necessarily in order of importance:

- 1) The material must be easily available or simple

### CHAPTER THREE

#### THE CHOICE OF MATERIAL FOR A TEST ELECTRODE

However, due to the limitations of a S.R.C. grant, the use of single crystals was ruled out by cost considerations. Arguably there is also a case for not using a single crystal on the grounds that any device destined for widespread use would most likely be polycrystalline, and any measurements should therefore be on a polycrystalline electrode. Also any comparison of polycrystalline to single crystal electrodes have found that the only difference exhibited was in the magnitude of the current - e.g. ref.(38). So the test material should be polycrystalline.

If the experimental work carried out in the literature reported in Chapter 2 is sieved through, the following five basic principles can be arrived at as a set of outlines for the choice of a suitable test material, assuming, obviously, that material exhibits a photo electrochemical effect. These are, not necessarily in order of importance:-

- 1) The material must be easily available or simple to produce. The majority of research into photoelectrochemistry has been carried out on single crystals. However, due to the limitations of a S.R.C. grant, the use of single crystals was ruled out by cost considerations. Arguably there is also a case for not using a single crystal on the grounds that any device destined for widespread use would most likely be polycrystalline, and any measurements should therefore be on a polycrystalline electrode. Also any comparison of polycrystalline to single crystal electrodes have found that the only difference exhibited was in the magnitude of the current - e.g. ref.(39). So the test material should be polycrystalline.

2) The semi-conducting material must have a reasonable conductivity. This is to minimise ohmic losses in the photo electrochemical cell. It limits somewhat the use of powder semi-conductors, as often they have very low conductivities. Infact single crystals normally need some form of treatment to enhance their conductivity e.g. ref.(2).

3) The formation of a non-rectifying ohmic contact between the semi-conductor and the current collector must be possible and straight forward. The ohmic contact is made with a metal whose work function falls below the Fermi level of the semi-conductor. This is normally a material such as indium and it is applied to the semi-conductor surface by processes such as sputtering or evaporation.e.g. ref(2). Once the metal layer is formed, the current collector wire may be attached to it by the use of silver araldite.

4) The material should not be porous. This is to prevent the electrolyte getting into contact with the ohmic contact or the current collector. If this happens, then corrosion will occur, especially of the ohmic contact, as indium is readily attacked at the potentials being used. Such corrosion will lead to the breakdown of the ohmic contact or the resultant corrosion currents swamping any possible photo currents. This is an acute problem with any powder semi-conducting materials, as they usually have their electrodes fabricated as a sintered disk, and as such, unless a very full sinter is obtained, are porous, permitting the electrolyte to make contact with the ohmic contact and the current collector.

5) The material should have a band gap which will enable as much of the solar spectrum as possible to be utilized. Besides the desire to use as much as possible of the light energy available, this parameter was also a reflection of the cost limitations on the research. High band gap materials require a high energy ultra-violet light

an ohmic contact and to connect the current collector.

and this was not available.

Several materials were tried, but these were ruled out due to a failure to meet one of the 5 criteria. The main stumbling blocks were the formation of a good ohmic contact which could not be attacked by the electrolyte. Finally flame oxidized iron was settled upon, as it fitted all the requirements.

- 1) The electrode was simple and cheap to fabricate.
- 2) It had a good conductivity, and, as the oxide film was thin, the resistance was low.
- 3) The great advantage of flame oxidized iron was that it formed the ohmic contact during its fabrication. The ohmic contact can be considered to be the oxide layer-base metal interface. This also meant that as a nickel wire could be spot welded to the iron before flame oxidation, no elaborate steps had to be taken after the making of the semi-conductor, to provide an ohmic contact and to connect the current collector.

- 4) The oxide film was consistent and non-porous.
  
- 5) The band gap of flame oxidized iron was 2.1eV, which meant that it could utilize white light.

So flame oxidized iron provided a good material to be used as a test electrode.

THE PHOTO-ELECTROCHEMICAL BEHAVIOR OF FLAME OXIDIZED IRON

## Introduction

The use of flame oxidized iron as an electrode for the photoelectrochemical electrolysis of water was first reported by Van Haeckel and Ruckenstein (54). The potential use of flame oxidized iron for the study of photoelectrochemical behaviour has produced a great deal of interest due to its favourable characteristics. These were:

### CHAPTER FOUR

#### THE PHOTO ELECTROCHEMICAL BEHAVIOUR OF FLAME OXIDIZED IRON

- 1) The electrodes were easily made.
- 2) The wavelength response was that of a semi-conductor with an energy band gap of 2.1 eV, enabling utilization of radiation in the visible range (55).
- 3) The material exhibited interesting transient behaviour under illumination (56).

These properties have led to investigations into various forms of production of  $Fe_2O_3$  electrodes for study e.g. solid state sintering (57-59), vapour deposition (60, 61), anodic oxidation (62, 63), and the growth of a thin layer on an iron electrode (64). These studies have added to the knowledge of the photoelectrochemistry

#### 4.1 Introduction

The use of flame oxidized iron as an electrode for the possible photo-assisted electrolysis of water was first reported by Yeh and Hackerman<sup>(64)</sup>. The potential use of flame oxidised iron for the study of photoelectrochemical behaviour has provoked a great deal of interest due to its favourable collection of properties. These were:-

- 1) The electrodes were easily made.
- 2) The wavelength response was that of a semi-conductor with an energy band gap of 2.1 eV, enabling utilisation of radiation in the visible region<sup>(65)</sup>.
- 3) The material exhibited interesting transient behaviour under illumination<sup>(64)</sup>.

These properties have led to investigations into various forms of production of  $Fe_2O_3$  electrodes for study e.g. solid state sintering<sup>(61-63)</sup>, chemical vapour deposition<sup>(72,73)</sup>, anodizing<sup>(65)</sup> and the passive layer on an iron electrode<sup>(91)</sup>. These studies have added to the knowledge of the photoelectrochemistry



of  $\text{Fe}_2\text{O}_3$  but the difficulty in consistent electrode preparation ruled against them for the purposes of this study.

An interesting use of a flame oxidised Iron photo anode was proposed by P.G.P. Ang and A.F. Sammells<sup>(67)</sup>. They have made a photoelectrochemical solar cell using a flame oxidised iron photo anode and a fuel cell oxygen cathode (platinised porous nickel). This iron oxide/oxygen photovoltaic cell had an open circuit voltage of up to 400 mV and a short circuit current density of up to  $1\text{ma}/\text{cm}^2$  under illumination of a 150 watt Xenon light source. Such devices present an interesting route for the exploitation of photoelectrochemical devices.

Various attempts have been made to increase the photo efficiency of photo anodes based on iron oxide semi-conductors. Sammells and Ang<sup>(68)</sup> found that incorporating platinum into a flame oxidised electrode by sputtering platinum on to such an electrode then reheating. This electrode showed a higher photo current than a normal flame oxidised iron electrode under the same illumination, above -40mV from the  $\text{Hg}/\text{HgO}$  reference electrode. They also showed that additions of Hydrogen Peroxide also increased the photo current efficiency. Liou, Yong and Levine have developed a heterojunction electrode of chemically

vapour deposited titanium dioxide on thermally oxidised iron<sup>(69)</sup>. This has shown that the relatively large flat band potential of titanium dioxide and the spectral threshold of iron oxide can be combined to provide a useful photoelectrochemical device. Candeu has investigated the use of thermally oxidized iron/nickel alloys as photo anodes<sup>(92)</sup>. He found that a 44% nickel, 56% iron alloy suitably fabricated into an electrode, gave an increased photo current efficiency and potential necessary for the onset of the photo current was apparently moved more cathodic than iron oxide. Kennedy, Anderman and Shinar have prepared various iron oxide photo anodes doped with differing levels of group IVA elements<sup>(71)</sup>. They have shown the photo current onset voltage, the spectral response and photo current efficiency of a material can be altered by doping to varying levels with different dopants.

While work is in its early stages, iron oxide photo anodes appear to have an important place in the future development of photoelectrochemical devices. The subtle alteration of its basic semi-conducting properties possibly will result in a cheap, efficient photo electrode material being available in the future.

#### 4.2 The structure of thermally oxidised iron

Before moving on to the experimental work and the discussion of the results of that work, it would be worthwhile considering the structure and form of flame oxidized iron.

The physical properties and the crystal structure of thermally formed iron oxide have been reported in detail by a number of authors<sup>(93-97)</sup>. At temperatures up to about 570°C the high temperature oxidation of iron leads to the formation of a 2 layer scale of  $\text{Fe}_3\text{O}_4$  and  $\text{Fe}_2\text{O}_3$ . A three layer scale of  $\text{FeO}$ ,  $\text{Fe}_3\text{O}_4$  and  $\alpha\text{-Fe}_2\text{O}_3$  is formed at higher temperatures. This three layer oxide film of mainly  $\text{FeO}$  and  $\text{Fe}_3\text{O}_4$  with an outer layer of  $\alpha\text{-Fe}_2\text{O}_3$ . This outer layer is only about 1-5% of the oxide film thickness<sup>(66)</sup>. The two inner layers have a metal like conductivity<sup>(98)</sup> so the semi-conducting properties of the iron oxide are due only to the non-stoichiometry of the  $\alpha\text{-Fe}_2\text{O}_3$  layer. The oxide film is structurally highly disordered and may be described as glassy with short range crystalline order. The mean diameter of the crystal grains is approximately 1-2nm<sup>(66)</sup>. X-ray studies have indicated that the electrodes studied are of the 3 layered variety. This will be covered in more detail later.

It would appear that this layer structure is the cause of the non-rectifying ohmic contact between the current carrier (the original piece of iron) and the semi-conductors (the  $\alpha$   $\text{Fe}_2\text{O}_3$  layer). The ease of formation of this contact - inherent in the fabrication of the electrode is one of the advantages of using flame oxidised iron as a photo electrode.

#### 4.3 Electrode Preparation

A 1cm square piece of 1mm thick 99.999% pure iron sheet (Koch Light Ltd.) was spot welded on to a nickel wire. The face of the electrode was abraded with emery paper to remove the oxides formed by spot welding, degreased in acetone, rinsed in distilled water, etched in concentrated sulphuric acid until hydrogen evolution was evident then rinsed again in distilled water then acetone and dried. The electrode was then heated in a Fisher burner for between 1 and 15 minutes. This timing was from when the electrode reached red heat. The electrodes were then allowed to cool in air. After cooling, the electrodes were inspected, and were normally found to have a smooth even layer of grey oxide. Any electrodes with apparent cracks or irregularities were not used. However, the oxide layer was easily removed so the pieces could be used again. The nickel wire and the face of the electrode to which it was attached were covered in Silicone Rubber leaving only one face of the electrode

exposed to the electrolyte. This was to ensure that only flame oxidised iron was exposed to the solution and hence the electrochemical properties measured were that of only flame oxidised iron.

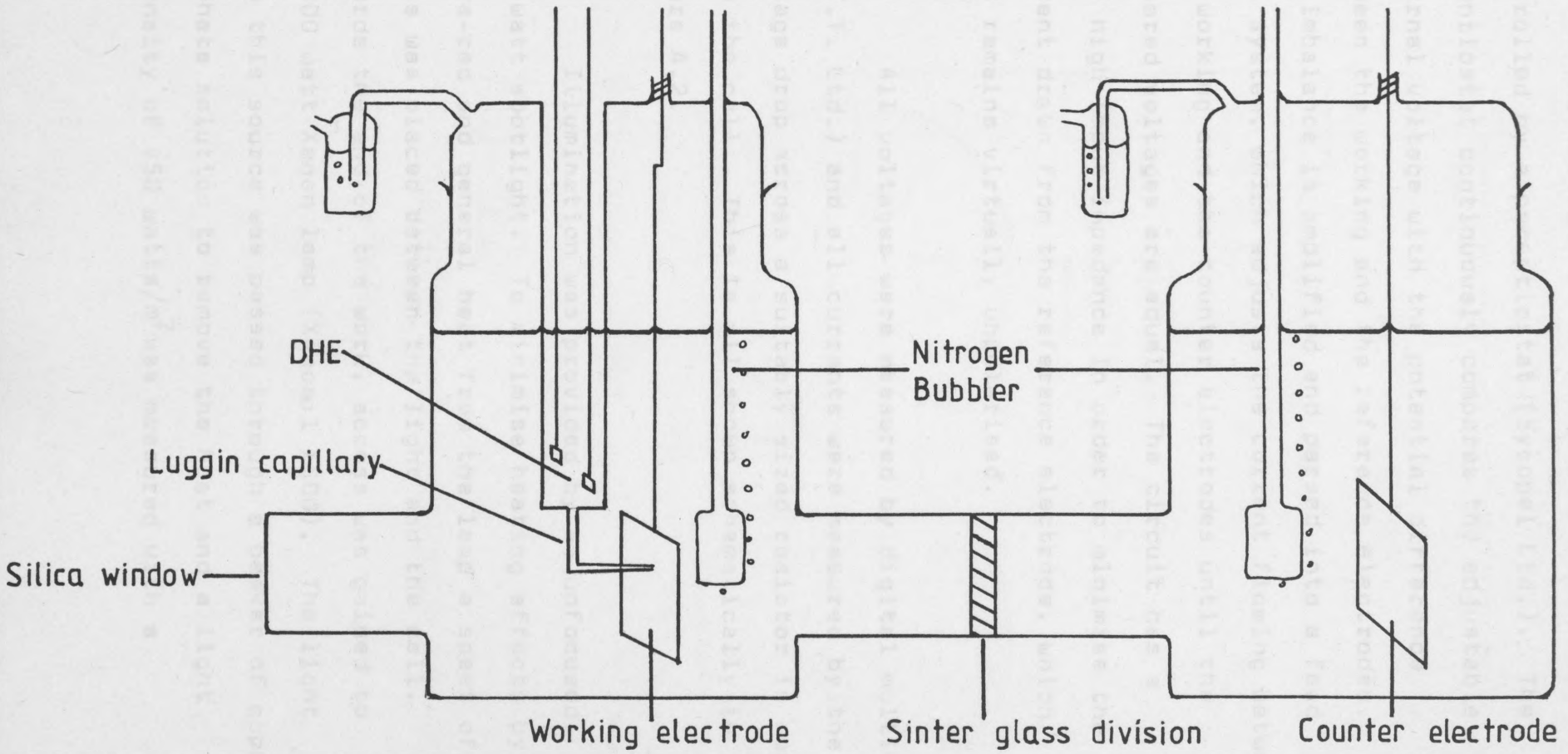
#### 4.4 Electrochemical experimental set up

All experiments were carried out in a specially made glass cell. This consisted of 2 compartments joined by a sintered glass disk. The compartment containing the working electrode had a silica window (to enable U.V. light to pass through) and an assembly to hold the working electrode near the Luggin capillary and contain the reference electrode (a dynamic hydrogen electrode or D.H.E.). The other compartment contained the counter electrode - a piece of platinum gauze<sup>Z</sup>. The working electrode was separated from the counter electrode to prevent any reaction products such as hydrogen interfering with the working electrode's electrochemical reactions.

The electrolyte used was 5M potassium hydroxide and this was de-aired in both compartments by a stream of white spot nitrogen. The cell is shown in Figure 4.1.

Fig 4.1

Diagram of an experimental cell.



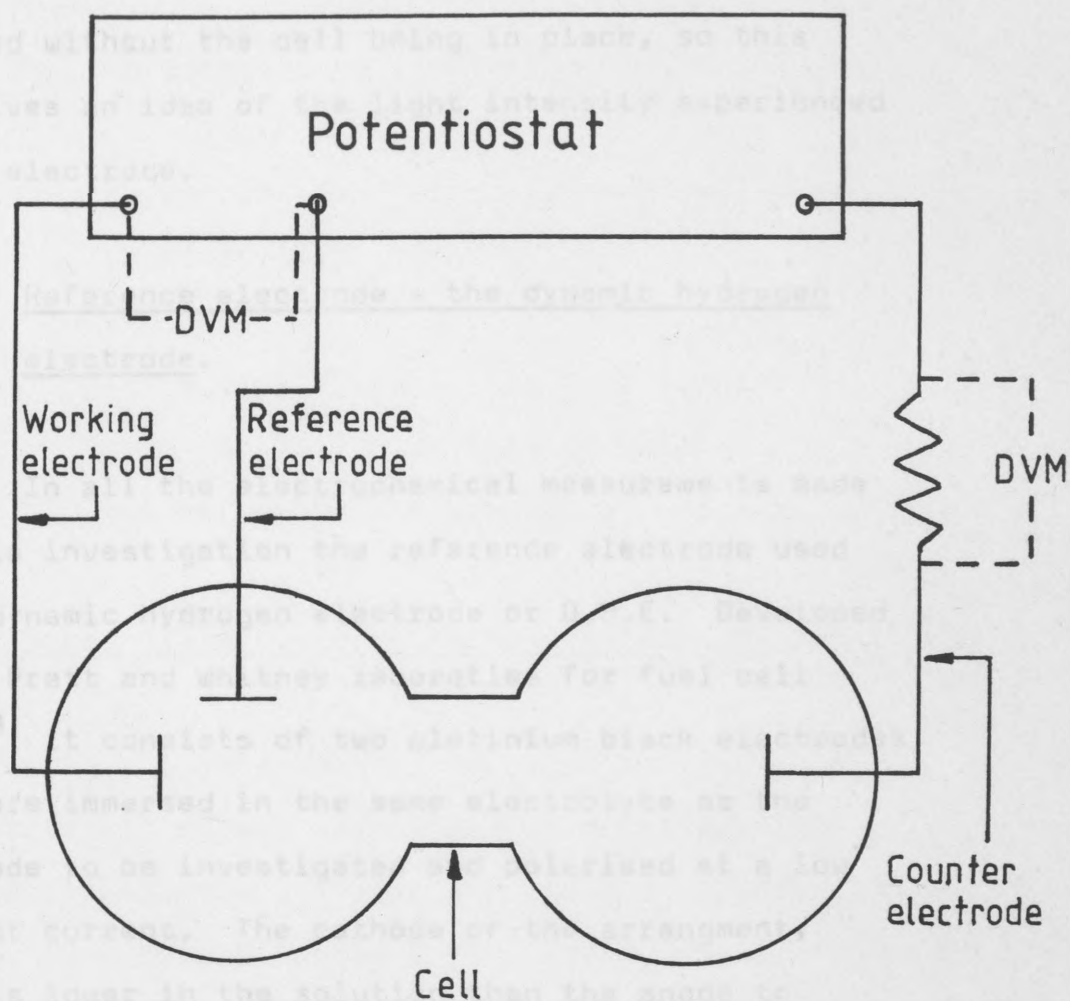
**Fig 4.1**

Diagram of an experimental cell.

The voltage of the working electrode was controlled by a potentiostat (Sycopel Ltd.). The potentiostat continuously compares the adjustable internal voltage with the potential difference between the working and the reference electrodes. Any imbalance is amplified and passed into a feedback system, which adjusts the current flowing between the working and the counter electrodes until the compared voltages are equal. The circuit has a very high input impedance in order to minimise the current drawn from the reference electrode, which thus remains virtually unpolarised.

All voltages were measured by digital multimeter (I.T.T. Ltd.) and all currents were measured by the voltage drop across a suitably sized resistor in series with the cell. This is all shown schematically in Figure 4.2.

Illumination was provided by an unfocused 150 watt spotlight. To minimise heating effects by infra-red and general heat from the lamp a sheet of glass was placed between the light and the cell. Towards the end of the work, access was gained to a 1600 watt Xenon lamp (Xenosol 1600). The light from this source was passed through a beaker of copper sulphate solution to remove the heat and a light intensity of  $450 \text{ watts/m}^2$  was measured with a



DVM - Digital Voltmeter

**Fig 4.2**

Schematic circuit diagram for potentiostatic measurements



photometer (Macam R101) at the distance from the light the working electrode was positioned. This had to be measured without the cell being in place, so this only gives an idea of the light intensity experienced by the electrode.

#### 4.5 Reference electrode - the dynamic hydrogen electrode.

In all the electrochemical measurements made for this investigation the reference electrode used was a dynamic hydrogen electrode or D.H.E. Developed in the Pratt and Whitney laboratories for fuel cell work<sup>(99)</sup> it consists of two platinum black electrodes which are immersed in the same electrolyte as the electrode to be investigated and polarised at a low constant current. The cathode of the arrangement, which is lower in the solution than the anode to prevent gaseous contamination, evolves hydrogen and maintains a steady voltage about 20-30mV cathodic of the Standard Hydrogen electrode potential. It is this electrode which is used as the reference electrode.

The D.H.E. has the following advantages:-

- 1) It is a easily used and mechanically simple electrode.

- 2) There is no introduction of impurities such as mercury or chloride ions.
- 3) No temperature limitation.
- 4) No pH differential due to salt bridges or diaphragms.
- 5) It is very suitable for fast transient work due to low resistance between the reference and working electrodes.

#### 4.6 Steady State Electrochemical Performance

Using the experimental set up outlined in 4.4 steady state  $V/i$  curves were measured under varying states of illumination. These are shown in Figure 4.3 and 4.4. It should be noted that a steady state dark anodic current is not achieved until about +1250mV vs D.H.E. whereas under illumination the steady state anodic photo current is achieved at about +500 mV vs D.H.E. However this voltage means that flame oxidised iron cannot be used by itself as a photo anode for the electrochemical photolysis of water as it is more anodic than the hydrogen evolution potential of any typical cathode material. However, it could be used in conjunction with a suitable p-semi-conducting electrode under illumination, as they

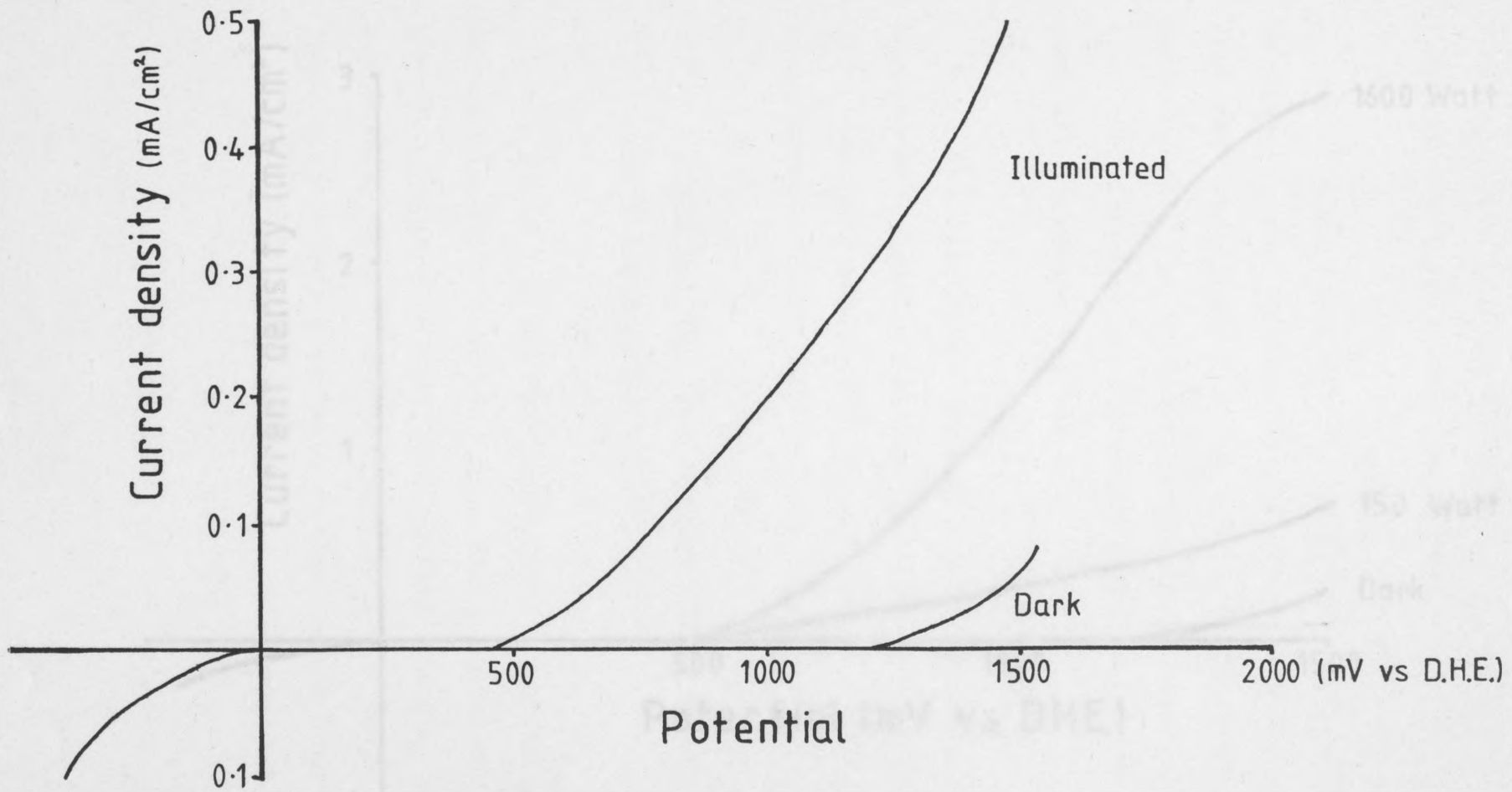


Fig 4.3

Voltage/current curve for a Flame Oxidised Iron electrode in 5M KOH with and without illumination with a 150 watt spotlight.

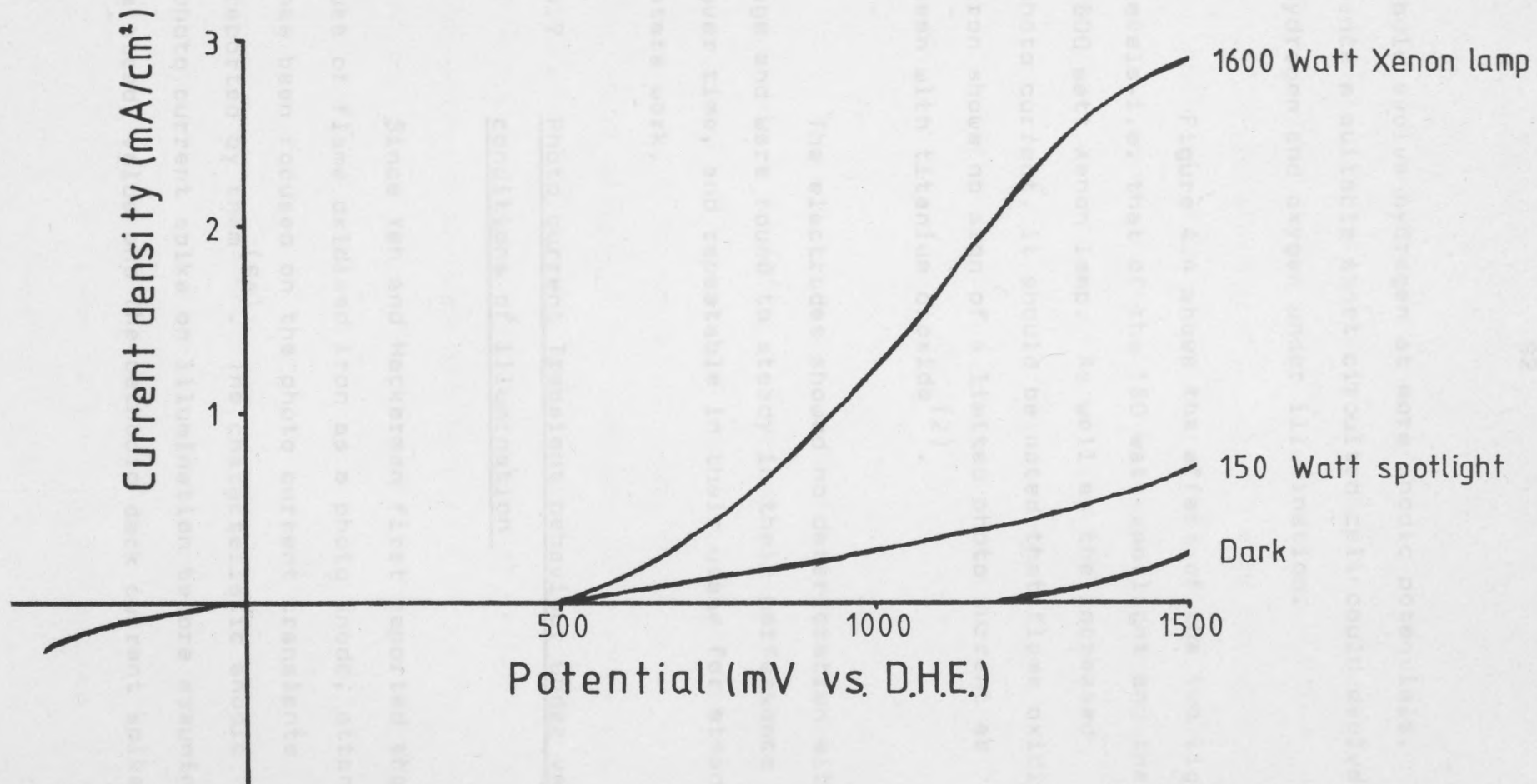


Fig. 4.4

Voltage/current curves for a flame oxidised Iron electrode in 5M KOH electrolyte under varying levels of illumination.

could evolve hydrogen at more anodic potentials, hence a suitable short circuited cell could evolve hydrogen and oxygen under illumination.

Figure 4.4 shows the effect of the two light levels-i.e. that of the 150 watt spotlight and the 1600 watt Xenon lamp. As well as the increased photo current, it should be noted that flame oxidised iron shows no sign of a limited photo current as seen with titanium dioxide<sup>(2)</sup>.

The electrodes showed no deterioration with age and were found to steady in their performance over time, and repeatable in their usage for steady state work.

#### 4.7 Photo current Transient behaviour under varying conditions of illumination

Since Yeh and Hackerman first reported the use of flame oxidised iron as a photo anode, attention has been focused on the photo current transients reported by them<sup>(64)</sup>. The characteristic anodic photo current spike on illumination before assuming a steady value and the cathodic dark current spike

1) It is due to the bulk properties of the semi-conductor.

2) It is due to the creation and destruction of a reaction intermediate.

before the resumption of the low level dark current on removal of illumination has been reported by several authors (63-65,70,73). If this behaviour could be explained then it may give an insight into the photo-assisted evolution of oxygen and could indicate which direction is necessary to increase the photo efficiency of this material.

The photo current transients were produced as follows:-

The electrode was mounted in the cell described previously and held at a fixed voltage using the potentiostat. The electrode was then illuminated for a period of time, the light being interrupted by an electrical switch on the spotlight or a shutter with the Xenosol 1600. The resultant photo current and dark current transients were recorded as the voltage drop across a suitable resistor on a x-y-t recorder (Bryans 2900 A4) in the x-t mode. A typical transient is shown in Figure 4.5.

The explanation of the transients can be considered to come from one of two areas. These are:-

- 1) It is due to the bulk properties of the semi-conductor.
- 2) It is due to the creation and destruction of a reaction intermediate.

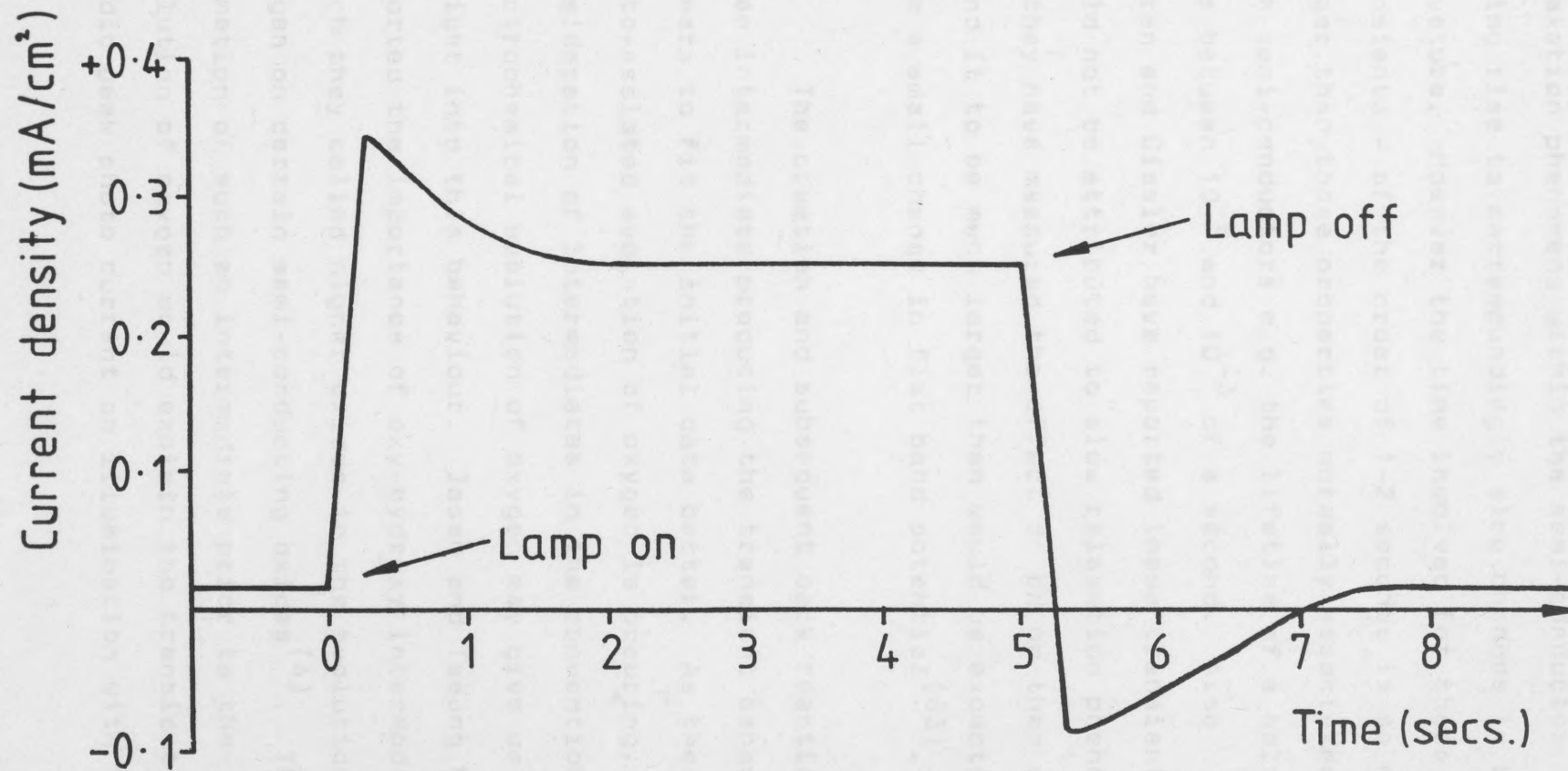


**Fig 4.5**

Current transients of a flame oxidised Iron electrode under illumination.  
(Held at +800 mV vs. DHE, 5M KOH electrolyte.)

The first area of consideration could give rise to an explanation based on a relatively slow relaxation phenomena within the semi-conductor giving rise to correspondingly slow changes in band curvature. However the time involved for these transients - of the order of 1-2 seconds is so much larger than those properties normally associated with semi-conductors e.g. the lifetime of a hole lies between  $10^{-9}$  and  $10^{-3}$  of a second. Also Curran and Gissler have reported these transients could not be attributed to slow relaxation phenomena as they have measured the effect of pH on them and found it to be much larger than would be expected from a small change in flat band potential<sup>(63)</sup>.

The creation and subsequent back reaction of an intermediate producing the transient behaviour appears to fit the initial data better. As the photo-assisted evolution of oxygen is occurring, consideration of intermediates in the conventional electrochemical evolution of oxygen may give us an insight into this behaviour. Jasem and Tseung have reported the importance of oxy-hydroxy intermediates which they called higher oxides in the evolution of oxygen on certain semi-conducting oxides<sup>(4)</sup>. The formation of such an intermediate prior to the evolution of oxygen would explain the transient anodic peak photo current on illumination with the



subsequent reduction of such an intermediate giving rise to the transient dark cathodic current peak when the illumination ceases. This explanation is favoured by Curran and Gissler who supported it with evidence of charge transfer to a monolayer of an intermediate species<sup>(63)</sup>. It was also favoured by Hardee and Bard<sup>(73)</sup>. However the premise of an intermediate and its nature have never been fully developed.

It was on this basis that several pieces of experimental work were carried out to ascertain if the transient behaviour was due to an oxy-hydroxy intermediate.

The investigation first centered on the production of cyclic voltammograms of flame oxidised iron with and without illumination. The use of linear sweep voltammetry is well established in the study of electrochemical reactions<sup>(100)</sup>.

In <sup>✓</sup> Voltammetry the potential of the working electrode is continuously changed linearly with time. The resultant current potential plot (voltammogram) consists of a series of current maxima whose magnitude and associated potential are characteristic of the electrode process. These maxima are caused

by mass transfer constraints on an increasing current leading to depletion and hence a maxima. The voltammograms were obtained by using a linear sweep generator (Chemical Electronics) in conjunction with the potentiostat and the cell. They were plotted using a x-y-t pen recorder (Bryans Model 29000 A4) in the x-y mode. This is shown diagrammatically in Figure 4.6.

The resultant voltammograms can be seen in Figure 4.7. They show the characteristic peak for an oxy-hydroxy intermediate at  $+600 \rightarrow 700$ mv vs the D.H.E. under illumination and at  $+1450 \rightarrow 1550$ mv vs the D.H.E. without illumination. The nature of the peak at about  $+900$  mv vs the D.H.E. is not known. However, it is common to the dark and light curves.

If the premise about the oxy-hydroxy intermediates is correct then if the transient photo current is observed at potentials where it is already formed, then the characteristic peaks will not be seen. As the cyclic voltammograms tell us that this potential is about  $+1450 \rightarrow 1550$  mv vs the D.H.E. this can be done. As Figure 4.8 shows this is the case.

As the formation of any oxy-hydroxy

Schematic circuit for cyclic voltammetry.

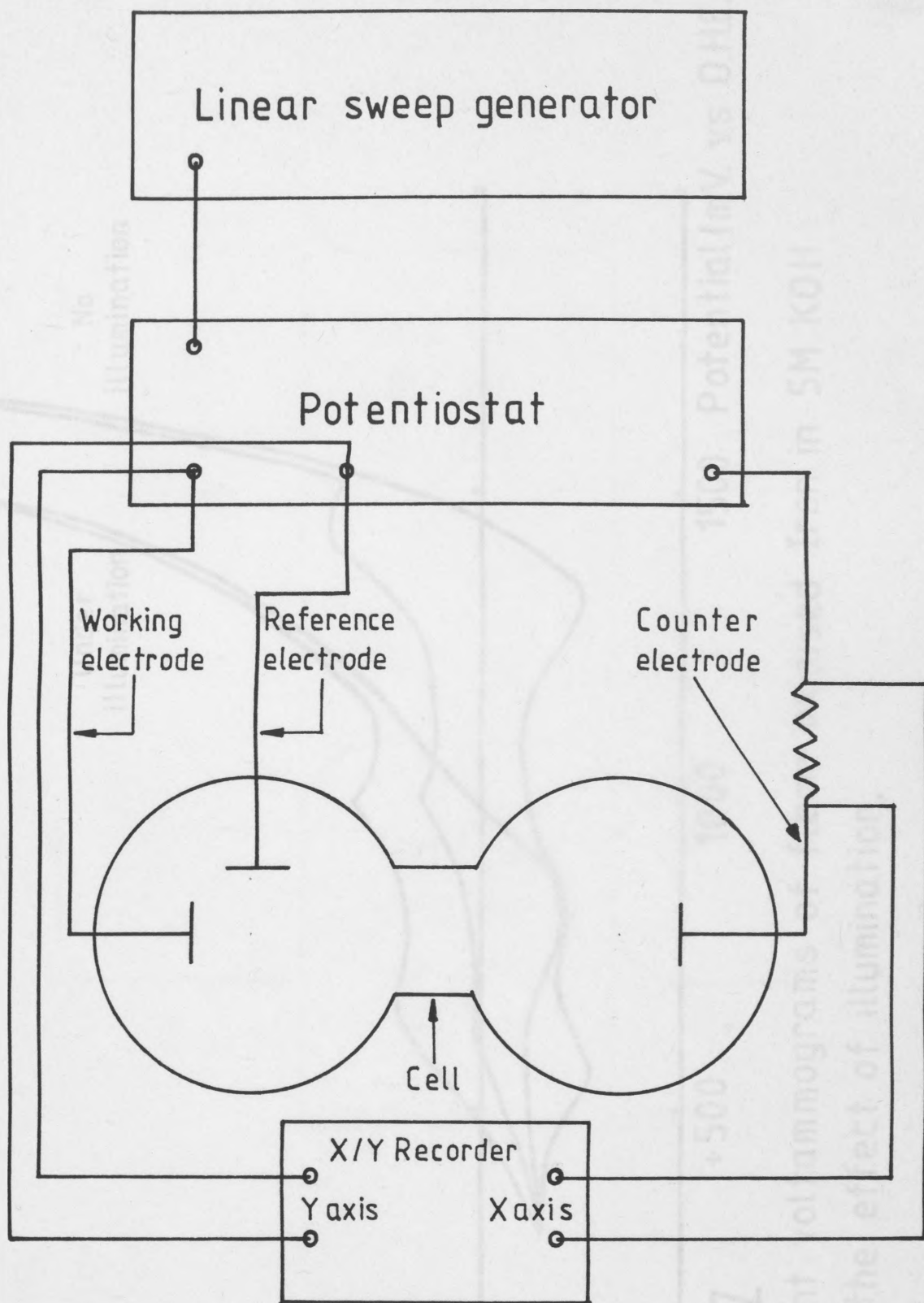
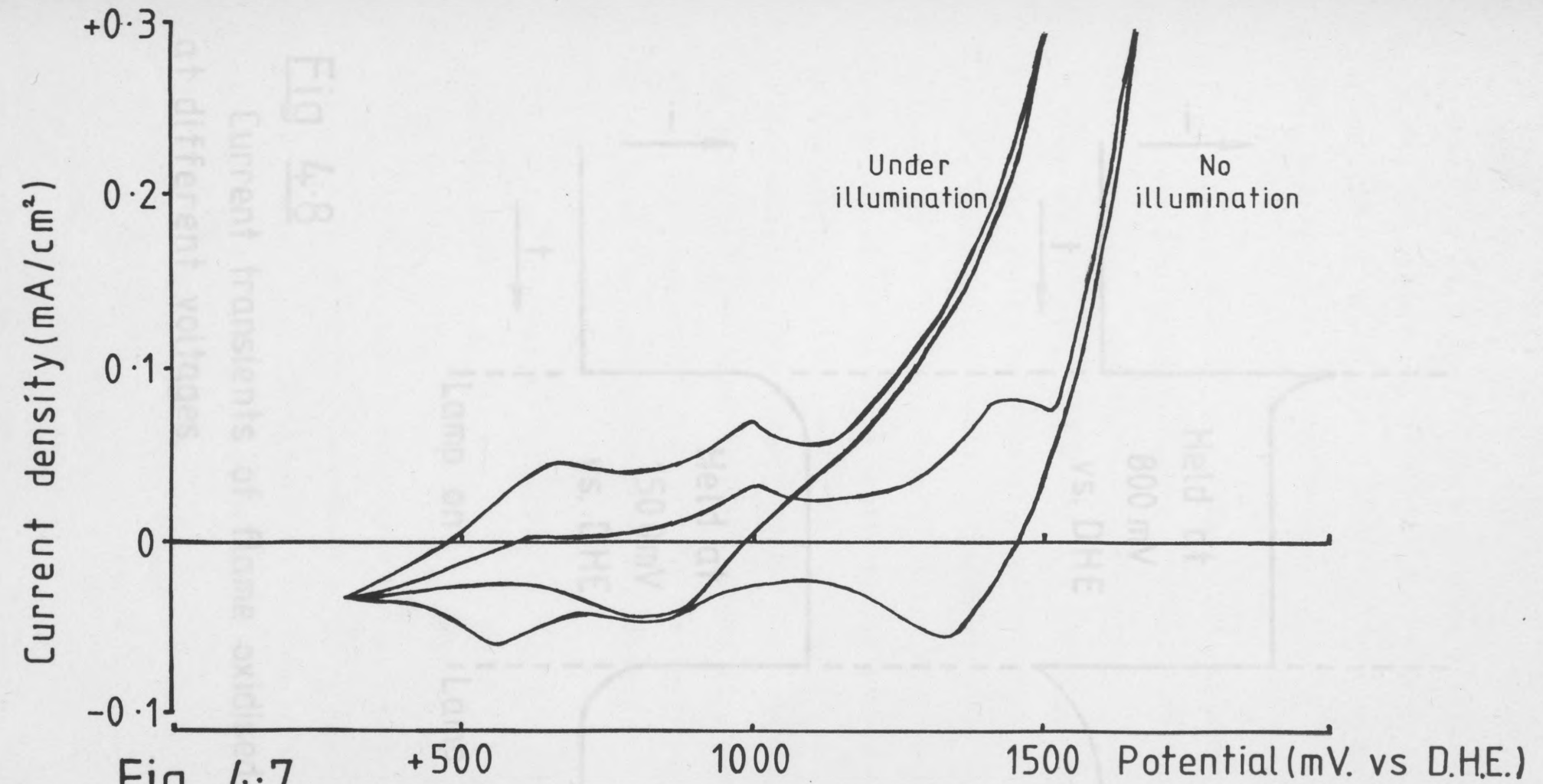


**Fig 4.6**

Schematic circuit for cyclic voltammetry.



Current voltammograms of flame oxidised Iron in 5M KOH showing the effect of illumination.

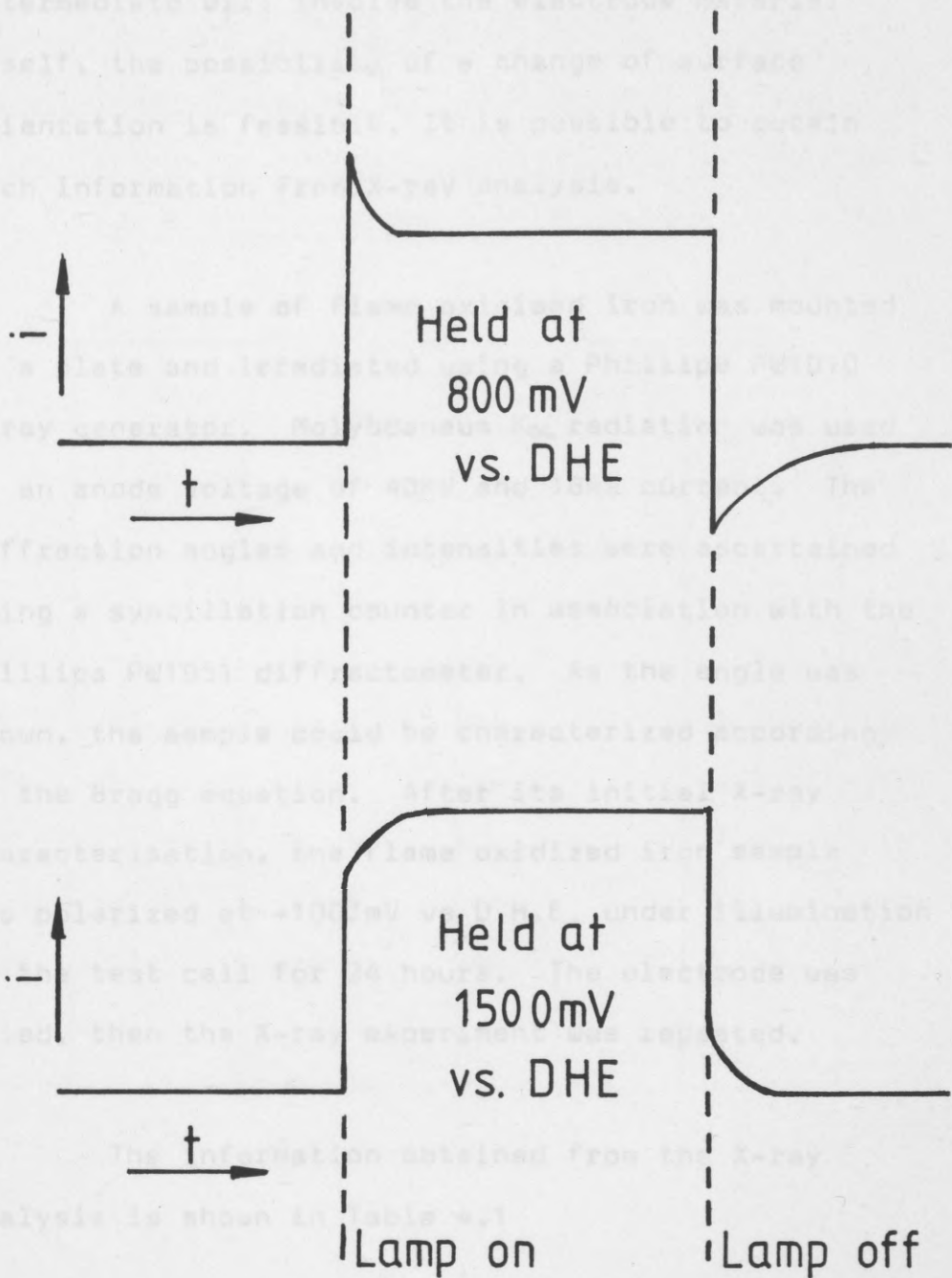


**Fig 4.8**

Current transients of flame oxidised Iron at different voltages.

intermediate will involve the electrode material itself, the possibility of a change of surface orientation is feasible. It is possible to obtain such information from X-ray analysis.

A sample of flame oxidised iron was mounted on a plate and irradiated using a Phillips PW1010 X-ray generator. Molybdenum  $K\alpha$  radiation was used at an anode voltage of 40KV and 16ma current. The diffraction angles and intensities were ascertained using a syntillation counter in association with the Phillips PW1051 diffractometer. As the angle was known, the sample could be characterized according to the Bragg equation. After its initial X-ray characterisation, the flame oxidized iron sample was polarized at +1000mV vs D.H.E. under illumination in the test cell for 24 hours. The electrode was dried, then the X-ray experiment was repeated.

The information obtained from the X-ray analysis is shown in Table 4.1

Although these results are not conclusive and are clouded by the limitations of the method (this is not a true picture of the surface as there is penetration to the substrate by the X-rays), they do indicate two things:-

TABLE 4.1

Intensities of various lattice spacings of flame oxidised iron before and after polarization at +1000mv vs D.H.E. in 5MKOH for 24 hours

d Å	I/I <sub>0</sub> new	I/I <sub>0</sub> after 24 hours	Assignment		
			Compound	dÅ	hk1
2.97	17.0	11.5	Fe <sub>3</sub> O <sub>4</sub>	2.97	220
2.70	13.8	32.3	*Fe <sub>2</sub> O <sub>3</sub>	2.69	104
2.534	100	100	Fe <sub>3</sub> O <sub>4</sub>	2.530	311
2.169	38.6	34.6	*Fe <sub>2</sub> O <sub>3</sub>	2.20	113
2.155	92.8	73.8	FeO	2.153	200
2.099	23.1	92.3	Fe <sub>3</sub> O <sub>4</sub>	2.097	400

- 1) A change has occurred.
- 2) This change appears to be in the direction of a higher iron valence state i.e. a Fe O line has decreased and a  $\text{Fe}_3\text{O}_4$  line and a  $\alpha\text{-Fe}_2\text{O}_3$  line have increased.

So the evidence of the cyclic voltammograms, the high potential photo current transients and the X-ray analysis confirm the theory that the photo current transients are caused by the formation and back reaction of an oxy-hydroxy intermediate.

#### 4.8 Discussion of the oxy-hydroxy intermediate model

Now to the oxy-hydroxy intermediate model has been established, it is worth considering how it can be used in explaining its photoelectrochemical behaviour. This can be considered in two parts:-

- 1) Its application in explaining certain aspects of the results obtained with the photo current transients on flame oxidised iron.
- 2) A review of the literature with reference to reaction intermediates in photoelectrochemical reactions.

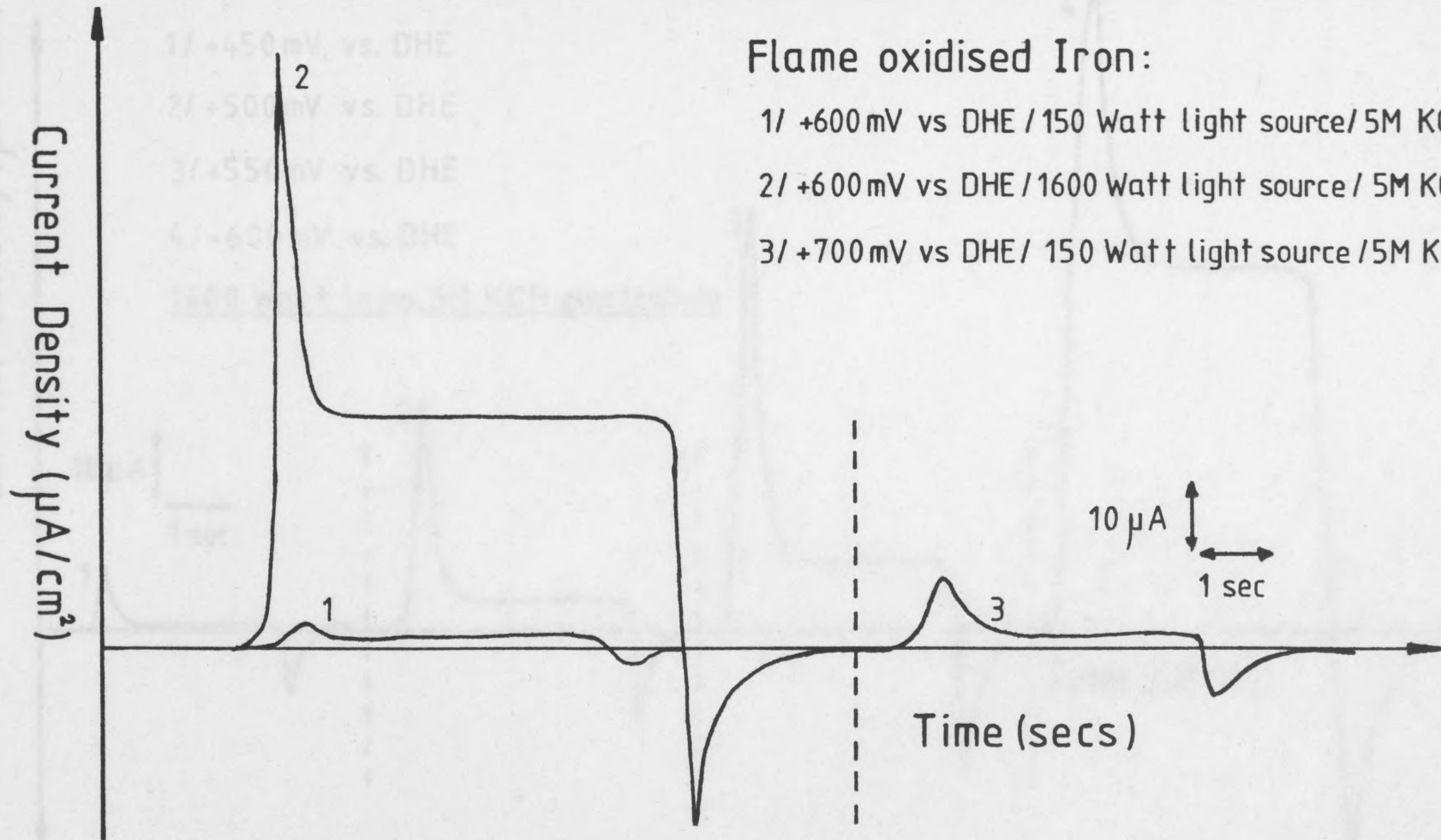


First the effect of increased levels of illumination can be considered. As the model says that the electrode undergoes the photoelectrochemical reaction of formation of the intermediate and results have shown that an increase in light level will give a higher photoelectrochemical reaction rate resulting in an increase in the photo current. If a comparison is made of the transients recorded at the same voltage for 150 watt and 1600 watt illumination, this can be seen to be the case. This is shown in Figure 4.9. The increase in light level has caused a large increase in the magnitude of the photo current spike. If the model holds true then as the voltage at which the transient has been recorded increases anodically the photo electrochemical reaction rate should increase. This would result in an increase in the anodic photo current spike. This can be seen to be so in Figure 4.10. Figure 4.10 also shows that transient peaks are present at +450 mV vs the D.H.E. where no steady state photo current occurs. Figure 4.10 also shows that the ratio of peak photo current to steady state photo current decreases with increasing anodic voltage. This would suggest that as the photo electrochemical reaction rate of the production of the intermediate is increased and, as the intermediate is limited in its reaction to the total

Current Density ( $\mu\text{A}/\text{cm}^2$ )

Fig. 4.9

Comparison of photocurrent transients under various levels of illumination



### Flame oxidised Iron:

- 1/ +600 mV vs DHE / 150 Watt light source / 5M KOH electrolyte
- 2/ +600 mV vs DHE / 1600 Watt light source / 5M KOH electrolyte
- 3/ +700 mV vs DHE / 150 Watt light source / 5M KOH electrolyte

**Fig 4.9**

Comparison of photocurrent transients under various levels of illumination.

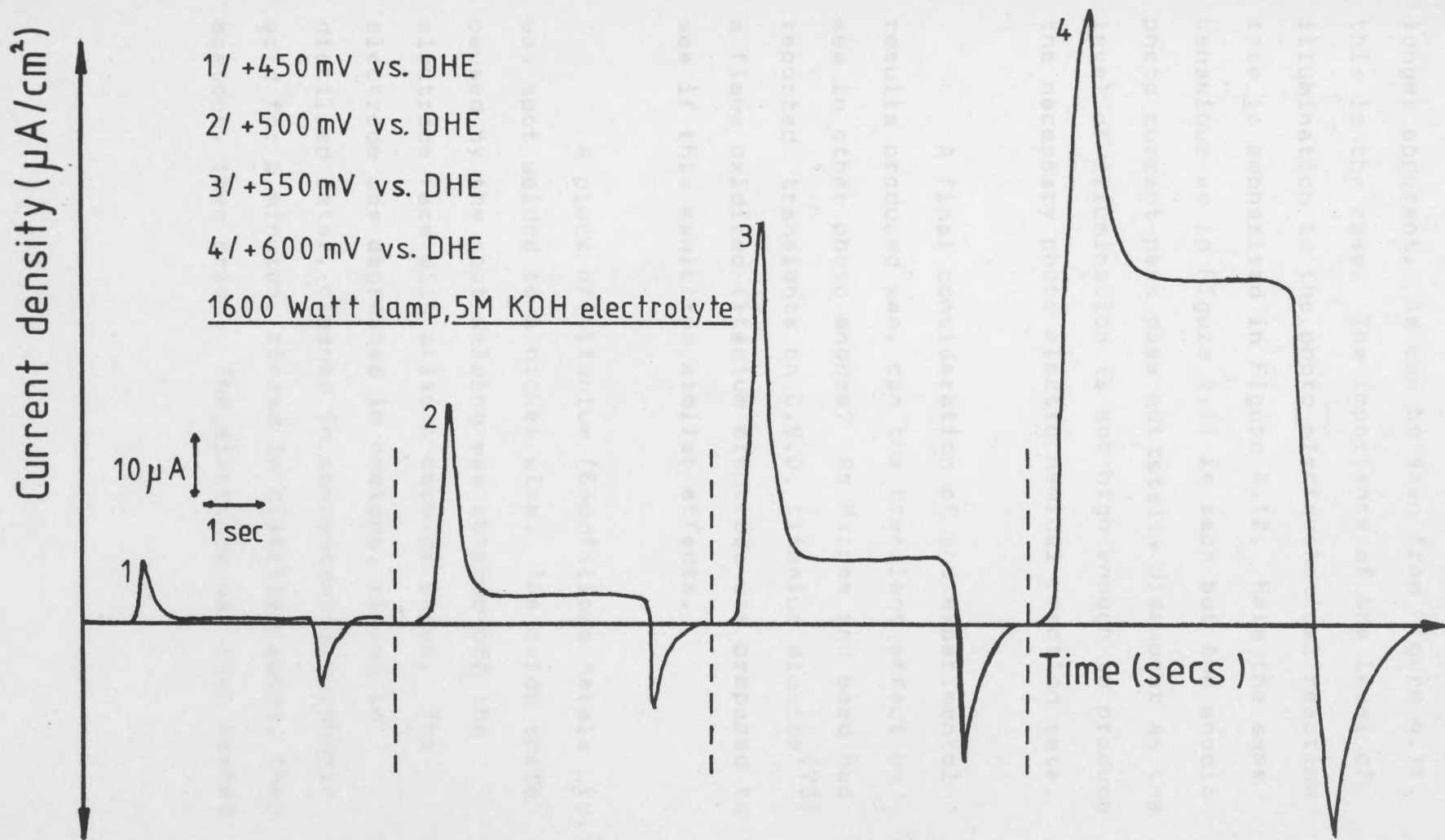


**Fig 4-10**

Effect of voltage on flame oxidised Iron photocurrent transients.

conversion of the electrode surface, then the anodic photo current peak should diminish until it was no longer apparent. As can be seen from Figure 4.11, this is the case. The importance of the level of illumination to the photoelectrochemical reaction rate is emphasised in Figure 4.12. Here the same behaviour as in Figure 4.11 is seen but the anodic photo current peak does not totally disappear as the level of illumination is not high enough to produce the necessary photo electrochemical reaction rate.

A final consideration of the experimental results produced was, can the transient effect be seen in other photo anodes? As Hardee and Bard had reported transients on C.V.D. titanium dioxide<sup>(73)</sup> a flame oxidized titanium electrode was prepared to see if this exhibited similar effects.

A piece of titanium (Goodfellows Metals Ltd.) was spot welded to a nickel wire. The oxide scale caused by the spot welding was abraded off the electrode face with silicon carbide paper. The electrode was degreased in acetone, rinsed in distilled water, cleaned in concentrated sulphuric acid for 5 minutes, rinsed in distilled water, then acetone, then dried. The electrode was then heated

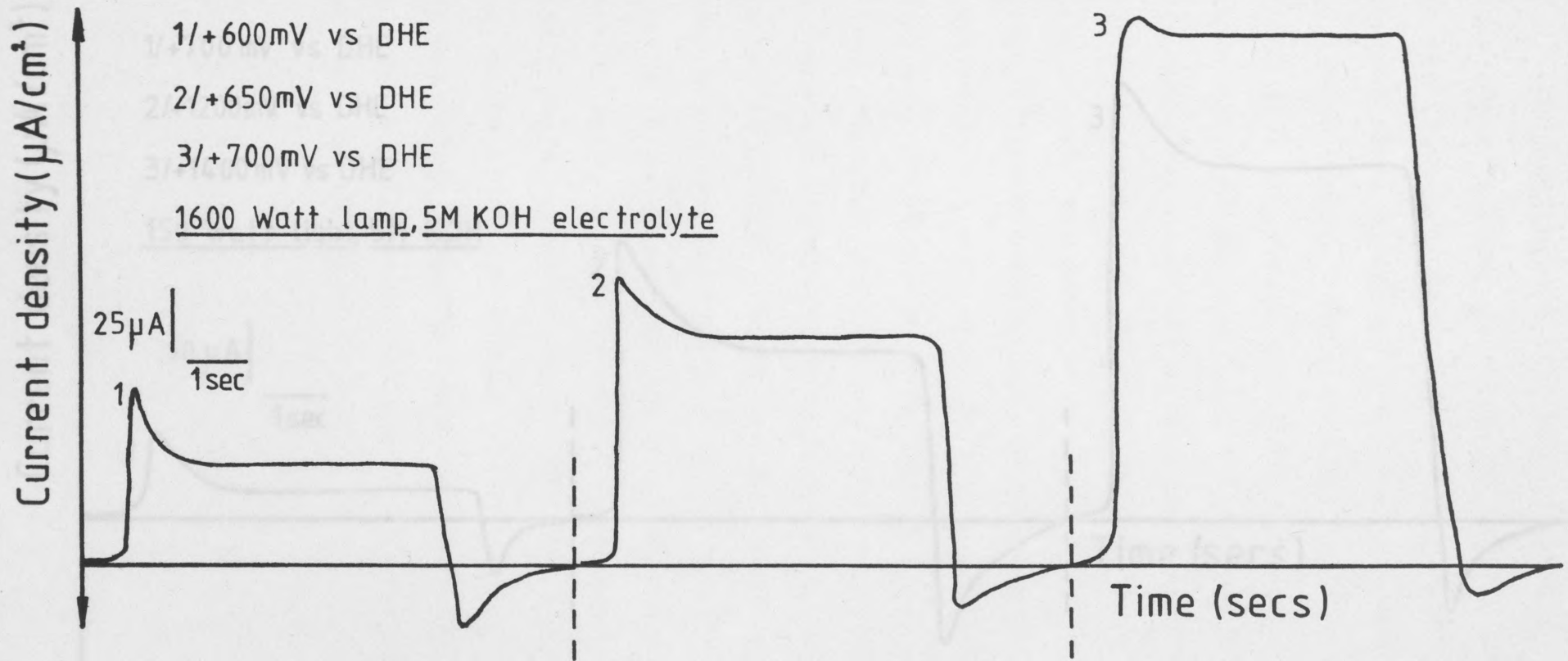


Fig 4.11

Effect of voltage on flame oxidised Iron photocurrent transients at high illumination levels.

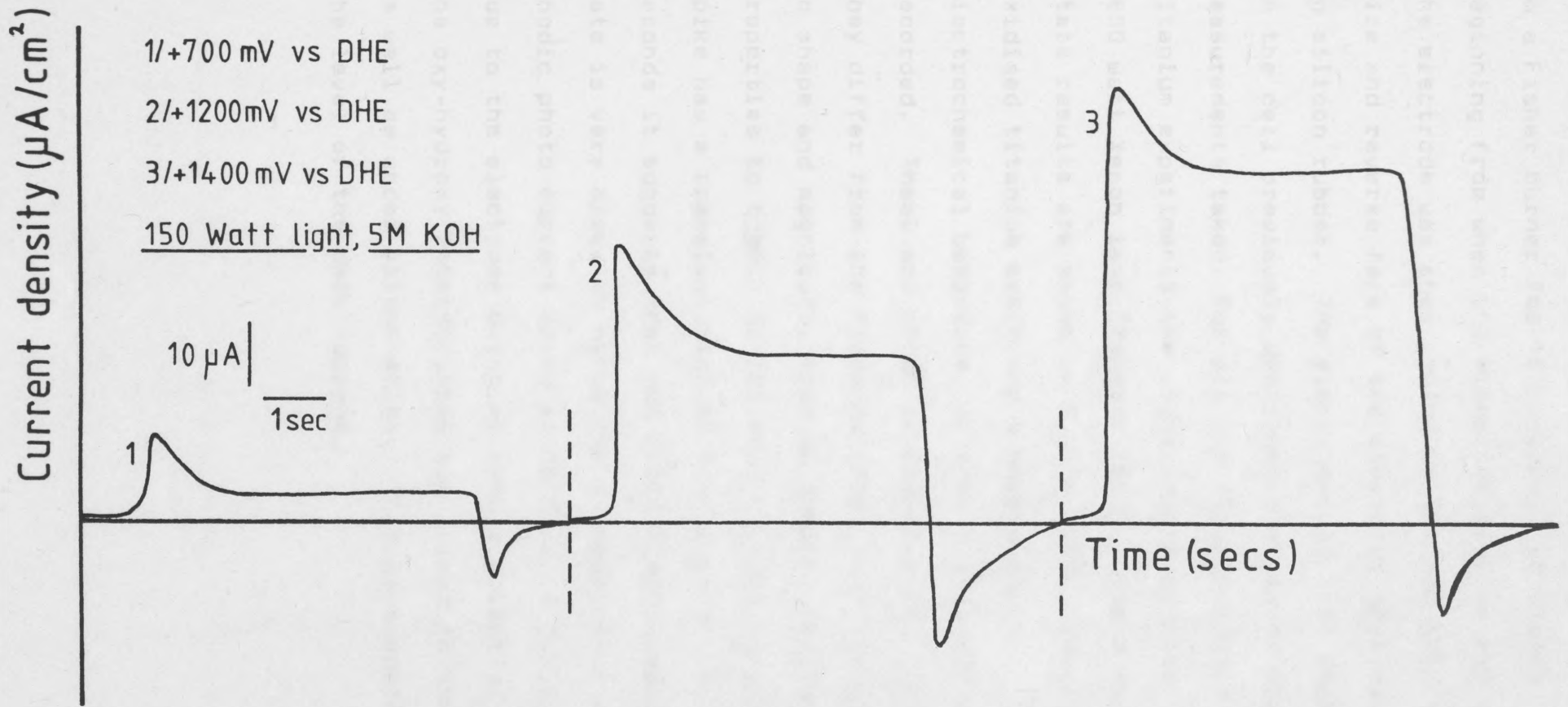
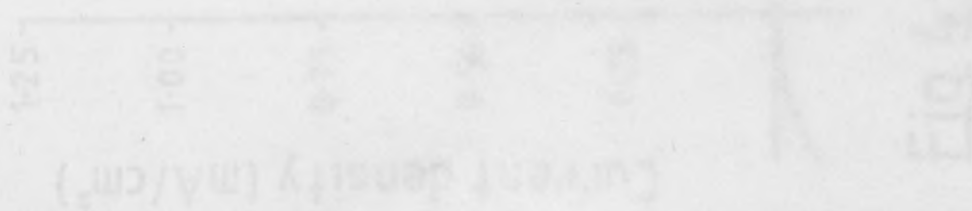
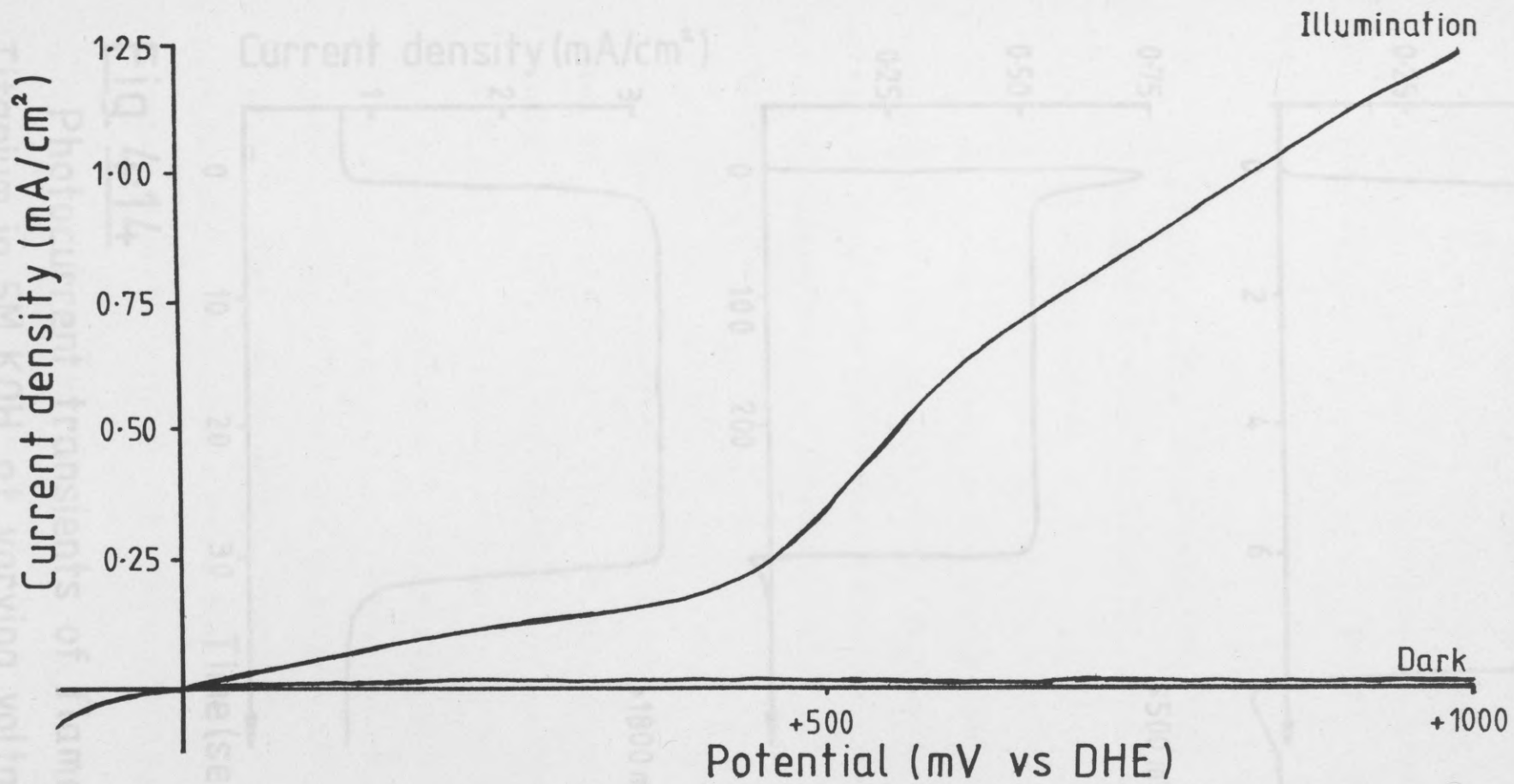


Fig 4-12

Effect of voltage on flame oxidised Iron photocurrent transients at reduced illumination levels.

in a Fisher burner for 15 minutes, the timing beginning from when the electrode reached red heat. The electrode was then cooled in air and then the wire and reverse face of the electrode were sealed in silicon rubber. The electrode was then mounted in the cell previously described and steady state measurements taken. For all the flame oxidized titanium experiments the light source was the 1600 watt Xenon lamp (Xenosol 1600). These steady state results are shown in Figure 4.13. The flame oxidised titanium exhibited a marked photo electrochemical behaviour, so some transients were recorded. These are shown in Figure 4.14. Although they differ from the flame oxidized iron transients in shape and magnitude, they do exhibit similar properties to them. As the anodic photo current spike has a transient time of the order of 25 seconds it suggests that the photo electrochemical rate is very slow, so hence the disappearance of the anodic photo current spike at 1800 mv vs D.H.E. is due to the electrode being at such a potential that the oxy-hydroxy intermediates are formed in the dark as well as under illumination. This is supported by the level of the dark current.





**Fig. 4.13**

Voltage/current curves for flame oxidised Titanium in 5MKOH under illumination by a 1600 Watt Xenon lamp and under darkness.



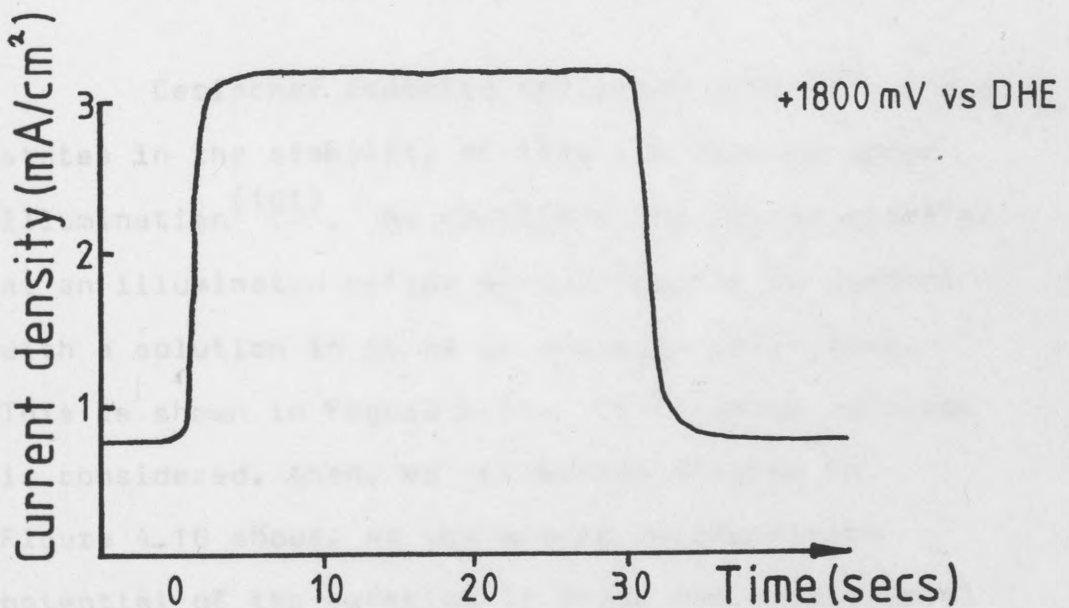
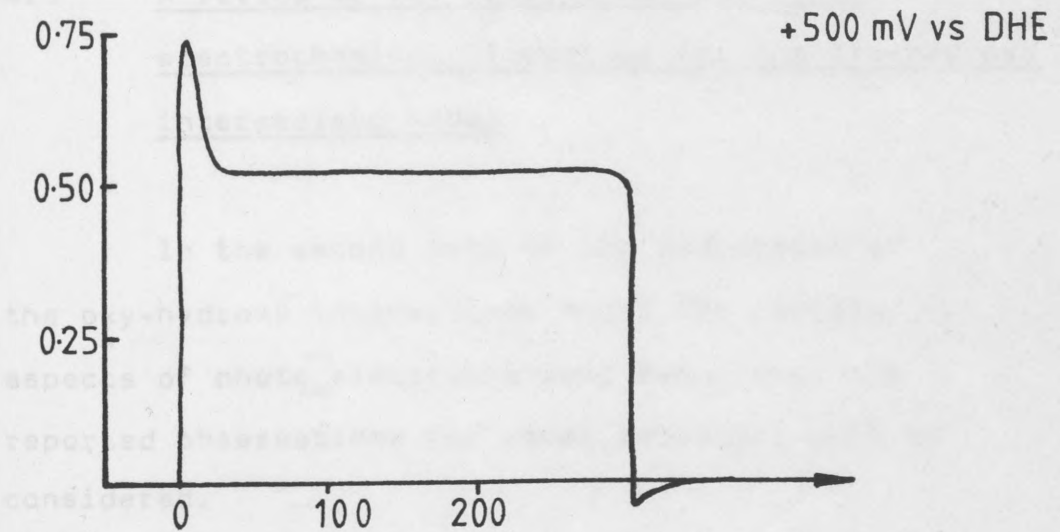
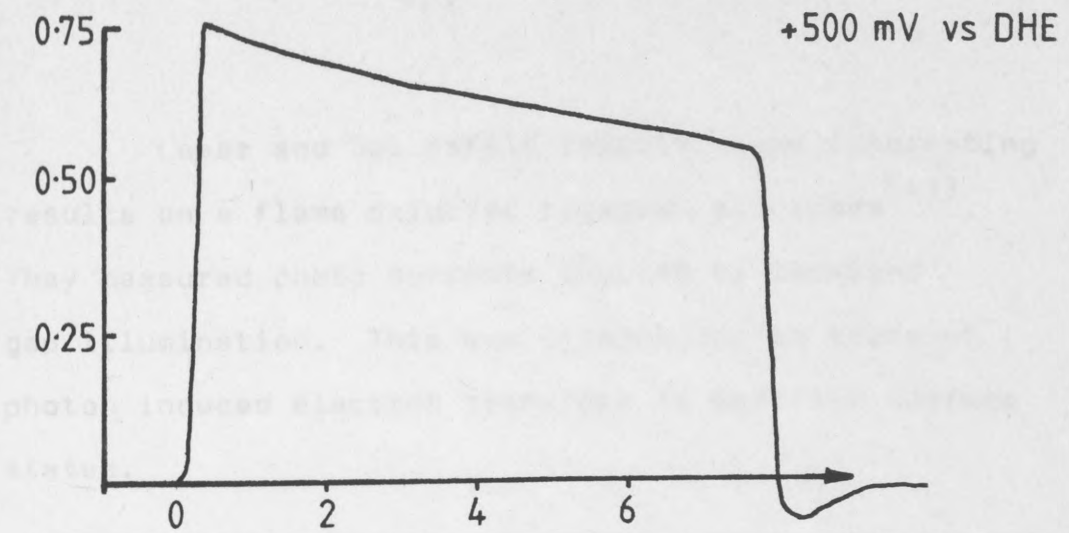


Fig. 4.14

Photocurrent transients of flame oxidised Titanium in 5M KOH at varying voltages.

Laser and Gottesfeld reported some interesting results on a flame oxidized titanium electrode<sup>(43)</sup>. They measured photo currents induced by sub-band gap illumination. This was interpreted in terms of photon induced electron transfers to and from surface states.

4.9 A review of the evidence in the photo electrochemical literature for the oxy-hydroxy intermediate model

In the second part of the discussion of the oxy-hydroxy intermediate model for certain aspects of photoelectrochemical behaviour, the reported observations for other materials will be considered.

Gerischer reported the importance of surface states in the stability of titanium dioxide under illumination<sup>(101)</sup>. He described the charge transfer at an illuminated n-type semi-conductor in contact with a solution in terms of a quasi-fermi level. This is shown in Figure 4.15. If titanium dioxide is considered, then, as the energy diagram in Figure 4.16 shows, as the anodic decomposition potential of the material is below the energy level for water oxidation, it is the latter which is the

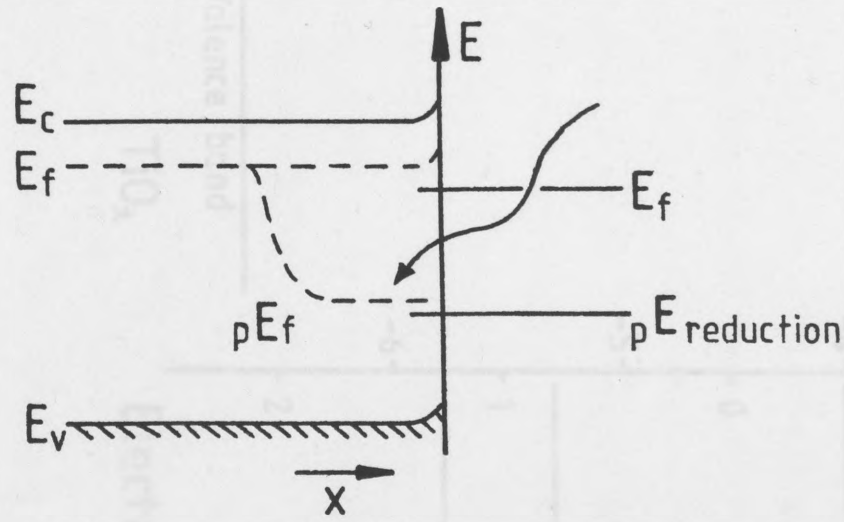


**Fig 4.15**

Quasi-Fermi levels in an illuminated space charge layer at steady state in the presence of a charge transfer reaction by minority carriers at the surface.

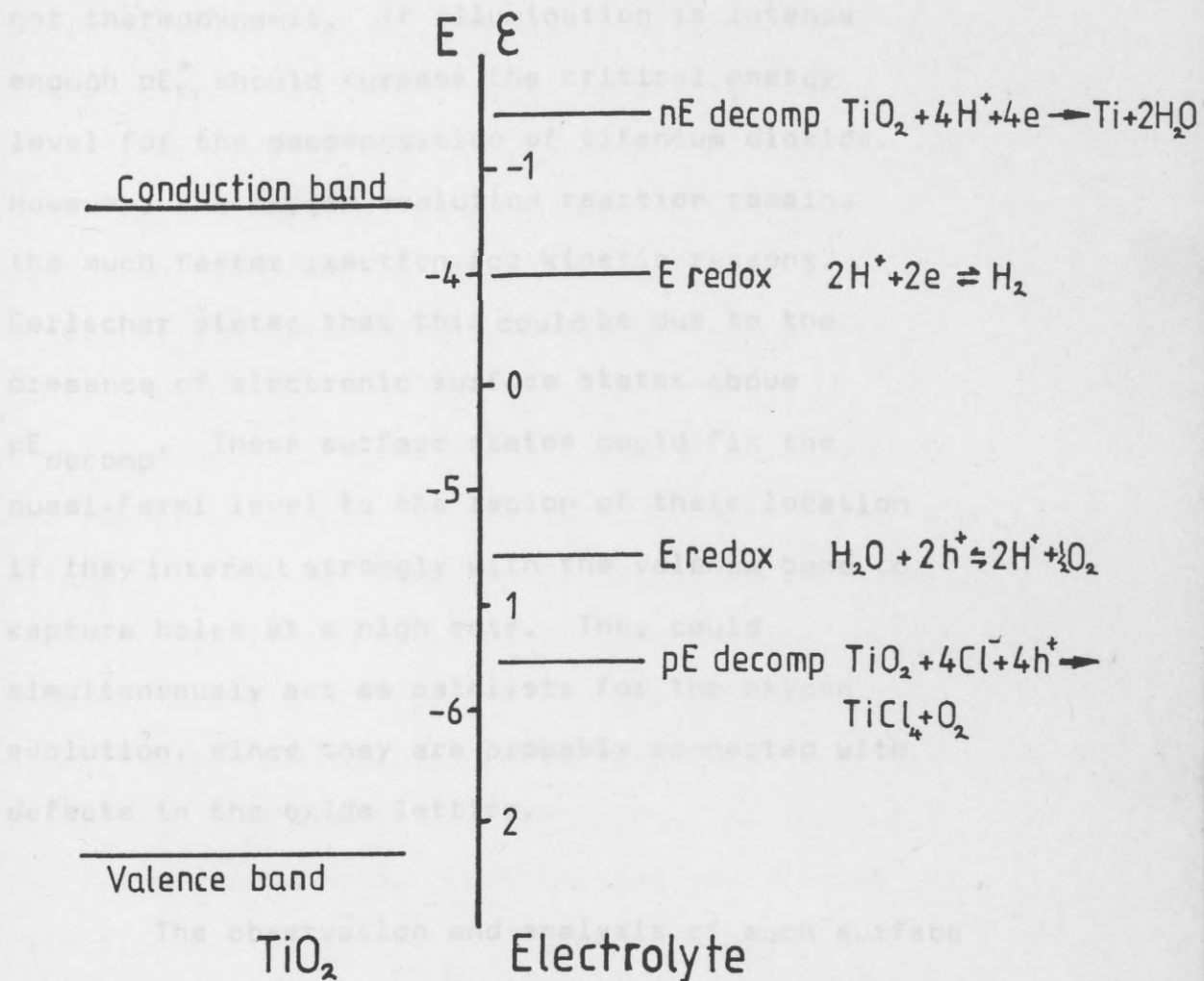


**Fig 4.16**

Energy correlation between band edges and the Fermi energies of electrode reactions in aqueous solution at pH 7 for  $\text{TiO}_2$ .

preferred reaction, not <sup>s</sup>dis<sup>s</sup>olution of the semiconductor. However, this stability is kinetic not thermodynamic. If illumination is intense enough  $pE_F^+$  should surpass the critical energy level for the decomposition of titanium dioxide. However, the oxygen evolution reaction remains the much faster reaction for kinetic reasons. Gerischer states that this could be due to the presence of electronic surface states above  $pE_{\text{decomp}}$ . These surface states could fix the quasi-Fermi level to the region of their location if they interact strongly with the valence band to capture holes at a high rate. They could simultaneously act as catalysts for the oxygen evolution, since they are probably connected with defects in the oxide lattice.

The observation and analysis of such surface states as postulated by Gerischer was reported by Wilson<sup>(29)</sup>. Wilson reported that when a titanium dioxide electrode was held at a suitable voltage under illumination, a photo current was observed. If that electrode was subsequently swept to move negative voltages in the dark a negative current in excess to the normal dark current was observed.

The growth and decay of this peak was analysed as a reduction by conduction band electrons of surface states that were oxidized by valence band holes during the photo excitation. Wilson interpreted these results as showing that the surface states were intermediates of the reaction leading to oxygen evolution. However, he also stated that this interpretation was not unequivocally established.

Kowalski, Johnson and Taller have used the self-consistent-field  $X\alpha$  scattered wave (SCF- $X\alpha$ -SW) method to calculate the cluster molecular orbitals of the interface of titanium dioxide and water<sup>(18)</sup>. They used as a basis for their model the interaction of a  $(TiO_5)^{6-}$  cluster with a hydroxide ion. It was found that when the  $(TiO_5)^{6-}OH$  cluster was formed, the oxygen atom of the hydroxide ion radical was more strongly bonded to the titanium atom than the oxygen atoms of the lattice. This would suggest that the oxygen gas evolved originates from the lattice. These oxygen atoms leaving the surface layer would create vacancies which could be occupied by oxygen ions originating from the adsorbed hydroxide ions.

Tributsch used an intermediate model in the study of the photoelectrochemical behaviour of

molybdenum selenide<sup>(78)</sup>. It was found that molybdenum selenide undergoes photo dissolution into the  $\text{SeO}_3^{2-}$  ion in water, but not in acetonitrile. On this premise it was surmised that a chemical bond was formed between the illuminated semi-conductor and the hydroxide ions present in the water and that the oxidation of these ions was the primary step in the generation of anodic photo currents. However, the principal oxidation product was selenic acid not oxygen.

Rajeshwar has recently postulated a unified model for the charge transfer in photo electrochemical devices via interface surface states and applied it to the n gallium arsenide/room temperature molten salt and the n cadmium selenide/polysulphide interfaces<sup>(47)</sup>. N gallium arsenide was found to exhibit similar photo current transient behaviour to that of flame oxidized iron. The model, based on the mediation of charge transfer by an interface state which is interpreted to arise from specific adsorption of ionic species from the electrolyte was found to qualitatively explain the observed behaviour.

#### 4.10 Conclusions

Flame oxidized iron electrodes have been prepared. Their steady state and transient photo electrochemical properties have been observed. The transient behaviour of these electrodes have shown characteristic anodic photo current and dark cathodic current spikes. These have been explained in terms of the creation and subsequent reduction of an oxy-hydroxy intermediate for the evolution of oxygen. This has been supported by linear sweep voltametry, high potential transient measurements and X-ray analysis. The model postulated has been used to explain the effects of illumination intensity and potential on the current transients. Similar behaviour has been observed on flame oxidized titanium. The model has been found to be in agreement with those theories reported in the literature.

If photo electrochemistry is to provide an efficient solar energy conversion device, then the nature of these charge transfer intermediates will have to be fully understood. The results of this study suggest that photo electrochemistry can borrow from the techniques and theories of conventional electrochemistry to do this.



The two areas where substantial improvements might be made are in the areas of current efficiency and apparent voltage (i.e. the band gap of titanium dioxide is 3.0eV, but the oxygen evolution potential is only moved about 1.3 volts from its thermodynamic equilibrium potential of + 1.23V). As the importance of the oxy-hydroxy intermediates has been established, if these could be formed at close to the equilibrium potential for the evolution of oxygen, then possibly an increase in photo efficiency could occur. Tseung and Jasem have correlated the potential of the high/lower oxide couple of certain compounds to their observed oxygen evolution performance<sup>(4)</sup>. They showed that compounds of cobalt and nickel show the most interest as possible electrode materials for oxygen evolution, as their lower/higher oxide couples are close to the oxygen evolution potential. However, the reported band gaps for cobalt oxide (0.47eV at -23°C, 0.73eV at 100°C) and nickel oxide (3.7eV at 27°C) rule out the use of these compounds as possible photo electrode materials<sup>(102)</sup>.

So other cobalt and nickel compounds must be considered. One family of compounds which suggested

itself was the silicates. The electro catalytic nature of transition metal silicon alloys was known (103-105) and Shallaby and Kuhn have linked this to the presence of the silicate of the transition metal<sup>(5)</sup>. So the silicates of cobalt, nickel and (as a possible cross reference to flame oxidized iron) iron offer some potential as possible photo electrode materials and possible electro catalysts for the evolution of oxygen. Unfortunately the band gaps of these materials are not known and the ability to measure them was not available. However, their investigation, reported in the next two chapters, involved the fabrication of the materials, measurement of the steady state electrochemical behaviour and the use of transient methods to ascertain if oxy-hydroxy intermediates were formed on these materials. If the steady state performance and the precise nature of any oxy-hydroxy intermediates are known, then the possible use of these materials as photo electrodes can be evaluated.

Introduction

The electrochemical behaviour of various transition metal silicates, which have been studied in some detail (103-105), is now also being examined that on such compounds, especially those of the silicic acid type, under existing conditions a thin layer of oxide is formed (103-108).

CHAPTER FIVE

THE STEADY STATE ELECTROCHEMICAL BEHAVIOUR OF

TRANSITION METAL SILICATES

the siliceous film is a conductor, the siliceous film is a conductor and a semiconductor, and a semiconductor. To fully establish this theory it was decided to prepare exactly the same silicates as those mentioned above, fabricate it into an electrode and examine its electrochemical behaviour.

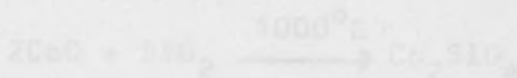
A parallel investigation into nickel and iron silicates was also carried out.

## 5.1 Introduction

The electrocatalytic behaviour of certain transition metal silicon alloys has been known for some time<sup>(103-105)</sup>. It had also been reported that on such compounds under a wide range of oxidising conditions a thin layer of silica was formed<sup>(106-108)</sup>. As silica is an insulator, the manner of the electrocatalytic activity exhibited provoked interest. Shallaby and Kuhn reported that, using X-ray diffraction methods, such species as cobalt silicate ( $\text{Co}_2\text{SiO}_4$ ) could be detected in the silica film on a cobalt silicon alloy electrode<sup>(5)</sup>. They postulated that as cobalt silicate was a semiconductor, the silica film was rendered both conductive and electrocatalytically active by their presence. To fully evaluate this theory it was decided to prepare cobalt silicate, characterise it, fabricate it into an electrode, and evaluate its electrochemical performance.

A parallel investigation into nickel and iron silicate was also carried out.

reaction is as follows:-

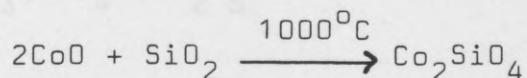


## 5.2 Literature review of transition metal silicates

The transition metal silicates are not very widely documented compounds. Often their study is in areas of geochemistry and as such, properties are measured under conditions of extreme temperature and pressure. As a result of this, information relevant to their use as electrocatalysts at or near ambient conditions is scant. However, the following has been found.

### 5.2.1 Cobalt Silicate

Cobalt silicate is a blue/violet crystalline solid. It is reported to have the olivine crystal structure and is a semi-conductor, although there is some uncertainty over the mechanism of conduction as to whether it is electronic or ionic conduction<sup>(109-112)</sup>. Kondo and Miyahara have reported that it is paramagnetic at room temperature<sup>(113)</sup>. The usual method of preparation of cobalt silicate is the solid state sintering of cobalt oxide and silica<sup>(109,110,113)</sup>. A variety of conditions are used but essentially the reaction is as follows:-



It has also been reported that cobalt silicate can be prepared by a co-precipitation from cobalt nitrate and tetraethyl silicate solution, followed by a similar heat treatment as the solid state sintering method<sup>(112,114)</sup>. The only method reported using co-precipitation only, is that of Kreshove et al using sodium glycerosilicate<sup>(115)</sup>. However, these were reported to be hydrated and ill-defined compounds.

Cobalt silicates appear to be virtually chemically inert. However, it has been reported that at high temperatures it is reduced by carbon monoxide<sup>(116-117)</sup>. Also Kondrasheva et al have reported that cobalt silicate in a polysilicate form will catalyse the reaction<sup>(118)</sup>.



The A.S.T.M. index lists the following as the information for cobalt silicate and related compounds:-

$\text{Co}_2 \text{SiO}_4$  - 15.865, 15-497

$\text{Co}_3 \text{Si}_4 \text{O}_{10} (\text{OH})_2$  - 15-387

$\text{Co}_3 (\text{OH})_2 (\text{Si}_2 \text{O}_5)_2$  - 21-871

$\text{Co}_3 (\text{OH})_4 (\text{Si}_2 \text{O}_5)$  - 21-872

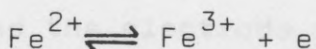
### 5.2.2 Nickel silicate

Nickel silicate is a green crystalline solid. At normal temperatures and pressures it has an olivine structure<sup>(111,113,119)</sup>. However, at high temperatures and pressures (700°C, 50,000 atmospheres), it converts to a spinel structure<sup>(120-121)</sup>. Kondo and Miyahara have reported it to be paramagnetic at room temperature<sup>(113)</sup>. Ringwood has reported its infra red spectrum<sup>(122)</sup>. Bradley et al have measured its electrical properties and found it to be a semi-conductor similar to cobalt silicate<sup>(109)</sup>. Nickel silicate can be prepared by similar solid state sintering and co-precipitation techniques to those reported for cobalt silicate<sup>(109,110,112-115)</sup>. Hofmann and Gruehn have reported<sup>(124)</sup> that single crystals can be prepared by chemical vapour deposition<sup>(123)</sup>. Kondrasheva has reported that nickel silicate showed a similar degree of activity to cobalt silicate in acting as a catalyst for the oxidation of carbon monoxide<sup>(118)</sup>. Burdese reported that nickel silicate could be reduced by carbon monoxide at high temperatures<sup>(117)</sup>. However, it is more easily reduced than cobalt silicate. The A.S.T.M. data card for nickel silicate is 3-0780.

### 5.2.3 Iron Silicate

Iron silicate has been more widely documented than nickel and cobalt silicates. Unfortunately, most of this work has been associated with slag formation in iron production, so most of the information is of limited use for the application desired.

Iron silicate is a brownish/green crystalline compound. It has an olivine structure<sup>(111)</sup>, but may be converted to a spinel structure at high temperature and pressure (35,000 bars, 520°C)<sup>(124)</sup>. Bradley et al have reported it to be an intrinsic semi-conductor with a conduction mechanism based on<sup>(124)</sup>.



Kondo and Miyahara have reported silicate to be paramagnetic at room temperature<sup>(113)</sup>. It can be prepared by similar methods to that of cobalt and nickel silicate<sup>(113,114,125)</sup>. Kondrasheva has reported that it is a catalyst for the oxidation<sup>tion</sup> of carbon monoxide, but it does not show as much activity as cobalt silicate<sup>(118)</sup>. It is more readily reduced by carbon monoxide than cobalt silicate<sup>(117,126)</sup>.



The reported A.S.T.M. dates for iron silicate is as follows:-

Iron silicate: 9-307, 9-484, 11-262

Iron silicate (spinel): 12-284

Of the transition metal silicates, iron silicate was the only compound for which any electrochemical activity was reported. Eguchi has reported that iron silicate has been used as an electrode material in the electrolysis of sodium acetate solution<sup>(127)</sup>. A 15% iron silicate electrode was used as an anode and although it gave a reasonable performance, it suffered from corrosion (23mg/A hr) and the performance deteriorated with time. After 50 hours operation the electrochemical activity was greatly reduced and the electrode surface had become scaly with a silica deposit left by the corrosion of the electrode.

### 5.3 The preparation of transition metal silicates

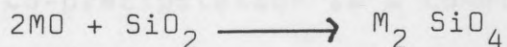
Three methods were used to prepare transition metal silicates. These were:-

- 1) Solid state sintering.

- 2) Co-precipitation from a sodium silicate solution.
- 3) A gelling method using tetra-ethyl ortho silicate as used by Hamilton and Henderson<sup>(114)</sup>.

### 5.3.1 Solid state sintering

The basis of this method was to mix intimately the metal oxide and silica and heat to a suitable temperature to enable the following reaction to occur:-



Analar quality nickel nitrate, cobalt nitrate or ferrous oxalate were ground with a stoichiometric amount of analar silicon dioxide with a pestle and mortar. This mixture was then warmed gently in an evaporating basin to allow the salts to dissolve in their own water of crystallisation. This enabled the metal salts to mix as intimately as possible. The slurry was then heated to dryness with a bunsen burner then vigorously heated to decompose the metal salts to the parent oxide. The resultant solid was ground again then heated at 1000°C for 24 hours in a muffle furnace. After sintering the compound was ground

again and washed first with 5M potassium hydroxide to remove any unreacted silica and secondly with concentrated nitric acid, to remove any unreacted metal oxide. The compound was then thoroughly washed with distilled water, dried at 100°C in an oven, re-ground and stored in a dry sample jar. The reaction gave approximately a 90% yield. The losses can be attributed to transfer and spitting in heat treatment.

### 5.3.2 Co-precipitation from a Sodium Silicate solution

Co-precipitation is a common method for preparing high surface area compounds such as cobalt ferrites<sup>(128)</sup> and antimony doped tin oxide<sup>(129)</sup>. As sodium silicate or water glass as it is commonly known, is the only soluble silicate, attempts were made to precipitate transition metal silicates from the appropriate solutions using a solution of sodium silicate.

To a well stirred solution of cobalt or nickel nitrate, a solution of sodium silicate was slowly added. This solution was the stoichiometric amount to fully react with all the nitrate present. The resultant precipitate was filtered off, washed

well with distilled water, dried at  $100^{\circ}\text{C}$  in an oven, ground in a pestle and mortar then stored in a dry bottle.

However, when the conductivity of these products were measured, they were very low. This was probably due to the sodium silicate solution being very alkaline, causing a precipitate of nickel or cobalt hydroxide, as opposed to the appropriate silicate. The product was then treated as per the solid state sintering method of heating to a  $1000^{\circ}\text{C}$  for 24 hours and subsequent treatment. This caused some improvement.

### 5.3.3 Gelling method with tetra ethyl ortho silicate (114)

To a solution of cobalt or nickel nitrate, the required weight of tetra ethyl ortho silicate was washed in with ethanol. Enough ethanol was added to enable the two solutions to become miscible.

Concentrated ammonium hydroxide was then added to the solution, until it was in a slight excess (detected by litmus paper). The resultant gel was dried, then heated with a bunsen burner to decompose the nitrates. The sample was then heat treated as per the solid state sintering method.

## 5.4 Characterisation of the electrode materials

The samples of cobalt, nickel and iron silicate produced were characterised by conductivity measurements, X-ray analysis and in the case of cobalt silicate surface area measurement.

### 5.4.1 Conductivity Measurements

To be of use as a possible electrocatalyst, a material must have a suitably high conductivity, or else the voltage gained in lowering an over voltage may be lost in ohmic losses, so the preparation of the electrocatalyst in a conducting form and the measurement of that conductivity is obviously important.

The conductivity of the prepared samples was measured using a Teflon die with brass end caps. This is shown in Figure 5.1. A sample of the catalyst was compressed between the brass end caps using a vice, care being taken that the end caps were electrically isolated from the vice. The electrical resistance of the compressed powder sample was measured with a digital multimeter (I.T.T. Co.Ltd.). As the geometry of the cell was known the specific

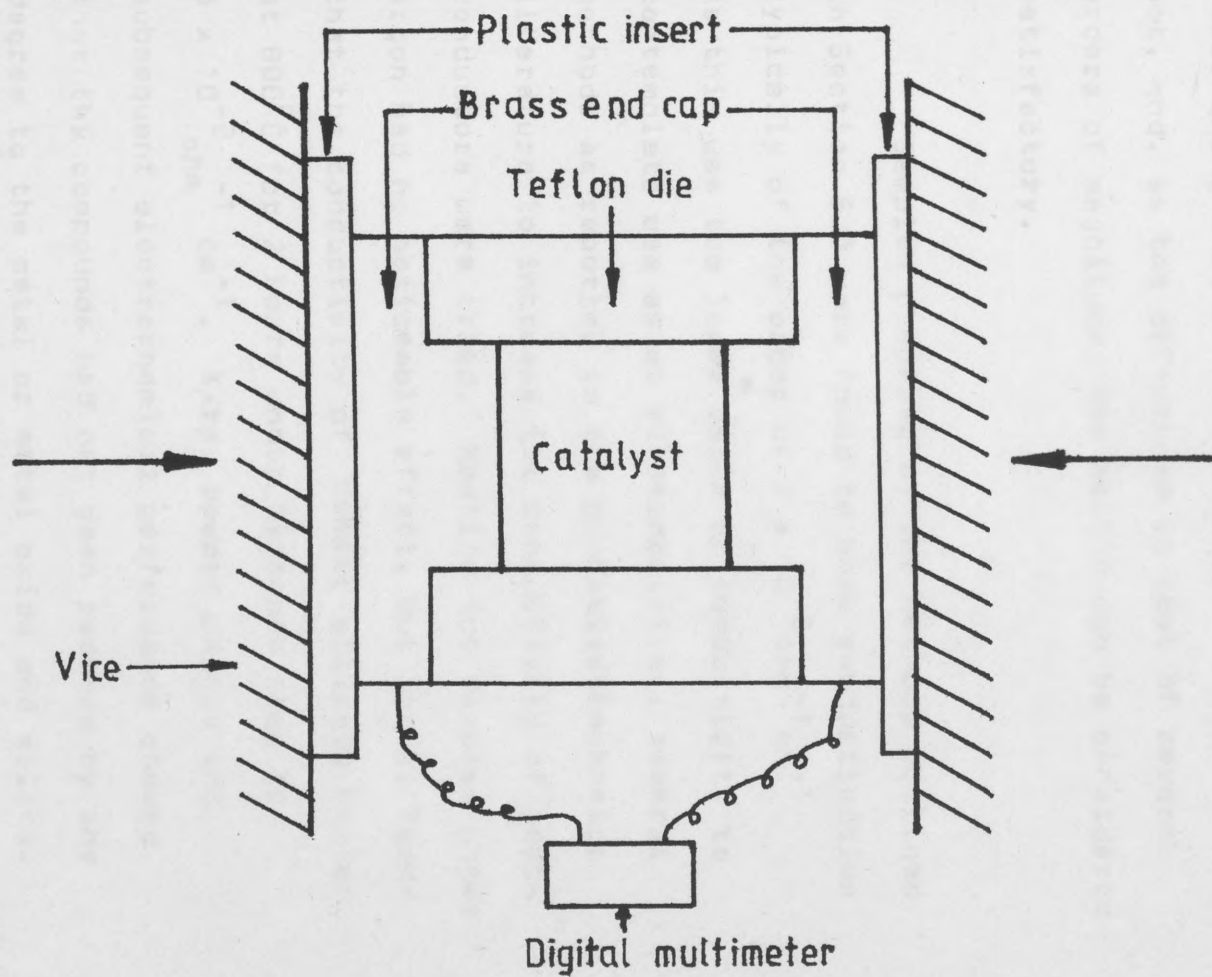


**Fig 5-1**

Powder conductivity measurement cell

conductivity could be calculated. The degree of accuracy of these results in absolute terms must be open to question as such properties as pressure, degree of compacting and absolute cell dimensions were not controllable. However, in terms of determining whether the material was suitable or not, and, as the difference is that of several orders of magnitude, the method can be considered satisfactory.

Samples prepared by the methods outlined in Section 5.3 were found to have conductivities typically of the order of  $2 \times 10^{-6} \text{ ohm}^{-1} \text{ cm}^{-1}$ . As this was too low<sup>a</sup> value of conductivity to contemplate use as an electrocatalyst, several methods as reported in the photoelectrochemical literature to increase the conductivity of semiconductors were tried. Heating the samples under argon had no noticeable effect, but it was found that the conductivity of cobalt silicate heated at  $800^{\circ}\text{C}$  for 2 hours under hydrogen rose to  $6 \times 10^{-2} \text{ ohm}^{-1} \text{ cm}^{-1}$ . X-ray powder photos and subsequent electrochemical performance showed that the compounds had not been reduced by any degree to the metal or metal oxide and silica.

Iron silicate exhibited some degree of partial reduction, but these products could be removed by subsequent acid and alkali washing as per 5.3.1. However, nickel silicate treated in the same way was completely reduced to nickel and silica. So the electrochemical investigations were carried out using cobalt silicate and iron silicate. However, the literature on the reduction of transition metal silicates by carbon monoxide (116,117,126) would suggest that if the reducing conditions were varied, then possibly conducting non-reduced iron and nickel silicate could be obtained.

#### 5.4.2 X-ray analysis

The samples produced were characterised at their various stages of manufacture, e.g. before and after hydrogen treatment by obtaining the X-ray powder photographs, indexing according to the Bragg equation.

$$2d \sin \theta = n\lambda$$

where  $d$  is the lattice spacing

$\theta$  is the angle of the X-ray beam on the crystal planes



$n$  is an integer

$\lambda$  is the wavelength of radiation used.

and comparing the lattice spacings and intensities of the samples with those in the A.S.T.M. index.

The work was carried out on a Phillips PW 1010 X-ray generator using an analytical camera of diameter 11.46 cm. Molybdenum K radiation was used at an anode voltage of 40 <sup>k</sup>KV and 16 mA current. The samples were mounted in Lindemann glass tubes of internal diameter 0.5 mm and exposure times of 5-6 hours were used.

#### 5.4.3 Surface Area Measurements

It is desirable for a catalyst to have as much surface area available for reaction per gram as possible hence the measurement of the surface area per gram of a potential catalyst is usually of great importance in its characterisation.

However, as the two compounds under investigation were made by high temperature solid state sintering methods, it was known that their specific surface areas would be very low. Because of this, not every sample had its specific surface area measured, but to determine what order of magnitude the specific area of these compounds was, two samples of cobalt silicate had their surface area measured.

#### 3.5.1 Fabrication of catalyst

The actual measurement presented a problem, as the expected specific surface area was outside the range of B.E.T. equipment available. This was resolved through the kind offices of Chlor - Alkad Limited, who measured the specific surface area of the two samples, using their argon absorption equipment. These were found to be  $1.96 \text{ m}^2 \text{ g}^{-1}$  and  $2.01 \text{ m}^2 \text{ g}^{-1}$  respectively. These results suggest bonded on to a path by following the mechanical strength and ease of fabrication, the dry channels existing in the reaction.

that most samples would have a specific surface area of the order of  $2\text{m}^2\text{gm}^{-1}$ . To give some idea of the comparative magnitude of this specific surface area, nickel cobalt oxide - an oxygen evolution electro-catalyst has a specific surface area of  $70\text{m}^2/\text{gm}$  and graphite - an oxygen reduction electro catalyst, has a specific surface area of  $700\text{m}^2/\text{gm}$  (130).

### 5.5. Steady state Electrochemical Measurements

#### 5.5.1 Fabrication of electrodes

Although polycrystalline samples such as the silicates can be sintered into solid disks, which can be used as electrodes, it is preferable to fabricate the electrode in such a way, that as much of the electrocatalyst is available for electrochemical reaction as possible. In recent years this has centered on the use of Teflon bonded electrodes. These electrodes consist of the electrocatalyst being bonded on to a mesh by Teflon. Besides mechanical strength and ease of fabrication, the teflon provides dry channels assisting the removal of gas evolved in the reaction.

The method of Giner et al<sup>(131)</sup>, later improved by Tantram and Tseung<sup>(132)</sup> was used for the preparation of the cobalt and iron silicate electrodes.

Weighed quantities of the electro catalyst and aqueous poly tetra fluoro ethylene (P.T.F.E.) dispersion were slurried together with distilled water in an ultra sonic bath. Initially these weighed quantities were in such a ratio that a catalyst/P.T.F.E. ratio of 10/3 would be produced on the final electrode. However, this produced an electrode which was too hydro phobic so the ratio was altered to 10/1. This produced satisfactory electrodes.

The slurry was then painted on to a pre-weighed piece of 100 mesh nickel screen which had previously been degreased in acetone. The piece of mesh was of such a shape, that after a strip of 1 x 0.2 cm nickel foil had been spot welded on to it to give support to the electrode and enable a wire to be attached, a 1 cm square of nickel mesh remained.

After an even coating of catalyst on both sides of the mesh had been obtained by the application of several coats of slurry with a paint brush and drying with a hairdryer, the electrode was dried at 100°C for 1 hour, then cured at 300°C for 1 hour. The curing

is shown in Figure 5.2.

removes the wetting agent (Triton X100) from the P.T.F.E. and causes partial sintering between the P.T.F.E. and electrode material particles, thereby increasing the hydrophobic character and strength of the electrode.

The temperature of curing is critical, as below  $265^{\circ}\text{C}$  the P.T.F.E. does not sinter and above  $330^{\circ}\text{C}$  it is transformed into a glassy state which produces a highly inactive electrode.

After curing, the electrodes are re-weighed so the catalyst, teflon loading can be calculated.

#### 5.5.2 General electro chemical testing

The electrodes were tested in a conventional, 2 compartment, 3 electrode cell. The reference electrode was the D.H.E. and the counter electrode was a large piece of platinum mesh. The electrolyte was 5M potassium hydroxide and this was de-aired in both compartments with a stream of white spot nitrogen. While de-aeration is not strictly necessary as oxygen is being evolved, the turbulence created by the nitrogen stream assisted the removal of gas bubbles from the electrodes and helped keep the temperature in the cell constant. The cell is shown in Figure 5.2.

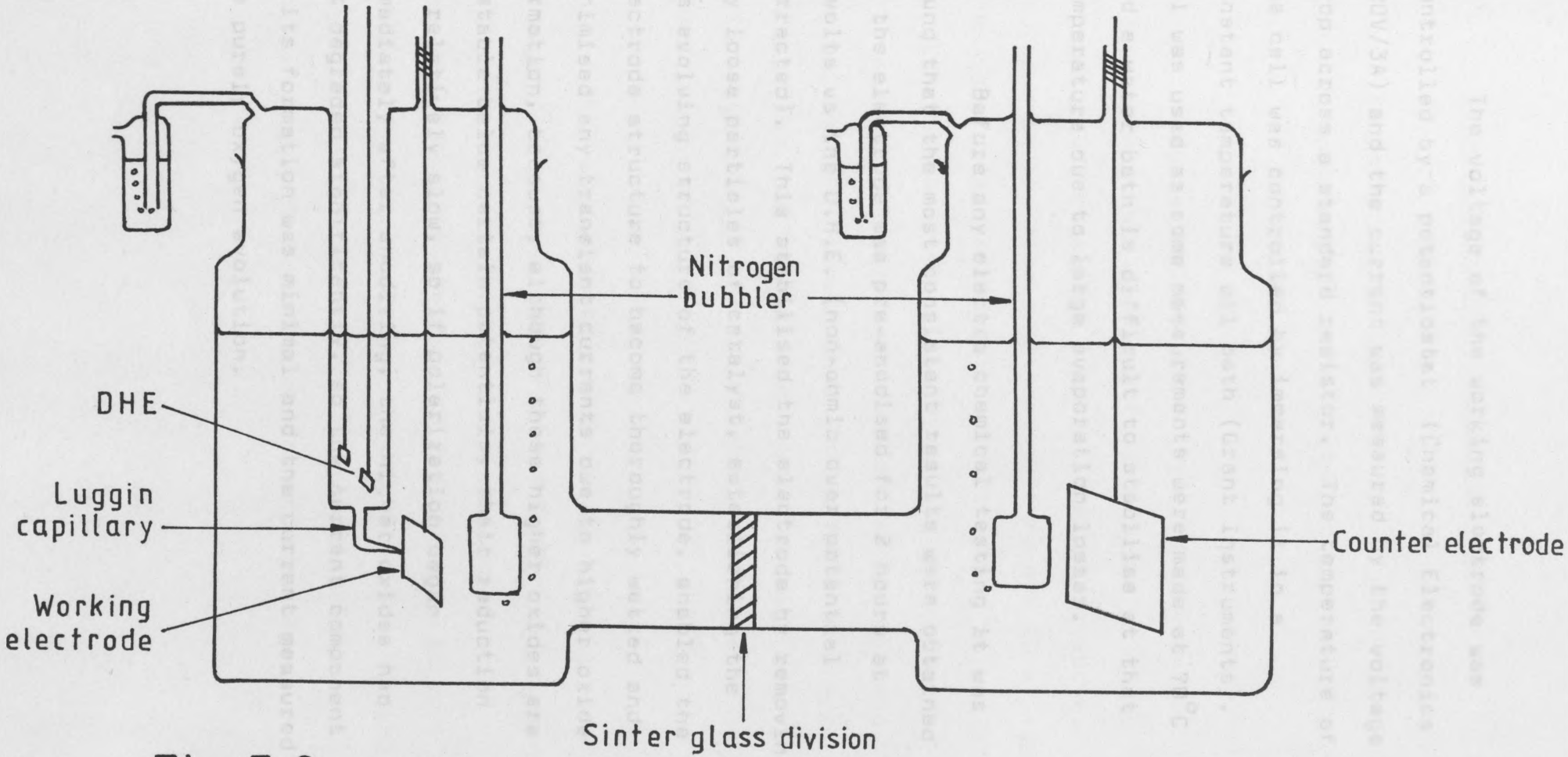


**Fig 5.2**

Diagram of an experimental cell

5.5.3 The voltage of the working electrode was controlled by a potentiostat (Chemical Electronics 120V/3A) and the current was measured by the voltage drop across a standard resistor. The temperature of the cell was controlled by immersing it in a constant temperature oil bath (Grant Instruments). Oil was used as some measurements were made at 70°C and a water bath is difficult to stabilise at that temperature due to large evaporation losses. losses occur due to the electrolyte resistance and to a lesser extent. Before any electro chemical testing it was found that the most consistent results were obtained if the electrode was pre-anodised for 2 hours at 2 volts vs the D.H.E. (non-ohmic over potential not corrected). This stabilised the electrode by removing any loose particles of catalyst, establishing the gas evolving structure of the electrode, enabled the electrode structure to become thoroughly wetted and minimised any transient currents due to higher oxide formation, because, although these higher oxides are unstable below certain potentials, their reduction is relatively slow, so if polarization began immediately after anodizing, the higher oxides had not degraded significantly, so the current component of its formation was minimal and the current measured was purely oxygen evolution.

### 5.5.3 Steady State polarisation curves

Steady state polarisation curves were obtained using the apparatus as per the block diagram in Figure 5.3.

As large currents were involved it was obviously desirable to correct the results obtained for ohmic over potential losses. These ohmic losses occur due to the electrolyte resistance and to a lesser extent the catalyst and cell connections. The use of a Luggin capillary which minimises the gap between reference and the working electrode and hence ohmic over potential will mean that low currents need not be corrected, but high currents lead to large errors so the magnitude of the ohmic over potential must be ascertained.

This was achieved by use of the interrupter technique<sup>(133)</sup>. This method is based upon the steady d.c. polarising current being interrupted at mains frequency (50 Hz) by means of a fast acting, mercury wetted relay. This produces a train of square current pulses through the cell. The circuit diagram is shown in Figure 5.4. As the source of the ohmic



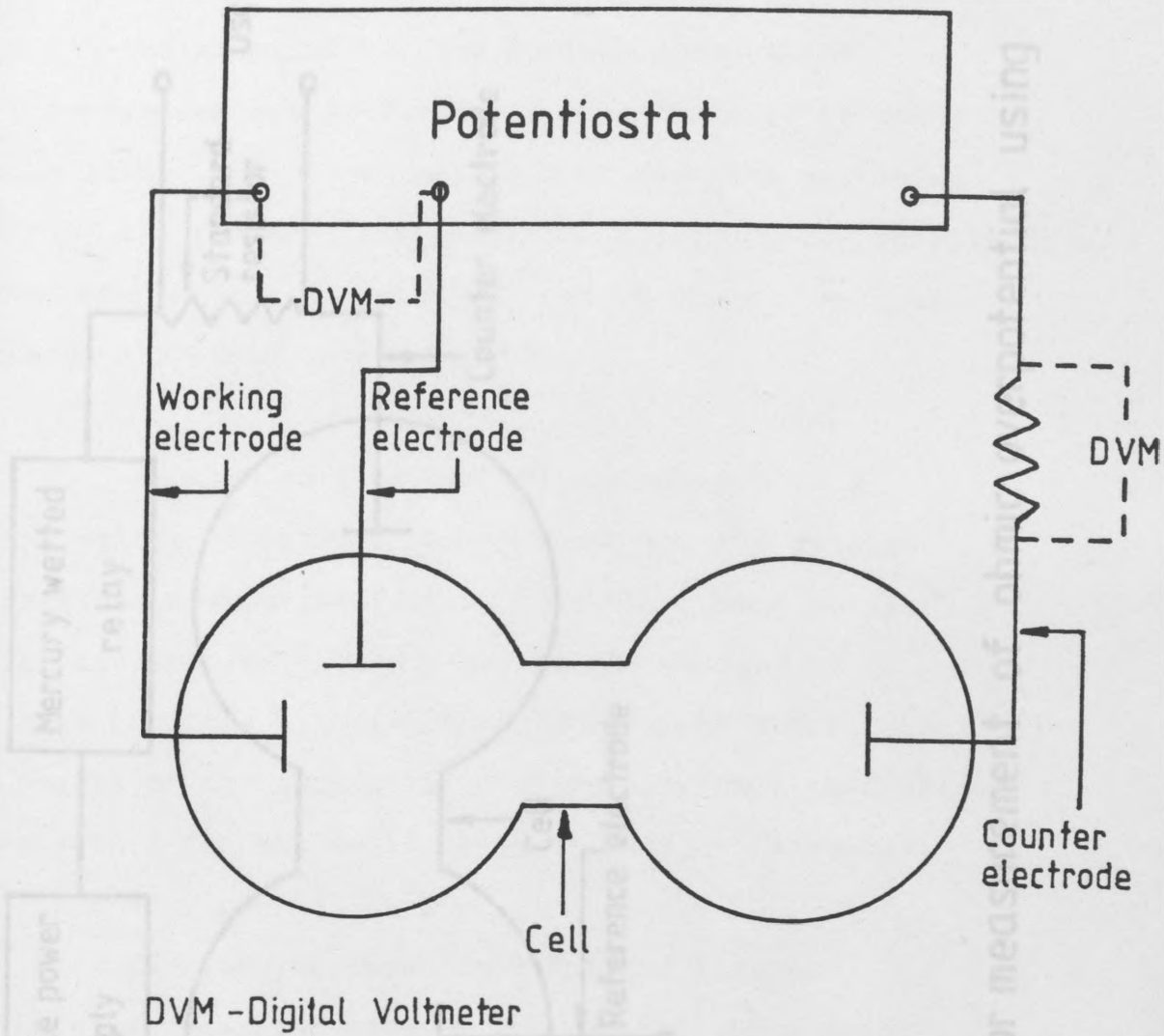


**Fig 5.3**

Schematic circuit diagram for potentiostatic measurements

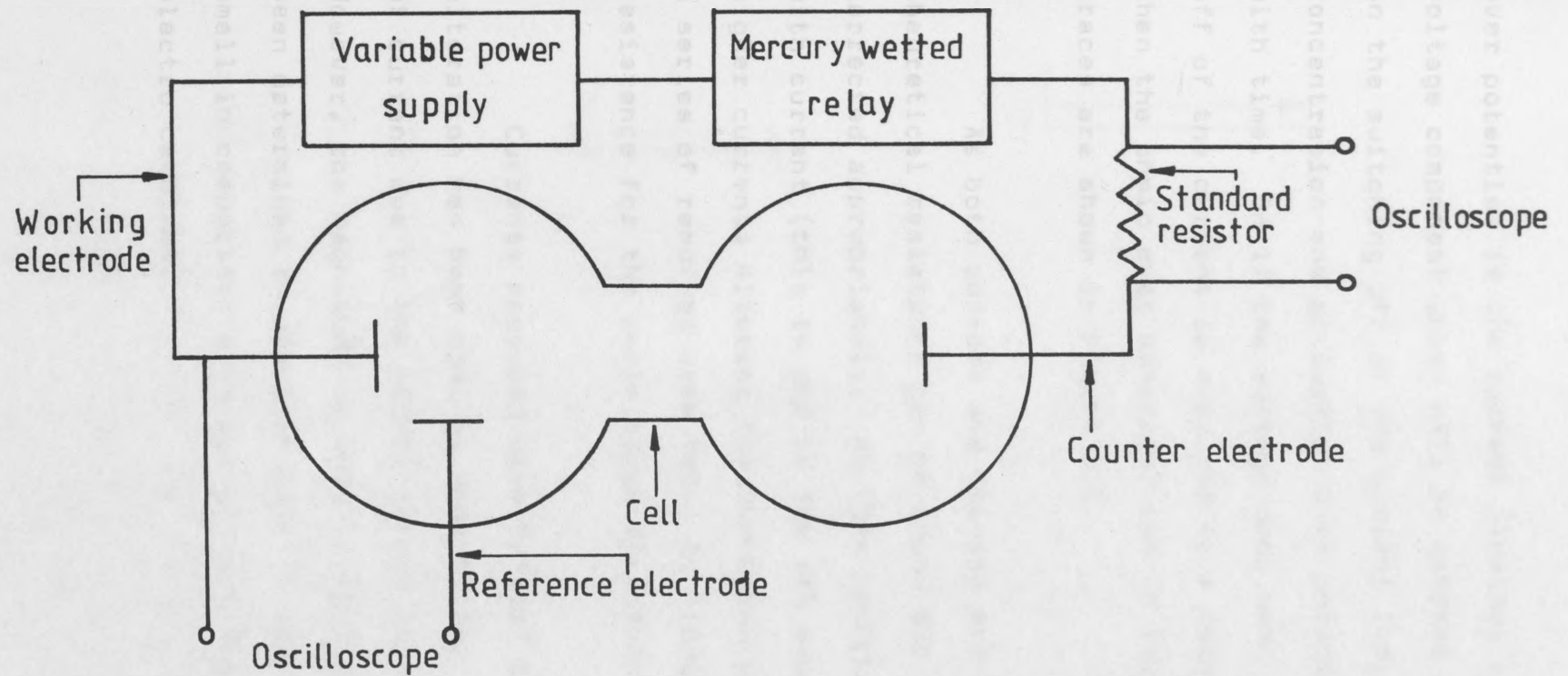


**Fig 5.4**

Schematic circuit for measurement of ohmic overpotential using the interruptor method.

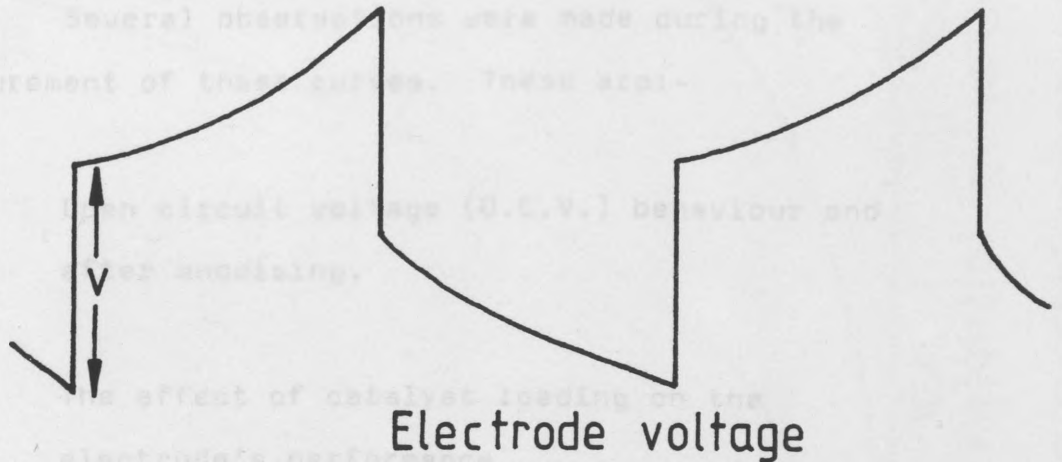
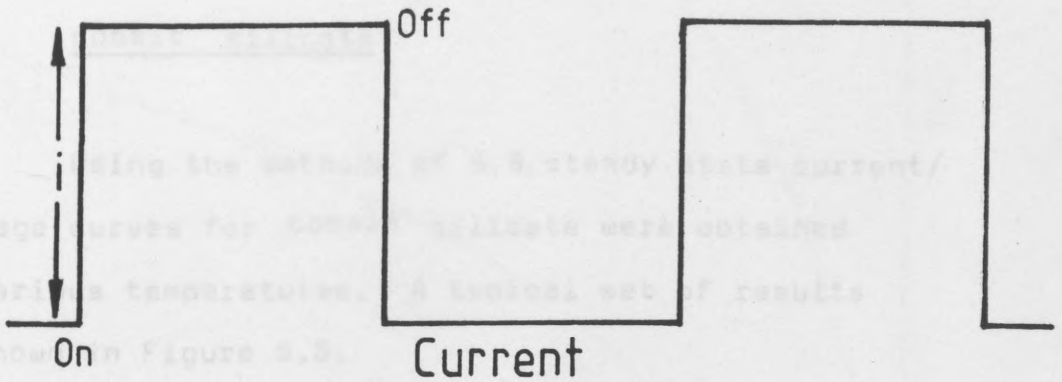
over potential is the current flowing, it is this voltage component which will be removed instantaneously on the switching off of the current leaving the concentration and activation over potentials to decay with time. So if the voltage drop upon the switching off of the current is measured by a cathode ray oscilloscope, then the ohmic over potential can be found. Typical traces are shown in Figure 5.5.

As both current and voltage are known, a theoretical resistance can be found and the results corrected appropriately. As this resistance varies with current (this is due to the gas evolved at higher currents altering the resistance of the electrolyte) a series of readings were taken to provide a theoretical resistance for the whole range of currents measured.

Currents measured were "gross" i.e. no alteration has been made to account for the element of current due to the nickel screen current collector. However, the magnitude of this current element has been determined in previous work<sup>(4)</sup> and found to be small in comparison with the current due to the electro catalyst.

## 5.0 Steady state electrochemical performance

### 5.0.1 Steady state electrochemical performance of



$V = \text{Ohmic overpotential for current } i$ . As  $V$  and  $i$  are known,

a theoretical resistance  $R$  may be calculated.

### Fig 5.5

Typical traces for determining Ohmic overpotential

## 5.6 Steady state electrochemical performance

### 5.6.1 Steady state electrochemical performance of cobalt silicate

Using the methods of 5.5 steady state current/voltage curves for cobalt silicate were obtained at various temperatures. A typical set of results is shown in Figure 5.6.

Several observations were made during the measurement of these curves. These are:-

- 1) Open circuit voltage (O.C.V.) behaviour and after anodising.
- 2) The effect of catalyst loading on the electrode's performance.

The O.C.V. was of the order of +1050 mvs vs the D.H.E. when the electrode was first introduced into the solution. The electrode was then pre-anodised for 2 hours and immediately after this treatment the O.C.V. has risen to +1370 → 1400 mV vs D.H.E. On standing this value would decay until eventually it would achieve equilibrium at approximately +1050mv vs the D.H.E. Similar behaviour has been reported

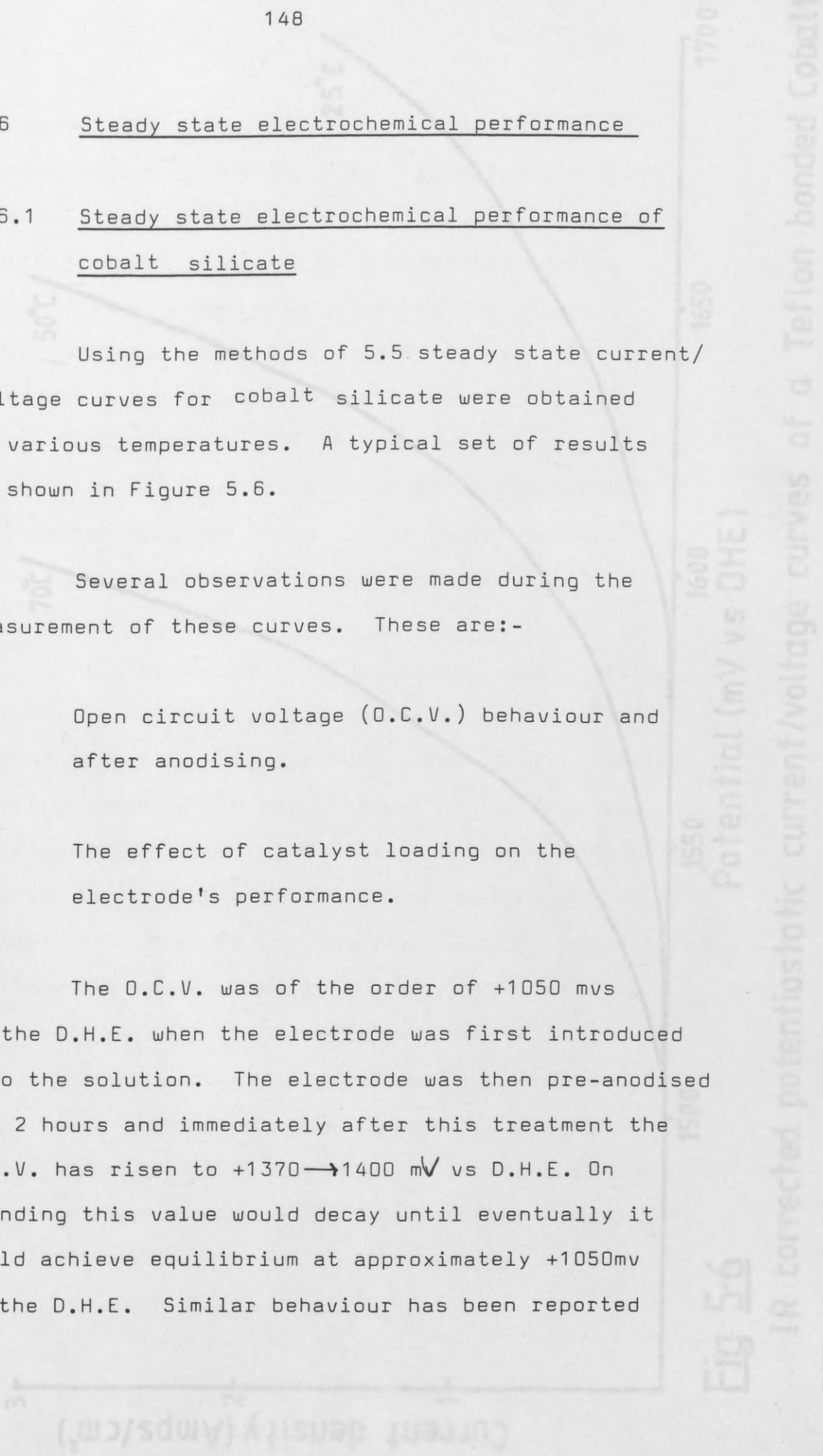
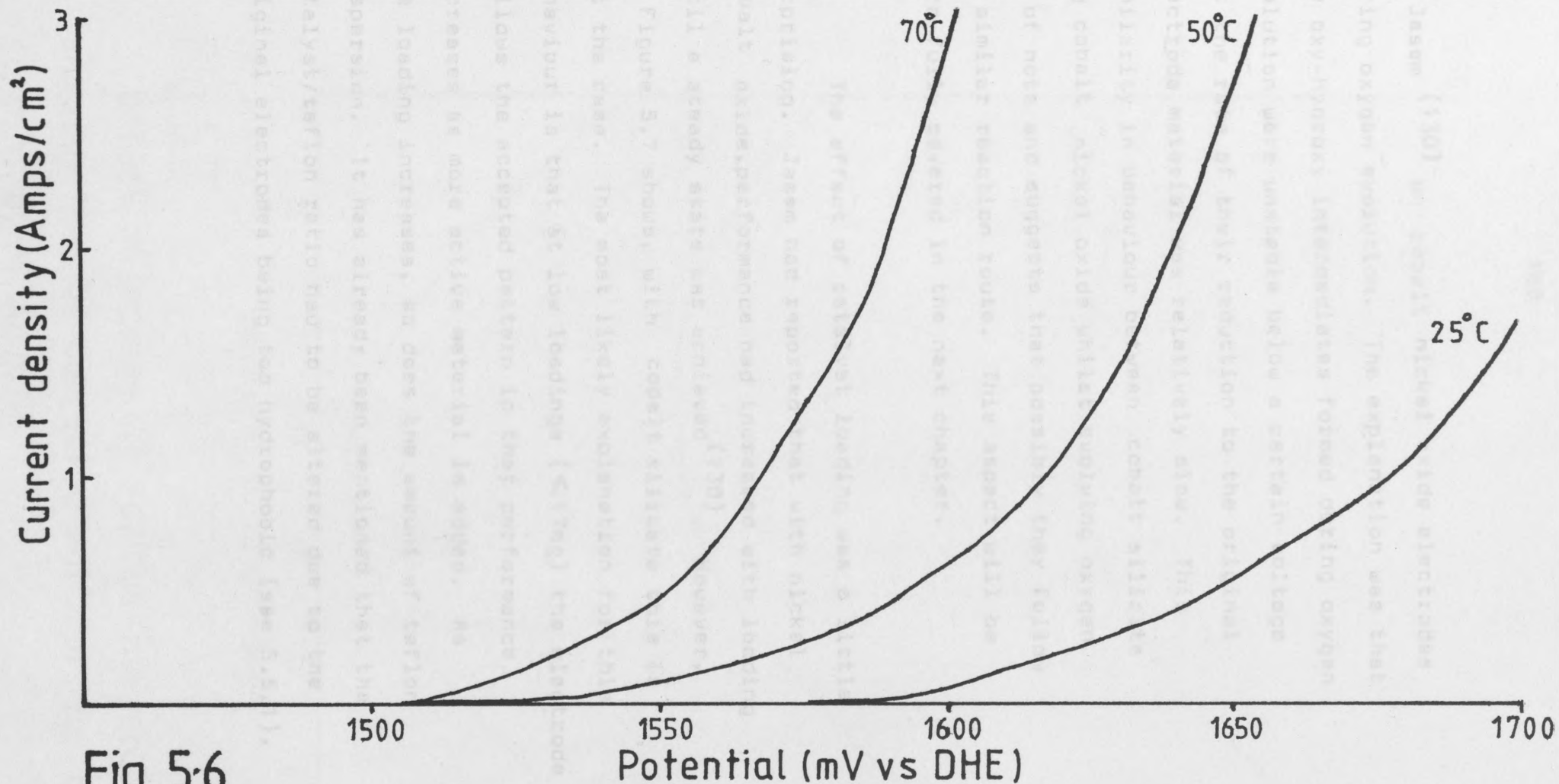


Fig 5.6



**Fig 5.6**

IR corrected potentiostatic current/voltage curves of a Teflon bonded Cobalt Silicate electrode (14.7mq loading) in 5M KOH at various temperatures.

by Jasem (130) on cobalt nickel oxide electrodes during oxygen evolution. The explanation was that the oxy-hydroxy intermediates formed during oxygen evolution were unstable below a certain voltage but the rate of their reduction to the original electrode material was relatively slow. This similarity in behaviour between cobalt silicate and cobalt nickel oxide whilst evolving oxygen is of note and suggests that possibly they follow a similar reaction route. This aspect will be more fully covered in the next chapter.

The effect of catalyst loading was a little surprising. Jasem had reported that with nickel cobalt oxide, performance had increased with loading until a steady state was achieved (130). However, as Figure 5.7 shows, with cobalt silicate this is not the case. The most likely explanation for this behaviour is that at low loadings ( $< 17\text{mg}$ ) the electrode follows the accepted pattern in that performance increases as more active material is added. As the loading increases, so does the amount of teflon dispersion. It has already been mentioned that the catalyst/teflon ratio had to be altered due to the original electrodes being too hydrophobic (see 5.5.1),

Fig 5.7

Effect of loading at various temperatures showing the IR corrected voltage for a current of 1 Amp.

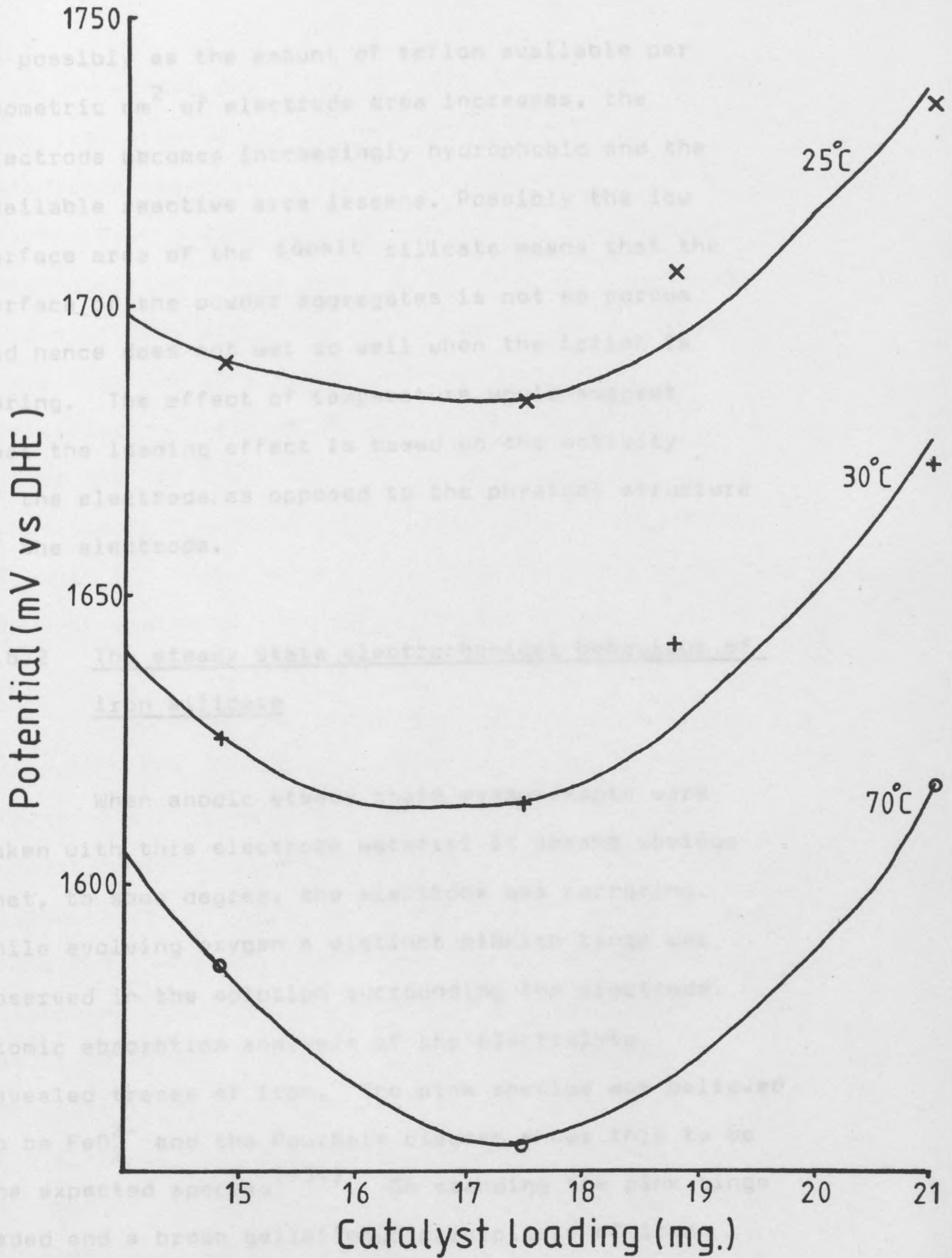


Fig 5.7

Effect of loading at various temperatures showing the IR corrected voltage for a current of 1 Amp.



so possibly as the amount of teflon available per geometric  $\text{cm}^2$  of electrode area increases, the electrode becomes increasingly hydrophobic and the available reactive area lessens. Possibly the low surface area of the cobalt silicate means that the surface of the powder aggregates is not so porous and hence does not wet so well when the teflon is curing. The effect of temperature would suggest that the loading effect is based on the activity of the electrode as opposed to the physical structure of the electrode.

#### 5.6.2 The steady state electrochemical behaviour of iron silicate

When anodic steady state measurements were taken with this electrode material it became obvious that, to some degree, the electrode was corroding. While evolving oxygen a distinct pinkish tinge was observed in the solution surrounding the electrode. Atomic absorption analysis of the electrolyte revealed traces of iron. The pink species was believed to be  $\text{FeO}_2^{2-}$  and the Pourbaix diagram shows this to be the expected species<sup>(134)</sup>. On standing the pink tinge faded and a brown gellatinous precipitate of iron hydroxide was visible. To ensure this phenomena

was the actual corrosion of the silicate and not of any iron present due to the fabrication of the electrode material, a long term test was run on an electrode. A 12mg loading iron silicate electrode was polarised anodically at  $1 \text{ A cm}^{-2}$  for 168 hours. The electrode after this polarisation was found to have lost 6mg of its catalyst loading. The polarisation curve of the electrode before and after the 168 hour run is shown in Figure 5.8. These results and the corrosion of iron silicate by Eguchi<sup>(127)</sup> suggests that it is the iron silicate and not traces of iron which are corroding.

Two observations can be made on these results. One is that apparently the inhibiting layer of silica reported by Eguchi<sup>(127)</sup> does not appear to form, as the performance after 168 hours, although it is lower, is not as poor as would be expected. Possibly this is due to the 5M potassium hydroxide electrolyte dissolving off the silica as it is formed. This would not have happened in Eguchi's case as he was using sodium acetate as the electrolyte. The other observation is that this is another indication of the importance of oxy-hydroxy intermediates in the evolution of oxygen. It is easy to postulate a mechanism for the generation of

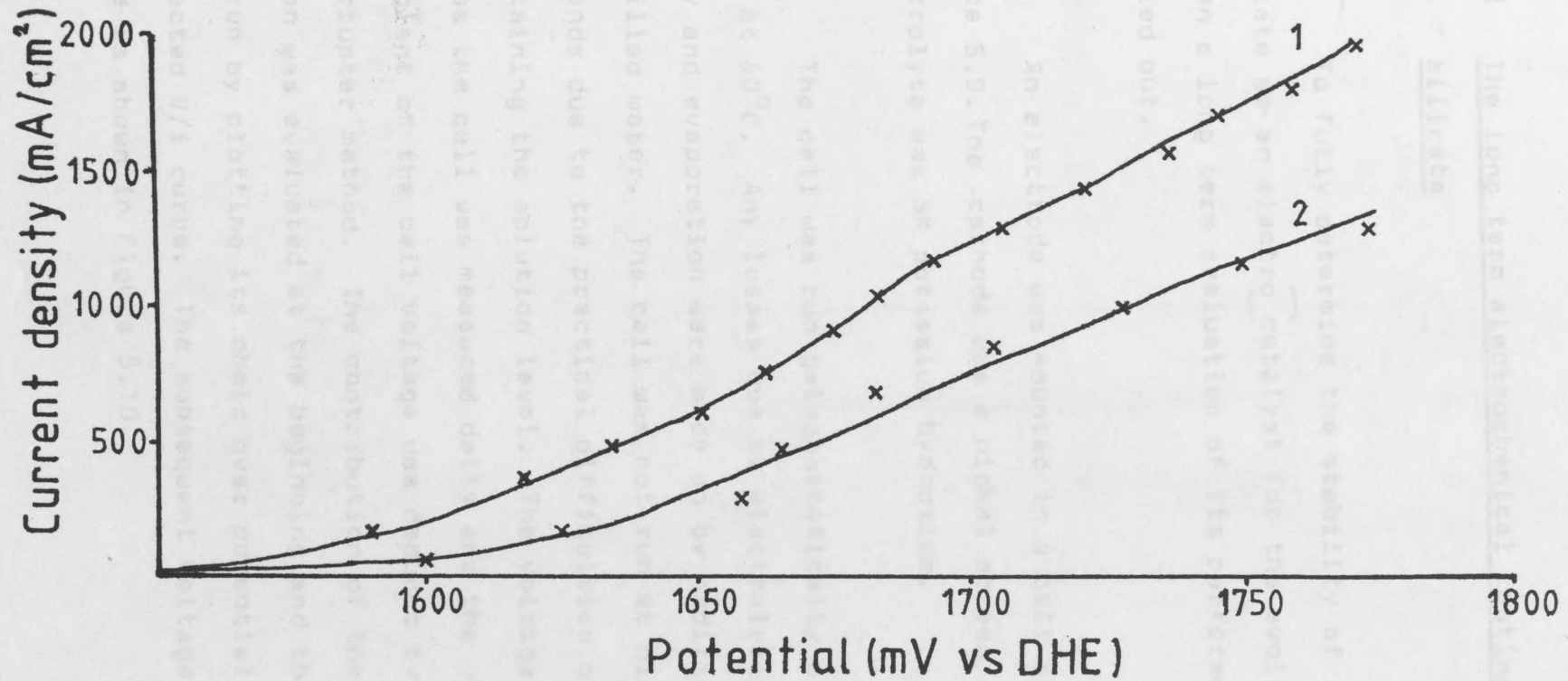


**Fig. 5-8**

Current/voltage curve (IR corrected) for  $\text{Fe}_2\text{SiO}_4$  before (1) and after (2) 168 hours polarisation at 1 Amp. 5M KOH electrolyte at 25°C.

Catalyst loading before polarisation 12mg

Catalyst loading after 168 hours of polarisation 6mg.

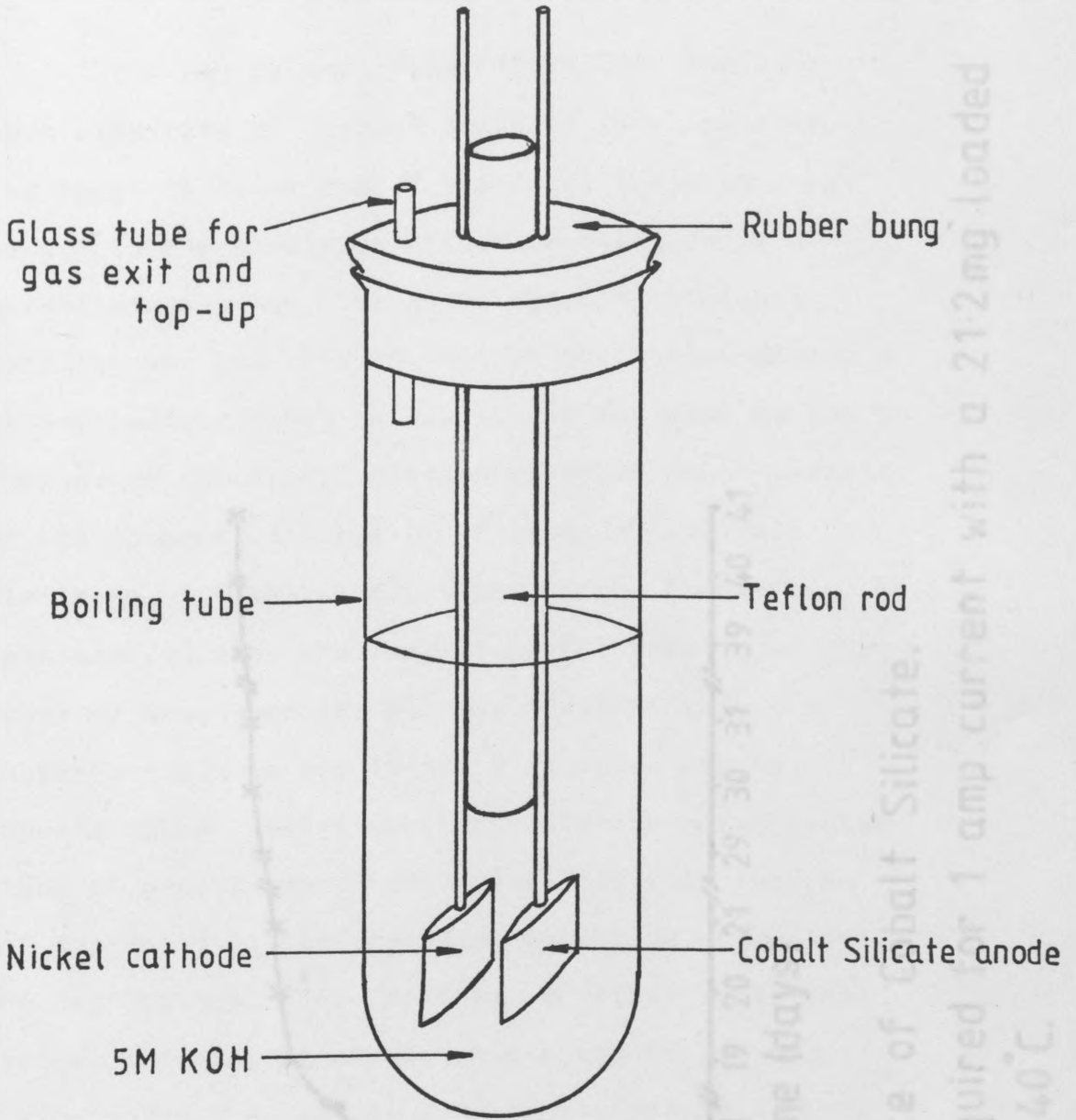
the  $\text{FeO}_2^{2-}$  ion by the breakdown of such an intermediate.

### 5.6.3 The long term electrochemical testing of cobalt silicate

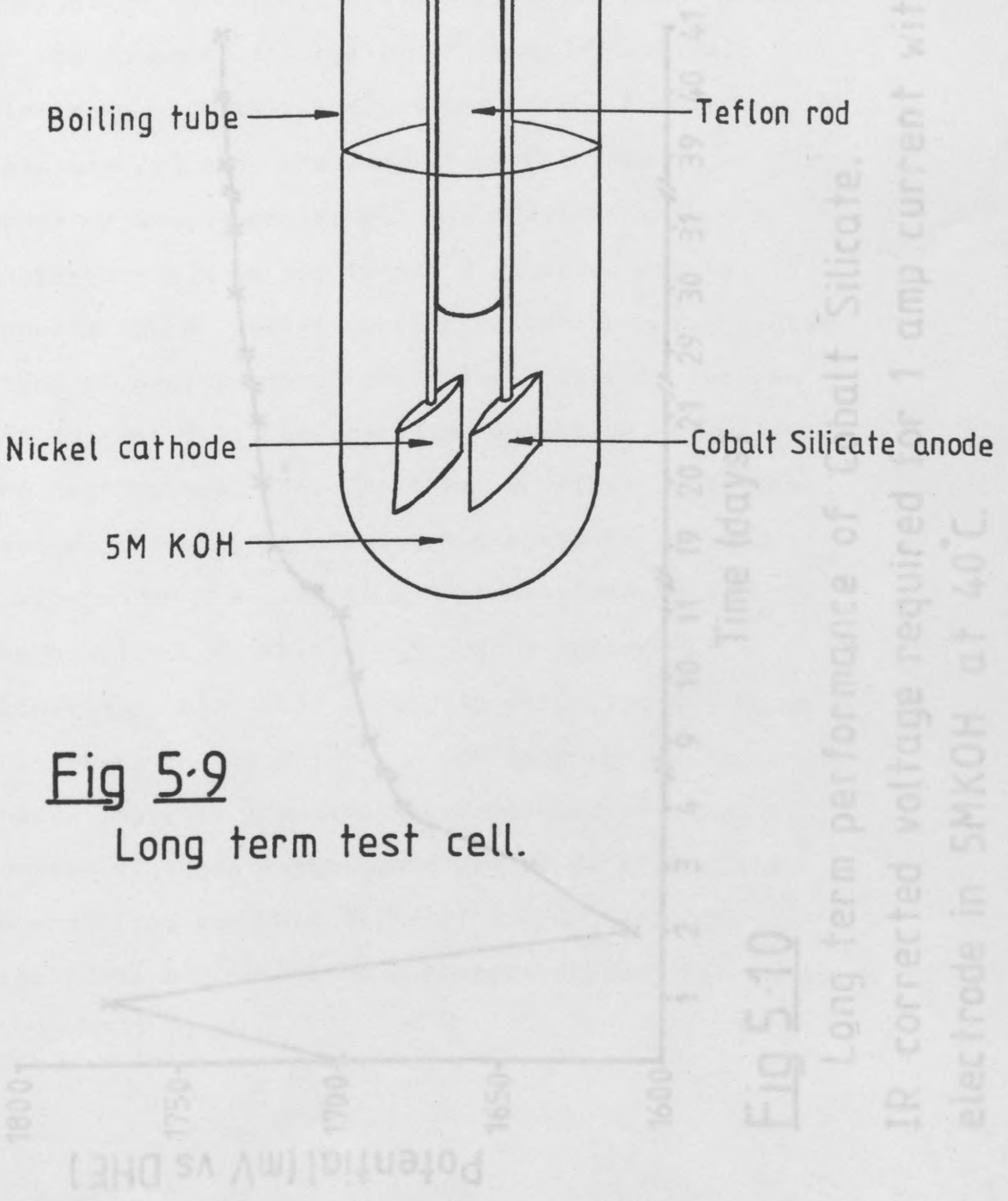
To fully determine the stability of cobalt silicate as an electrocatalyst for the evolution of oxygen a long term evaluation of its performance was carried out.

An electrode was mounted in a cell as per Figure 5.9. The cathode was a nickel screen and the electrolyte was 5M potassium hydroxide.

The cell was run galvanostatically at lamp at  $40^\circ\text{C}$ . Any losses due to electrolysis, spray and evaporation were made up by additions of distilled water. The cell was not run at night or weekends due to the practical difficulties of maintaining the solution level. The voltage drop across the cell was measured daily and the ohmic component of the cell voltage was deduced by the interrupter method. The contribution of the nickel screen was evaluated at the beginning and the end of the run by plotting its ohmic over potential corrected  $V/i$  curve. The subsequent voltage/time curve is shown in Figure 5.10.



**Fig 5-9**  
Long term test cell.



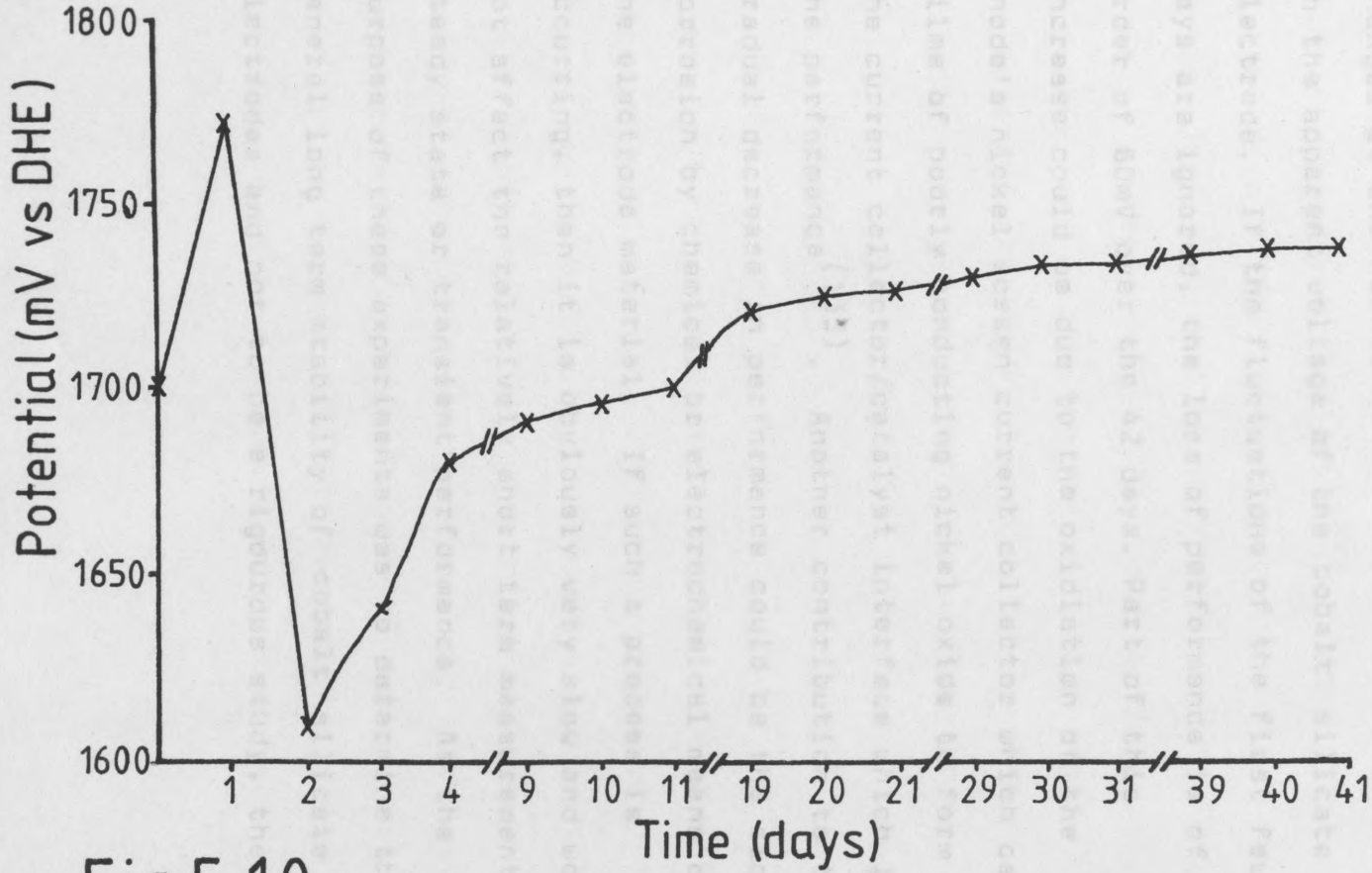


**Fig 5-10**

Long term performance of Cobalt Silicate..  
 IR corrected voltage required for 1 amp current with a 21.2mg loaded electrode in 5MKOH at 40°C.

As can be seen from Figure 5.10 the long term stability of cobalt silicate is reasonable. The large fluctuations of the first three days may be due to the electrode structure being fully established by such things as shedding of loose material and the cleaning out of the teflon channels of any loosely bound catalyst. It may also be due to changes at the nickel electrode, which would reflect on the apparent voltage of the cobalt silicate electrode. If the fluctuations of the first few days are ignored, the loss of performance is of the order of 60mV over the 42 days. Part of this increase could be due to the oxidation of the anode's nickel screen current collector which causes films of poorly conducting nickel oxide to form at the current collector/catalyst interface which limits the performance<sup>(135)</sup>. Another contribution to this gradual decrease in performance could be the slow corrosion by chemical or electrochemical means of the electrode material. If such a process is occurring, then it is obviously very slow and would not affect the relatively short term measurements of steady state or transient performance. As the purpose of these experiments was to determine the general long term stability of cobalt silicate electrodes and not to be a rigorous study, the precise

nature of this loss of performance has not been investigated further.

These long term results also support the premise that the current contribution of the nickel current collector is negligible. It has been reported that the current density associated with the nickel screen falls to an extremely low value with prolonged polarisation<sup>(130)</sup>. Hence after several days polarisation the nickel current collector current component must be very small and the current value is predominantly due to the electro catalyst. As can be seen on the 4th day when this should be the case the electrode in fact has a lower over voltage for 1 amp than when polarisation began.

## 5.7 Conclusions

Cobalt, nickel and iron silicate have been prepared. It was found that heating under hydrogen altered the conductivity of cobalt and iron silicate to a suitably high value to enable their use as electrode materials. In subsequent electrochemical experiments, it has been found that cobalt silicate is an active electro catalyst for the evolution of oxygen and that iron silicate has a reasonable



performance for the same reaction, but corrodes. Various experimental observations suggested that oxygen evolution on these materials is via an oxy-hydroxy intermediate. This prompted a mechanistic study of the evolution of oxygen on cobalt silicate (the corrosion of iron silicate ruling out its suitability for a mechanistic study). It is this study which forms the basis for the next chapter.

A MECHANISTIC STUDY OF OXYGEN EVOLUTION ON COBALT SILICATE

## Introduction

The results reported in Chapter 5 have shown cobalt silicate to have a reasonable activity for oxygen evolution. Several experimental observations have suggested that oxygen evolution occurs via oxy-hydroxy intermediates. To investigate this premise the reaction has been studied using cyclic voltammetry and concentration over potential corrected Tafel curves have been obtained using a potentiostatic pulse technique.

## CHAPTER SIX

### A MECHANISTIC STUDY OF THE EVOLUTION OF OXYGEN

#### ON COBALT SILICATE

#### 6.1 Cyclic Voltammetry

The usefulness of cyclic voltammetry in studying reaction mechanisms has already been established in 4.7. Using an experimental set up similar to that described in 4.7, cyclic voltammograms of Tafel coated cobalt silicate electrodes in 5M potassium hydroxide at 25°C were obtained. Where a sweep rate in excess of 50mV/s was applied, the ramp section of a wave form generator (Chemical Electronics type B1) was used instead of the linear sweep generator. A typical voltammogram is shown in Figure (6.1)

## Introduction

The results reported in Chapter 5 have shown cobalt silicate to have a reasonable activity for oxygen evolution. Several experimental observations have suggested that oxygen evolution occurs via oxy-hydroxy intermediates. To investigate this premise the reaction has been studied using cyclic voltammetry and concentration over potential corrected Tafel curves have been obtained using a potentiostatic pulse technique.

### 6.1 Cyclic Voltammetry

The usefulness of cyclic voltammetry in studying reaction mechanisms has already been established in 4.7. Using an experimental set up similar to that described in 4.7, cyclic voltammograms of teflon bonded cobalt silicate electrodes in 5M potassium hydroxide at 25°C were obtained. Where a sweep rate in excess of 50mV/s was desired, the ramp section of a waveform generator (Chemical Electronics type 01) was used instead of the linear sweep generator. A typical voltammogram is shown in Figure (6.1)

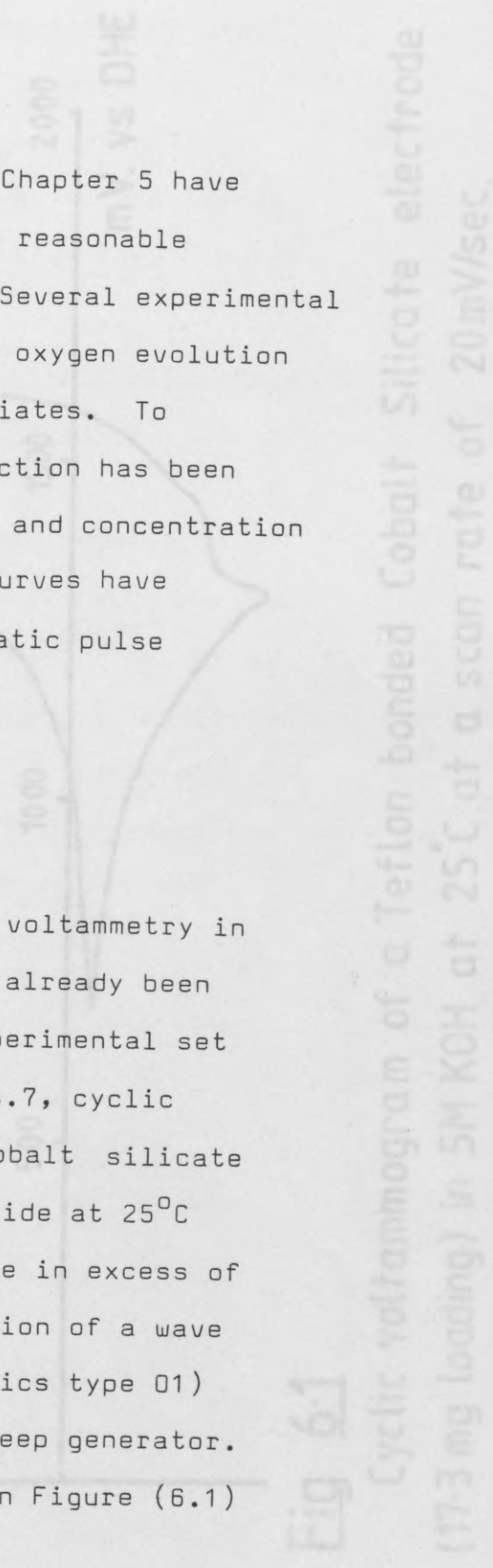
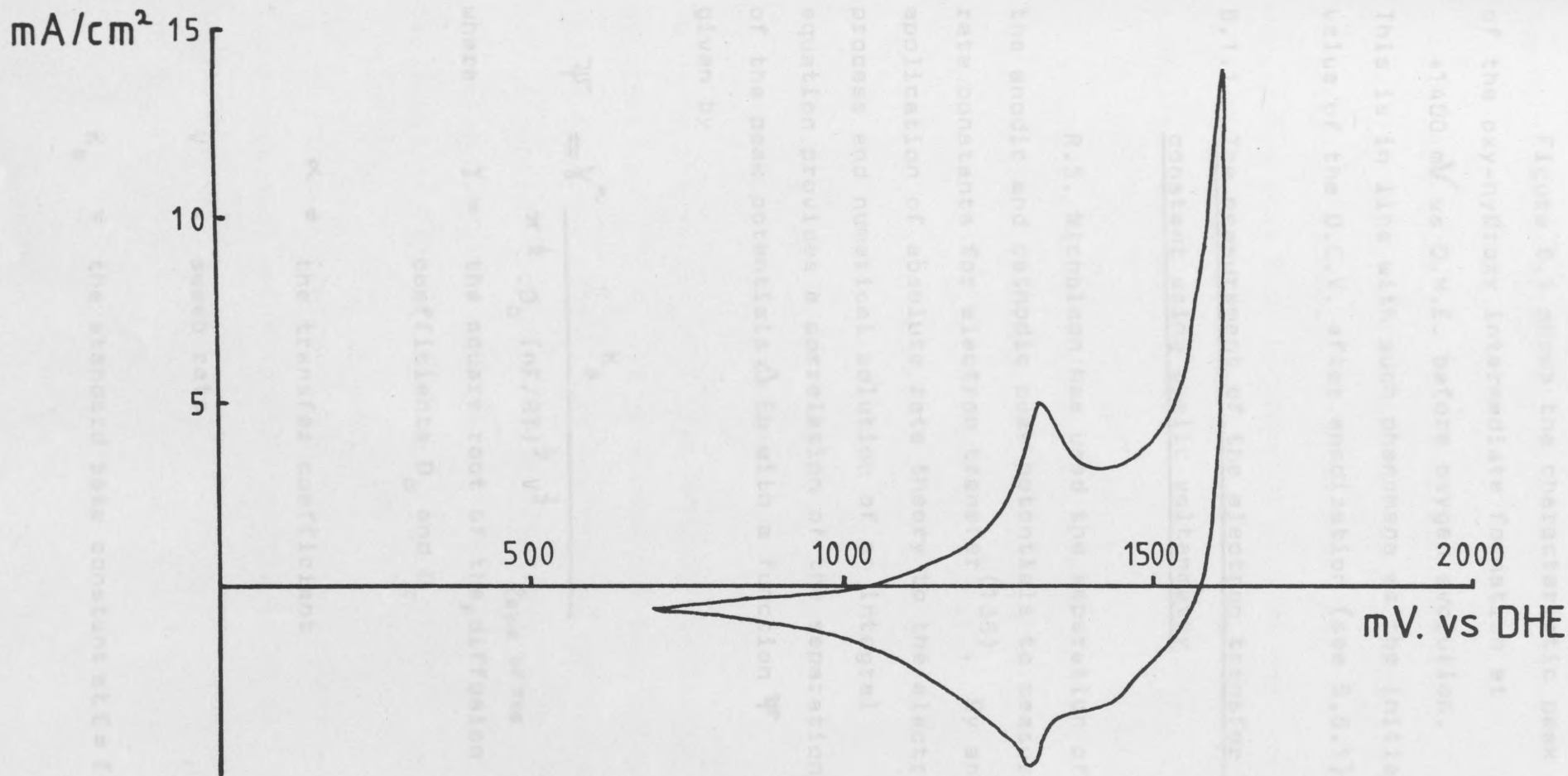


Fig 6.1  
Cyclic voltammogram of a Teflon bonded Cobalt Silicate electrode  
(17.3 mg loading) in 5M KOH at 25°C at a scan rate of 20mV/sec.



**Fig 6.1**

Cyclic voltammogram of a Teflon bonded Cobalt Silicate electrode (17.3 mg loading) in 5M KOH at 25°C at a scan rate of 20mV/sec.

Figure 6.1 shows the characteristic peak of the oxy-hydroxy intermediate formation at +1400 mV vs D.H.E. before oxygen evolution.

This is in line with such phenomena as the initial value of the D.C.V. after anodization (see 5.6.1).

### 6.1.1 The measurement of the electron transfer rate constant using cyclic voltammetry

R.S. Nicholson has used the separation of the anodic and cathodic peak potentials to measure rate constants for electron transfer<sup>(136)</sup>. By an application of absolute rate theory to the electrode process and numerical solution of an integral equation provides a correlation of the separation of the peak potentials  $\Delta E_p$  with a function  $\Psi$  given by

$$\Psi = \gamma^\alpha \frac{K_s}{\pi^{1/2} D_o (nF/RT)^{1/2} v^{1/2}}$$

where  $\gamma =$  the square root of the ratio of the diffusion coefficients  $D_o$  and  $D_r$

$\alpha =$  the transfer coefficient

$v =$  sweep rate

$K_s =$  the standard rate constant at  $E = E^0$

The other terms have their usual significance.

Since the difference in D values is ordinarily small,  $\gamma^\alpha$  is unity for many practical situations. Nicholson has also shown that in many situations  $\Psi$  is independent of  $\alpha$ , as  $\Delta E_p$  is unchanged due to equal changes to the anodic and cathodic peaks.

Adams simplified the above equation with the following approximations<sup>(137)</sup>. If  $\gamma^\alpha = 1$ ,  $D_o = 1 \times 10^{-5}$  cm<sup>2</sup>/sec and  $F/RT = 39.2V^{-1}$  then if V is in volts sec<sup>-1</sup>

$$\Psi \approx 28.8 \frac{K_s}{V^{1/2}}$$

So using the values of  $\Psi$  for various  $\Delta E_p$  quoted by Nicholson<sup>(136)</sup>  $K_s$  may be worked out for various values of sweep rate. This was carried out for a teflon bonded cobaltsilicate electrode in 5M potassium hydroxide at 25°C and the results are tabulated in Table 6.1.

The last entry on the table is probably the result most prone to experimental error as small differences in  $\Delta E_p$  give large differences in  $\Psi$ .

While the values are not absolute due to the assumptions made, the consistency of the results suggests that the reaction is totally

TABLE 6.1

Electron transfer rate constant - calculated at various voltage scan rates.

V (v/s)	$E_p$ (mv)	$\gamma$ 1	$K_s$ (cm <sup>-1</sup> sec <sup>-1</sup> )
0.3	131	0.3	$5.7 \times 10^{-3}$
0.1	106	0.5	$5.5 \times 10^{-3}$
0.03	85	1.0	$6.0 \times 10^{-3}$
0.02	80	1.25	$6.1 \times 10^{-3}$
0.01	67	3.5	$12.0 \times 10^{-3}$

Using diagnostic tests reported by Fletcher it is possible to obtain some further information about the reaction which is occurring (136).

1 - values obtained from Table 1 reference 136

to determine if a reaction is diffusion limited, kinetically controlled, or mixed, the relationship of  $I_p$  (peak current) and  $v$  must be considered. This gives various test results which are listed in Table 6.2.

While the values are not absolute due to the assumptions made, the consistency of the results suggests that the reaction is totally electro chemical and therefore no side chemical reactions of any consequence are occurring at that voltage. This observation is supported by the repeatability of subsequent cycles after the initial sweep. If any chemical reaction had occurred, the shape of subsequent curves would be different to the initial sweep.

Electrode process

Kinetically

Controlled

#### 6.1.2 Additional diagnostic tests of the cyclic voltammetry results

Using diagnostic tests reported by Pletcher it is possible to obtain some further information about the reaction which is occurring<sup>(138)</sup>.

Pletcher first states that if one wishes to determine if a reaction is diffusion limited, kinetically controlled, or mixed, the relationship of  $i_p$  (peak current) and  $V$  must be considered. This gives various test results which are listed in Table 6.2.



If  $i_p$  is plotted against  $V$  and  $\sqrt{V}$  one can deduce how the reaction is controlled.

These are shown in Figure 6.2 and 6.3. These show

that the reaction is controlled by a mixture of diffusion and kinetic limits.

TABLE 6.2

Diagnostic tests for reaction control  
using cyclic voltammetry results

Diffusion Limited Electrode process	Mixed Control	Kinetically Controlled Current
$i_p$ versus $\sqrt{V}$ is linear and passes through the origin.	$i_p$ depends on $V$ but $i_p$ versus $\sqrt{V}$ is non linear	$i_p$ independent of $V$

So if  $i_p$  is plotted against  $V$  and  $\sqrt{V}$  one can deduce how the reaction is controlled. These are shown in Figure 6.2 and 6.3. These show that the reaction is controlled by a mixture of diffusion and kinetic limits.

Pletcher further states that with peaks caused by adsorption steps (or reactions of an existing adsorbed layer) for which the surface reaction and not mass transfer is rate determining can be recognised by the fact that  $i_p$  is directly proportional to  $V$ . Also for adsorption - desorption steps or oxidation and reduction of the adsorbed layer  $\Delta E_p$  is zero. Figure 6.2 shows that  $i_p$  is directly proportional to  $V$ , but as was recorded in 6.1.1  $\Delta E_p \neq 0$ .

From this, the premise may be made that the reaction is surface controlled but not associated with a simple adsorption - desorption process or a reaction of an adsorbed species. This suggests that the reaction is the formation of an oxy-hydroxy intermediate previously mentioned.

Fig 6.2

Plot of peak current vs voltage scan rate for a Teflon bonded Cobalt Silicate electrode (17.3 mg loading) in 5M KOH at 25°C.

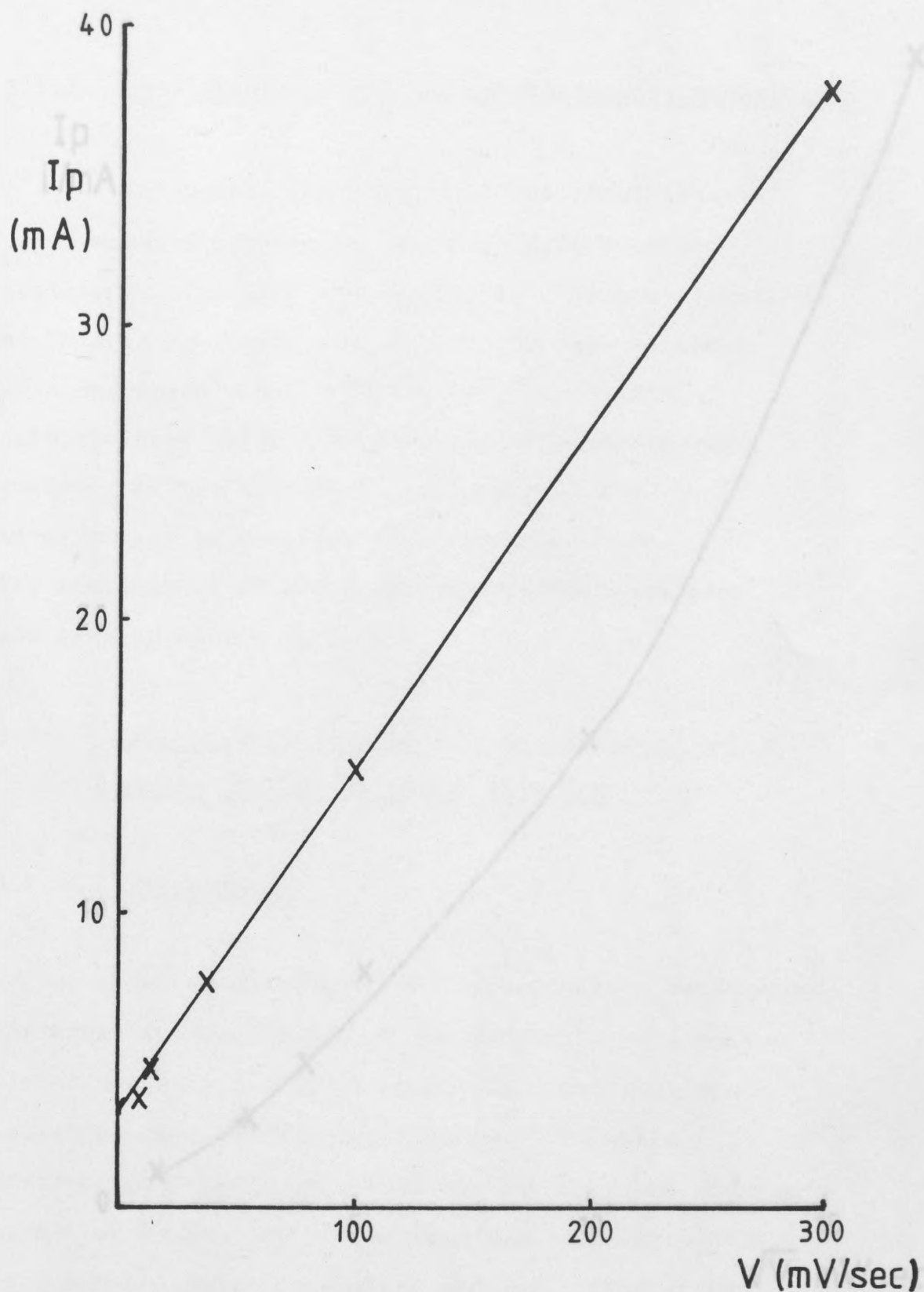


**Fig 6.2**

Plot of peak current vs voltage scan rate for a Teflon bonded Cobalt Silicate electrode (17.3 mg loading) in 5M KOH at 25°C.

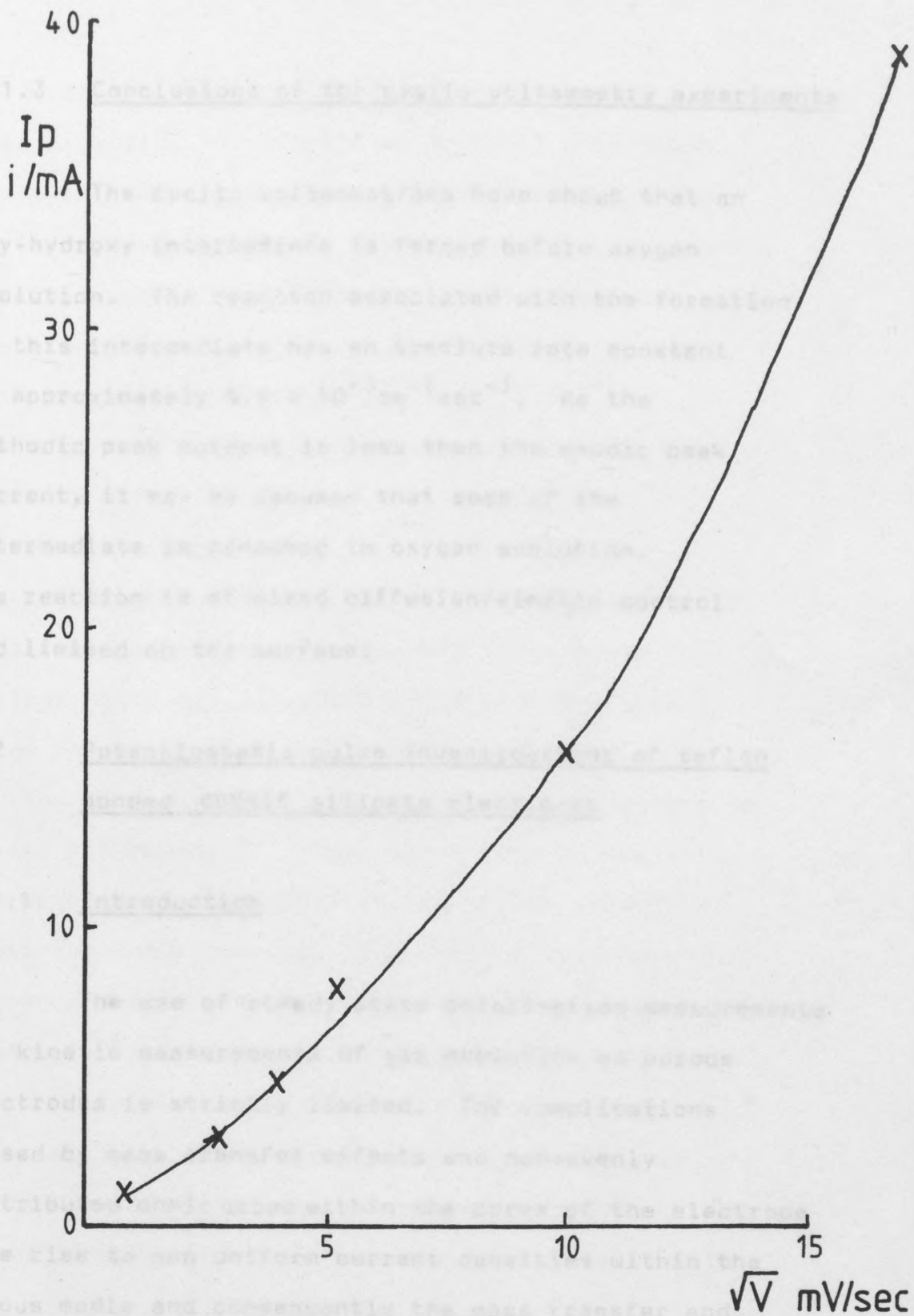


**Fig 6.3**

Plot of peak current vs square root of voltage scan for a Teflon bonded Cobalt Silicate electrode (17.3mg loading) in 5M KOH at 25°C.

### 6.1.3 Conclusions of the cyclic voltammetry experiments

The cyclic voltammograms have shown that an oxy-hydroxy intermediate is formed before oxygen evolution. The reaction associated with the formation of this intermediate has an absolute rate constant of approximately  $5.9 \times 10^{-3} \text{ cm}^{-1} \text{ sec}^{-1}$ . As the cathodic peak current is less than the anodic peak current, it may be assumed that some of the intermediate is consumed in oxygen evolution. The reaction is of mixed diffusion/kinetic control and limited on the surface.

### 6.2 Potentiostatic pulse investigations of teflon bonded cobalt silicate electrodes

#### 6.2.1 Introduction

The use of steady state polarisation measurements for kinetic measurements of gas evolution on porous electrodes is strictly limited. The complications caused by mass transfer effects and non-evenly distributed ohmic drops within the pores of the electrode give rise to non uniform current densities within the porous media and consequently the mass transfer and ohmic over potentials vary throughout the length of the pores<sup>(139)</sup>. Also the general evolution of gas

leads to gas bubbles forming at the base of the pores then expelling the electrolyte when at a suitable pressure. This leads to gas bubbles blocking the surface of the electrode and as a result a constantly varying area is available for electro chemical reaction. Added to this is the complication of oxide formation during oxygen evolution<sup>(140)</sup>. These factors make the application of the Tafel equation difficult.

However, if the current for a fixed voltage could be measured instantaneously after that voltage had been applied, as long as the higher oxide formation problem has been considered, then all the other effects should be able to be discounted. Tseung and Vassie<sup>(140)</sup> have shown that by measuring the potentiostatic transients of Teflon bonded platinum black and platinum foil electrodes, the exchange current density ( $i_0$ ) values for hydrogen evolution in 2.5M sulphuric acid at 25°C were essentially the same. This premise would suggest that, as long as allowances were made for higher oxide formation<sup>(4)</sup>, then potentiostatic pulse measurements should give us meaningful kinetic data.

the cycle. Hobbs, Vassie and Tseung have fully described the technique used<sup>(141)</sup>.

At the instant of applying an over voltage to an electrode, the mass transfer effects are negligible and the over voltage current relationship is governed solely by the charge transfer, if ohmic and double layer charging effects are taken into consideration. As reaction occurs, products are formed and reactants depleted and hence the mass transfer effects become significant. The electrode could be described as a "leaky" condenser and that at the instant of applying potential a very small but finite time is required to charge the electrode. This is known as the double layer charging time. This means that measurements cannot be taken at zero time but must be taken after the double layer is charged. For planar electrodes this time can be predicted using mathematical analysis, assuming semi-infinite diffusion<sup>(100)</sup>. However, the complex mass transfer situation of a porous electrode means that this can not be applied.

The answer to this problem is to measure the double layer charging time at a voltage where Faradaic processes are at a minimum. This can be found from

the cyclic voltammograms. For teflon bonded cobalt silicate electrodes in 5 molar potassium hydroxide in a <sup>n</sup> Nitrogen atmosphere this was found to be +800 mv with respect to the D.H.E. So the electrode was held at this voltage and pulsed anodically for 50-100mv steps. This produced typically the current time trace shown in Figure 6.4. The sharp spike is due to the charging of the double layer, whereas the minimum and the continuation of the trace could be attributed to a) an oscillatory effect in the potentiostat pulse generator and the cell circuit and b) a pseudo-capacity effect. The double layer charging time is measured as per Figure 6.4. It should be noted that the current peak magnitude is changed with voltage, but not the double layer charging time.

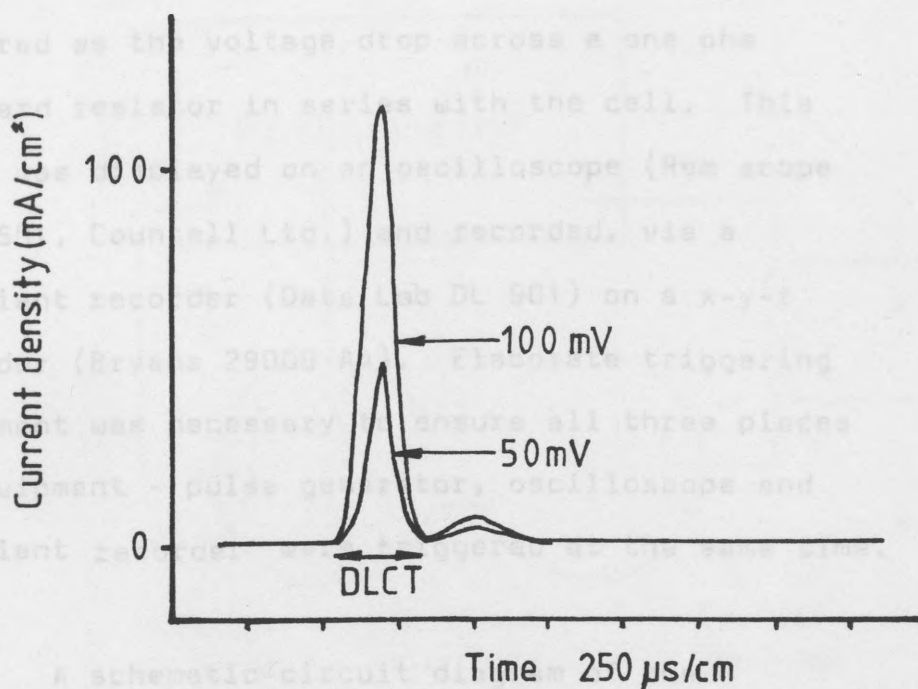
### 6.2.2 Experimental Procedure

The experimental procedure for the measurement of the transients was as follows:-

The electrode was mounted in the same cell as the other electrochemical testing was carried out in. The electrolyte was 5M potassium



hydroxide which had been pre-electrolysed with two platinum gauzes under a nitrogen atmosphere at 5ma for 48 hours. This was to remove any impurities present. The electrode was then held at the desired voltage by the potentiostat (Chemical Electronics 70V/3A) and the voltage pulse was applied as a discrete step by the pulse generator (Chemical Electronics type -Q1). The current transient was



DLCT - Double layer charge time.

### Fig 6.4

Double layer charging trace of a Teflon bonded Cobalt Silicate electrode in 5M KOH at 25°C in a N<sub>2</sub> atmosphere.

hydroxide which had been pre-electrolysed with two platinum gau<sup>z</sup>ses under a nitrogen atmosphere at 5ma for 48 hours. This was to remove any impurities present. The electrode was then held at the desired voltage by the potentiostat (Chemical Electronics 70V/3A) and the voltage pulse was applied as a discrete step by the pulse generator (Chemical Electronics type -01). The current transient was measured as the voltage drop across a one ohm standard resistor in series with the cell. This trace was displayed on an oscilloscope (Rem scope type S01, Countell Ltd.) and recorded, via a transient recorder (Data Lab DL 901) on a x-y-t recorder (Bryans 29000 A4). Elaborate triggering equipment was necessary to ensure all three pieces of equipment - pulse generator, oscilloscope and transient recorder were triggered at the same time.

A schematic circuit diagram of the potentiostatic pulse system is shown in Figure 6.5.

The over voltages pertaining to the transient currents were corrected for ohmic losses by measuring

the ohmic drop by a galvanostatic pulse method.  
This is shown schematically by Fig. 6.5.

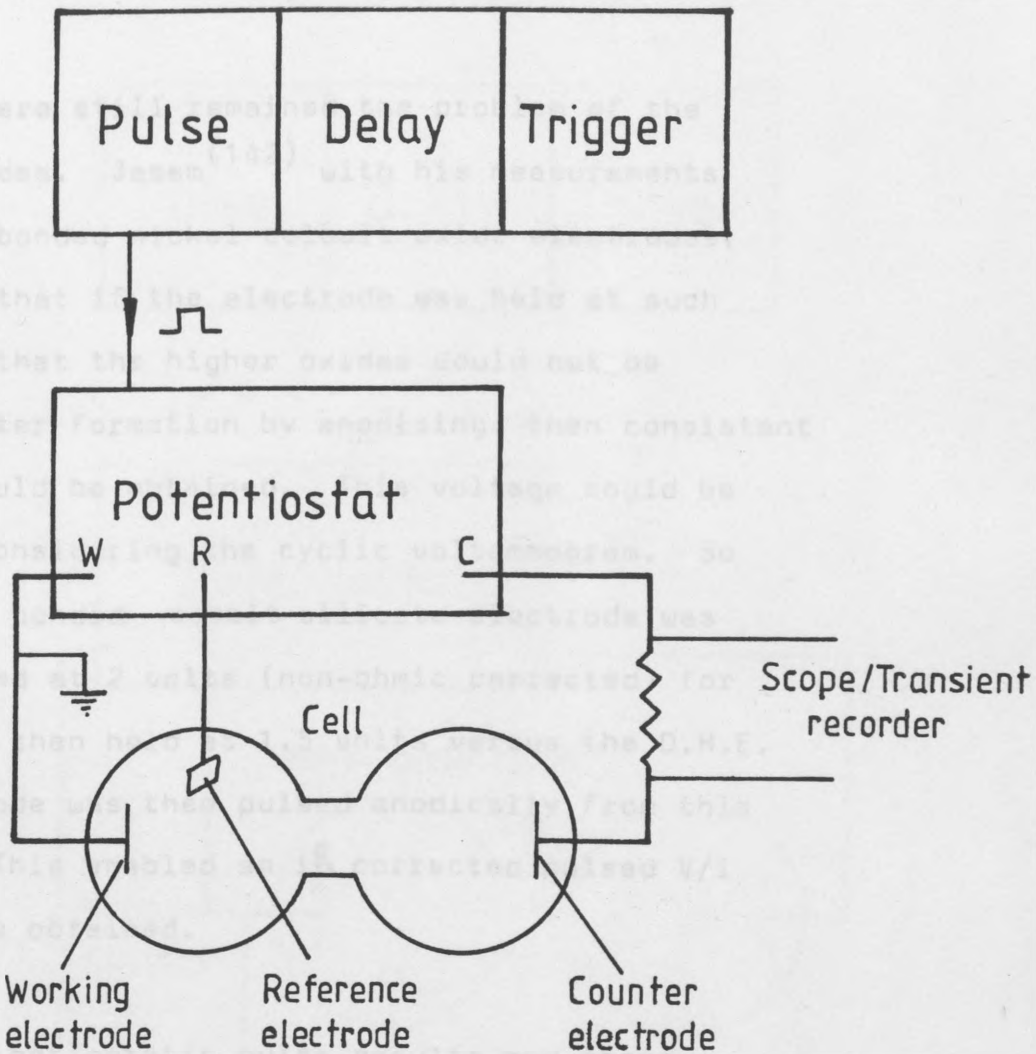


**Fig 6.5**

Schematic circuit diagram for potentiostatic pulse measurements.

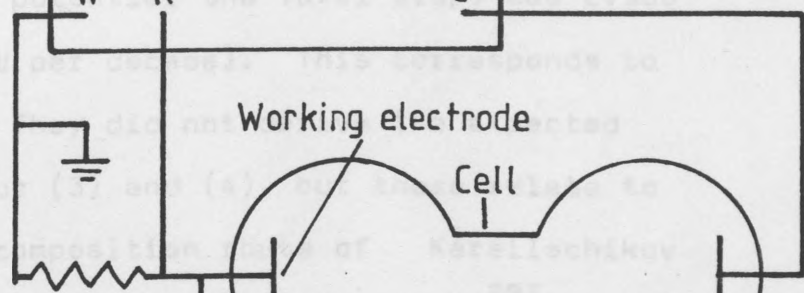
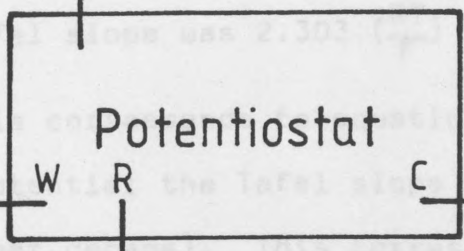
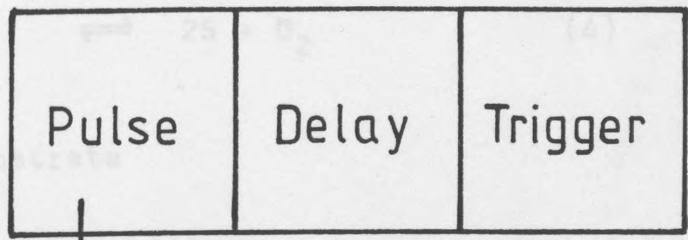
the ohmic drop by a galvanostatic pulse method. This is shown schematically in Figure 6.6.

There still remained the problem of the higher oxides. Jasem<sup>(142)</sup> with his measurements on teflon bonded nickel cobalt oxide electrodes, had found that if the electrode was held at such a voltage that the higher oxides would not be reduced after formation by anodising, then consistent results could be obtained. This voltage could be found by considering the cyclic voltammogram. So the teflon bonded cobalt silicate electrode was pre-anodised at 2 volts (non-ohmic corrected) for two hours, then held at 1.5 volts versus the D.H.E. The electrode was then pulsed anodically from this voltage. This enabled an  $iR$  corrected pulsed  $V/i$  curve to be obtained.

### 6.2.3 Potentiostatic pulse results and their interpretation

Iwakuru, Fukuda and Tamura have studied the evolution of oxygen on platinum oxide in alkaline solutions<sup>(143)</sup>. They formulated the following reaction sequence assuming Langmuir conditions:-

# Pulse Generator



Working electrode

Cell

Standard Resistor

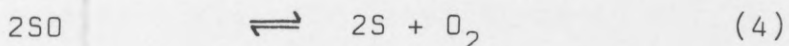
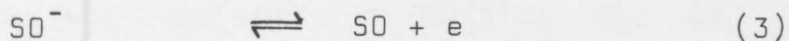
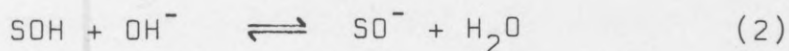
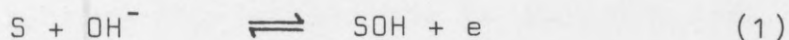
Scope/Transient recorder

Reference electrode

Counter electrode

**Fig 6.6**

Schematic circuit diagram for galvanostatic pulse measurements.



where S = the substrate

They found when  $\eta$  was plotted against  $\log i$  there were 2 distinct Tafel regions. At low over potential the Tafel slope was  $2.303 \left(\frac{RT}{F}\right)$  (or 60 mV per decade). This corresponds to equation (2). At higher over potential the Tafel slope was  $2.303 \left(\frac{2RT}{F}\right)$  (or 119mV per decade). This corresponds to equation (1). They did not derive the expected Tafel slopes for (3) and (4), but these relate to the "oxide" decomposition route of Karsilshikov and as such have Tafel slopes of  $2.303 \left(\frac{2RT}{3F}\right)$  (or 40 mV <sup>per</sup> decade) and  $2.303 \left(\frac{RT}{4F}\right)$  (or 15mV <sup>per</sup> decade) respectively (144).

Using the methods described in 6.2.1 a potentiostatic pulse voltage vs log current plot for a teflon bonded cobalt silicate electrode in 5M potassium hydroxide was obtained. This is shown in Figure 6.7. The plot shows 2 Tafel regions. At low

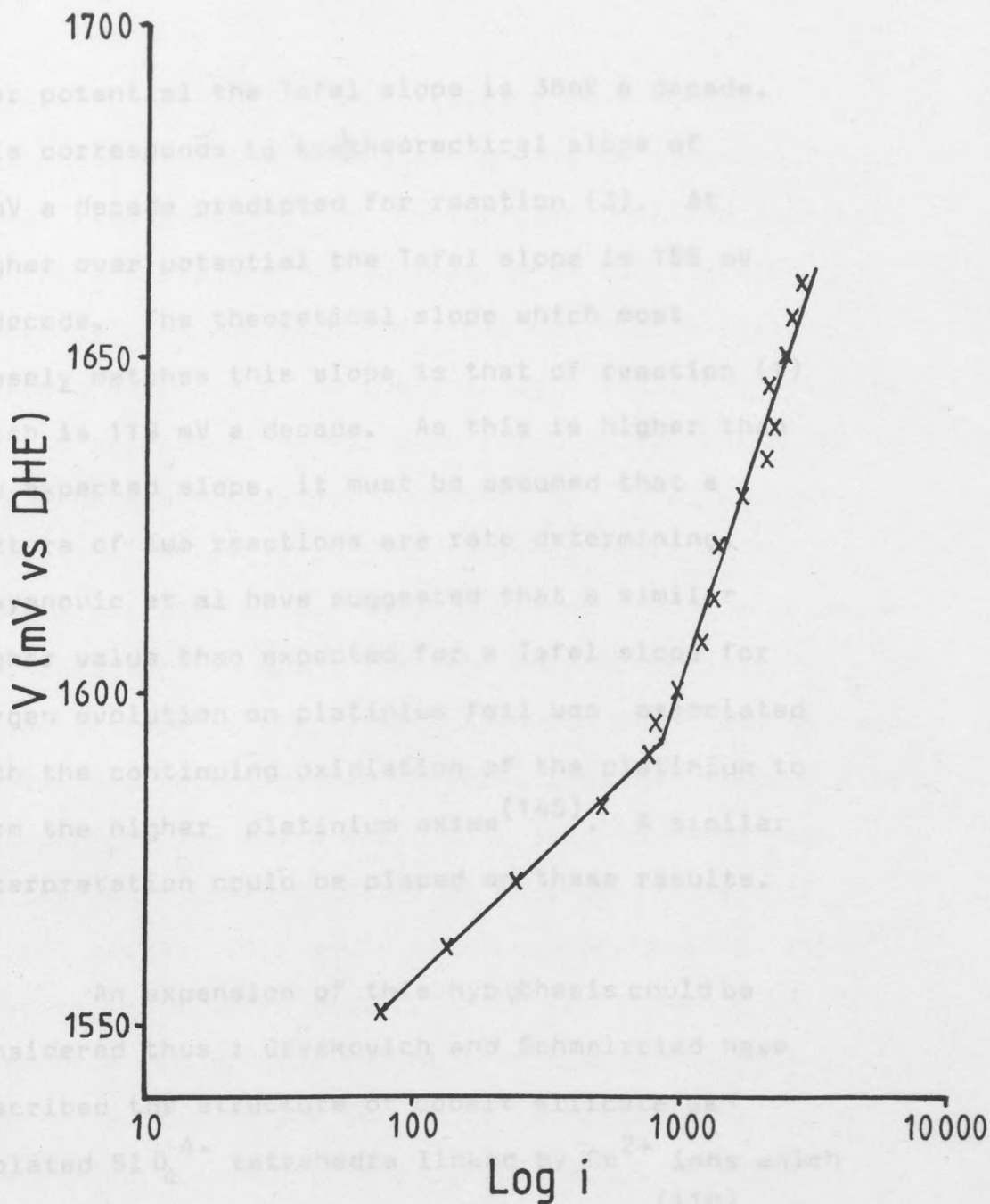


**Fig 6.7**

Tafel plot for a Teflon bonded Cobalt Silicate (17.4 mg loading) electrode in 5M KOH at 25°C.

over potential the Tafel slope is 36mV a decade. This corresponds to the theoretical slope of 40mV a decade predicted for reaction (3). At higher over potential the Tafel slope is 155 mV a decade. The theoretical slope which most closely matches this slope is that of reaction (1) which is 119 mV a decade. As this is higher than the expected slope, it must be assumed that a mixture of two reactions are rate determining. Danyanovic et al have suggested that a similar higher value than expected for a Tafel slope for oxygen evolution on platinum foil was associated with the continuing oxidation of the platinum to form the higher platinum oxide<sup>(145)</sup>. A similar interpretation could be placed on these results.

An expansion of this hypothesis could be considered thus : Greskovich and Schmalzried have described the structure of cobalt silicate as isolated  $\text{SiO}_4^{4-}$  tetrahedra linked by  $\text{Co}^{2+}$  ions which are in an octrahedral oxygen environment<sup>(110)</sup>. They state that cobalt silicate exhibits similar non-stoichiometry and hence electronic defects to the binary metal oxide  $\text{Co}_{1-\delta}\text{O}$ . This deviation from stoichiometry leads to defect concentrations associated with single ionised cation vacancies and electron holes in the form of  $\text{Co}^{3+}$  ions are



present. As the cobalt silicate used in these experiments was rendered conducting by hydrogen heat treatment, it must be surmised that the electrode surface has a high concentration of such defects. Such defects would be the ideal reaction sites for oxygen evolution. At low over potential, the reaction would proceed as normal with reaction (3) being the rate determining step. However, at higher over potential there would be greater competition for these reaction sites. This is mirrored in the movement to reaction (1) being the rate determining step. However, due to the tight octahedral structure of cobalt silicate, access to all possible reaction sites may be hindered. The extra energy required to reach such sites would exhibit itself as an increase in the Tafel slope. This would also possible explain the cyclic voltammetry results which found that the reaction was to some extent kinetically controlled at the surface (note the pulse technique as a cross reference has removed any consideration of the diffusion control present with the cyclic voltammetry results).

The other aspect to consider is the comparison between cobalt silicate's transient performance and steady state performance. This is shown in Figure 6.8. Tseung and Vassie have developed the concept of an electrode utilization factor to compare the transient

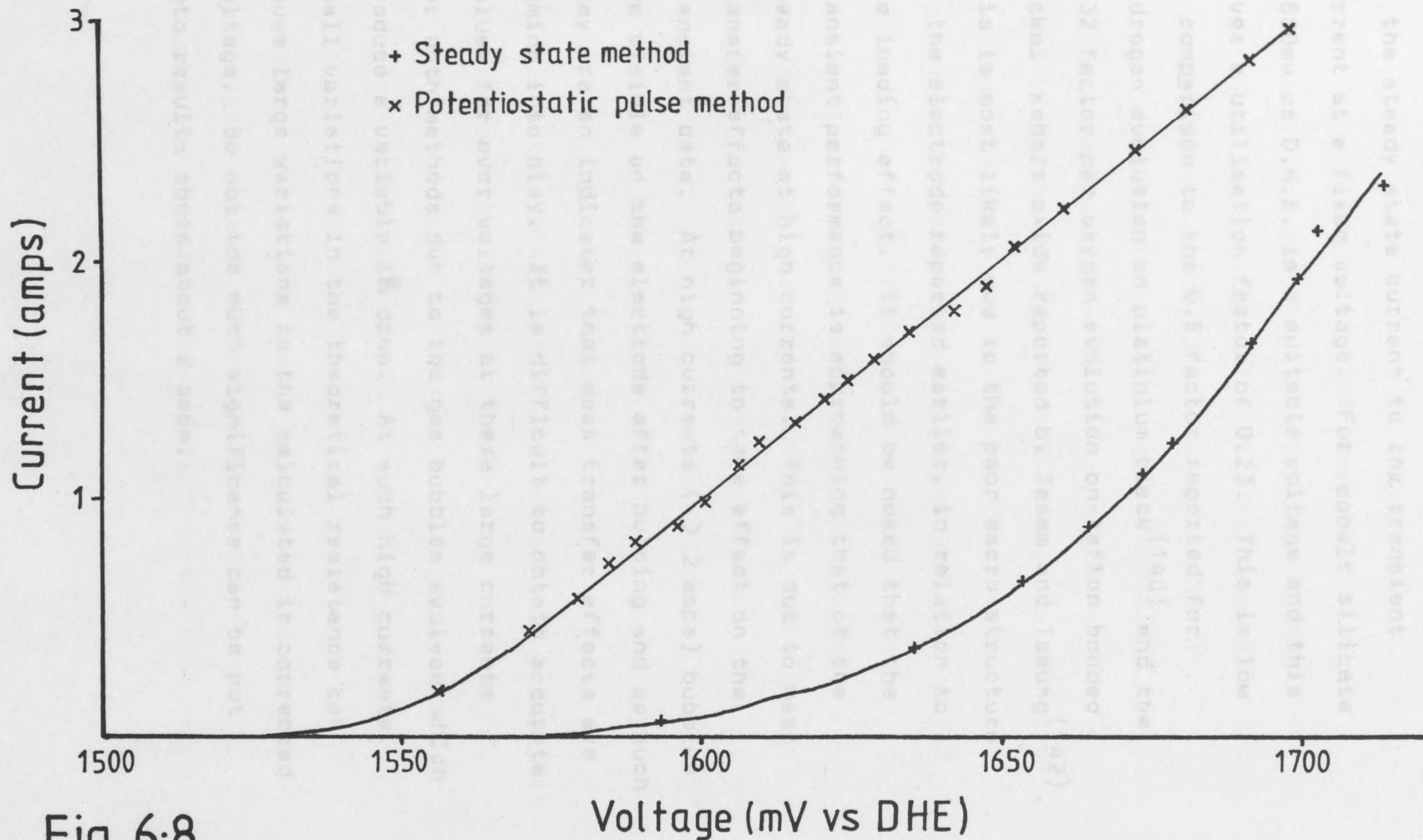


**Fig 6.8**

Comparison of  $V/i$  curves obtained for a Teflon bonded Cobalt Silicate electrode (17.4 mg loading) in 5M KOH at 25°C by steady state and pulse measurements

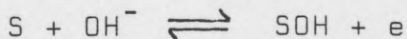
with steady state behaviour<sup>(140)</sup>. This is the ratio of the steady state current to the transient current at a fixed voltage. For cobalt silicate +1650mv vs D.H.E. is a suitable voltage and this gives a utilisation factor of 0.23. This is low in comparison to the 0.5 factor reported for hydrogen evolution on platinum black<sup>(140)</sup> and the 0.32 factor per oxygen evolution on teflon bonded nickel cobalt oxide reported by Jasem and Tseung<sup>(142)</sup>. This is most likely due to the poor macro structure of the electrode reported earlier, in relation to the loading effect. It should be noted that the transient performance is approaching that of the steady state at high currents. This is due to mass transfer effects beginning to take effect on the transient data. At high currents ( $> 2$  amps) bubbles are visible on the electrode after pulsing and as such they are an indicator that mass transfer effects are coming into play. It is difficult to obtain accurate values for over voltages at these large currents for both methods due to the gas bubbles evolved which produce a variable  $iR$  drop. At such high currents, small variations in the theoretical resistance can cause large variations in the calculated  $iR$  corrected voltage. So not too much significance can be put into results above about 2 amps.

### 6.3 Conclusions

The results obtained from the cyclic voltammetry and potentiostatic pulse investigations have shown that the creation of an oxy-hydroxy intermediate is the essential step in the evolution of oxygen on teflon bonded cobalt silicate in alkaline solutions. In the mass transfer effected environment of cyclic voltammetry the reaction was found to be under a mixture of diffusion and kinetic control by a reaction limited on the surface of the electrode. When the over potential caused by mass transfer effects was removed by using the potentiostatic pulse technique it was found that for low over potentials the reaction

$$SO^- \rightleftharpoons SO + e$$

was the rate limiting step. At higher over potentials it was found that the reaction



was the rate limiting step. A model involving the defect structure of cobalt silicate has been proposed to explain why the Tafel slope for higher

over potentials is larger than was predicted theoretically.

The results indicate that cobalt silicate behaves in a similar manner to cobalt oxide. Certainly the reaction centre can be considered to be similar to cobalt oxide. This would suggest that cobalt silicate is not viable as a possible photo electrode material, as the band gap of cobalt oxide ( $0.47\text{eV}$  at  $-23^{\circ}\text{C}$ ,  $0.73\text{eV}$  at  $100^{\circ}\text{C}$ ) is too low to be of use<sup>(102)</sup>. The acid test of this premise would be to study the photo electrochemical behaviour of cobalt silicate. However, time did not allow for this to be done, especially as any electrode would have to meet the requirements reported in Chapter 3. As cobalt silicate did not readily lend itself to these limitations on electrode fabrication, the development of a test electrode would be a long task.

## 7.1 Conclusions

Using finely oxidized iron as a test electrode the importance of oxy-hydroxy intermediates in the photo-assisted evolution of oxygen has been ascertained. The presence and nature of these intermediates have been ascertained by study of the transient photo current behaviour of the illuminated electrode. This connection between photo electrochemical behaviour and the oxy-hydroxy intermediates proposed

### CHAPTER SEVEN

#### CONCLUSIONS AND SUGGESTIONS FOR FURTHER WORK

silicates as potential photo-electrode materials. Nickel silicate could not be made in a suitably conducting form and iron silicate was found to corrode. However, cobalt silicate was found to be stable and gave a reasonable steady state performance for the evolution of oxygen. Investigations based on transient methods showed that oxy-hydroxy intermediates were formed during oxygen evolution and they played a crucial role in the reaction sequence. It was also found that the reaction centres of cobalt silicate could be considered to be similar to cobalt oxide and, as such, could be ruled out as a possible photo-electrode on grounds of a low band gap. Time and experimental considerations ruled out the testing of cobalt silicate as a photo-electrode material.

## 7.1 Conclusions

Using flame oxidized iron as a test electrode the importance of oxy-hydroxy intermediates in the photo-assisted evolution of oxygen has been ascertained. The presence and nature of these intermediates have been ascertained by study of the transient photo current behaviour of the illuminated electrode. This connection between photo electrochemical behaviour and the oxy-hydroxy intermediates prompted the investigation of cobalt, nickel and iron silicates as potential photo-electrode materials. Nickel silicate could not be made in a suitably conducting form and iron silicate was found to corrode. However, cobalt silicate was found to be stable and gave a reasonable steady state performance for the evolution of oxygen. Investigations based on transient methods showed that oxy-hydroxy intermediates were formed during oxygen evolution and they played a crucial role in the reaction sequence. It was also found that the reaction centres of cobalt silicate could be considered to be similar to cobalt oxide and, as such, would be ruled out as a possible photo-electrode on grounds of a low band gap. Time and experimental considerations ruled out the testing of cobalt silicate as a photo-electrode material.

## 7.2 Possible further investigations into photo electrochemistry

As outlined in Chapter 2, photo electrochemistry is a fertile field for multi-faceted experimental investigations. The three general areas for consideration arising out of this study are:

- 1) Methods to incorporate materials with low lower/higher oxide potentials e.g. cobalt into photo-electrodes. The use of such compounds as dopants is of interest, especially in light of the reported results of the visible light response of titanium dioxide (40,48). An electrode of a flame oxidized iron/cobalt alloy would be interesting.
- 2) The further study of the oxy-hydroxy intermediates formed in the photo-assisted evolution of oxygen by various electrochemical and surface analysis techniques will provide an insight into the reaction mechanism and possibly the nature of the charge transfer process.
- 2) An investigation into alternative preparation techniques, allied with the preparation of a conducting form of nickel silicate,



- 3) As the importance of reaction intermediates in photo electrochemistry has been highlighted, the investigation of the reaction mechanism of other photo electrochemical reactions involving such couples as sulphur/sulphide and iodine/iodide will provide an insight to improving on electrodes photo electrochemical efficiency.

In all such studies the key to success is the combination of conventional electrochemical techniques with the new methods of photo electrochemistry.

### 7.3 Further investigative work into the properties of cobalt silicate

Cobalt silicate has proved itself to be a reasonable electrocatalyst for the evolution of oxygen. This compound deserves study in the following areas:-

- 1) An optimisation of its performance and a full investigation of its long term stability.
- 2) An investigation into alternative preparation techniques, allied with the preparation of a conducting form of nickel silicate.

- 3) Fuller investigations into the nature of the oxy-hydroxy intermediates formed during the evolution of oxygen could be carried out. Various surface analysis techniques could be used, and the use of experiments using  $H_2O^{18}$  as the supporting electrolyte could test to what extent the lattice oxygen atoms are involved in oxygen evolution.
- 4) To confirm the theory put forward in Chapter 6, a suitable cobalt silicate electrode could be made within the limitations of Chapter 3. to be tested for any possible photoelectrochemical response. The other possibility is the measurement of the band gap of cobalt silicate.
1. A.C.C. Tsang and S.M. Jaseen, *Electrochim. Acta.*
2. A. Fujishima and N. Honda, *Bull. Chem. Soc. Japan*, 44, p.1148 (1971).
3. H. Garischer, *J. Electroanal. Chem.*, 58, p.263 (1975).
4. S.M. Alkhatib and R.D. Armstrong, Paper presented to the Spring meeting of the Electrochemical Society, Boston, U.S.A. (1975).
5. J.M. Bolts and N.S. Wilson, *J. Phys. Chem.*, 80, p.2847 (1976).
6. R.D. Armer, *J. Appl. Electrochem.*, 5, p.77 (1975).

REFERENCES

1. J.I.B. Wilson, Solar Energy, Wykeham (London), (1979).
2. A. Fujishima and K. Honda, Nature, 238, p.37 (1972).
3. N. Biederman, K. Darrow Jr. and A. Konopka, Research project 320-1, final report Aug.(1975) Institute of Gas Technology - Chicago.
4. A.C.C. Tseung and S.M. Jasem, Electrochim. Acta, 22, p.31 (1977).
5. H. Shallaby and A.T. Kuhn, Electrochim. Acta, 25, p.745 (1980).
6. E. Becquerel, C.R. Acad.Sci., 9, p.561 (1839).
7. Yu.V. Pleskov, S.A. Rotenberg, J. Electroanal. Chem., 20, p.1 (1960).
8. H. Gerischer, Adv. Electrochem. Eng., 1, P.139 (1961).
9. A. Fujishima and K. Honda, Bull. Chem. Soc. Japan, 44, p.1148 (1971).
10. H. Gerischer, J. Electroanal.Chem., 58, p.263 (1975).
11. S.A. Alkaitis and R.D. Rouh, Paper presented to the Spring meeting The Electrochemical Society, Boston, U.S.A. (1979).
12. J.M. Bolts and M.S. Wrighton, J. Phys.Chem., 80, p.2647 (1976).
13. M.D. Archer, J. Appl. Electrochem., 5, p.17 (1975).

14. R. Memming, *Electrochim. Acta*, 25, p.77 (1980).
15. H. Gerischer and W.Mindt, *Electrochim. Acta*,  
13, p. 1329 (1968).
16. J.M. Kowalski, K.H. Johnson and H.L. Tuller,  
Paper presented to the Spring Meeting The  
Electrochemical Society, Boston, U.S.A., (1979).
17. R. Wilson, *J. Appl. Phys.*, 48, p.4292 (1977).
18. J.M. Kowalski, K. Johnson and H. Tuller,  
*J. Electrochem. Soc.*, 127, p.1969 (1980).
19. D. Ullman, *J. Electrochem. Soc.*, 128, p.1269  
(1981).
20. K. Ohashi, J. McCann and J.O'M Bockris, *Nature*,  
226, p. 610 (1977).
21. B. Kraeutler and A.J. Bard, *J.Am.Chem.Soc.*,  
99:23, p.7729 (1977).
22. R.N. Noufi, P.A. Kohl, S.N.Frank and A.J. Bard,  
*J. Electrochem. Soc.*, 125, p. 246 (1978).
23. A.J. Nozik, *Nature*, 257, p. 383 (1975).
24. L.A. Harris, P.R. Cross and M.E. Gerstner,  
*J. Electrochem. Soc.*, 124, p.839 (1977).
25. P.J. Boddy, *J. Electrochem. Soc.*, 115, p.199  
(1968).
26. A. Fujishima, K. Sakamoto and K. Honda, *Seisan  
Kenkyu*, 21:7, p.450, (1969).
27. F. Decker, J.F. Juliao and M. Abramovich,  
*Appl. Phys, Lett.*, 35 (5), p.397 (1979).
28. J. Vandermolen, W.P. Gomes and F. Cardon,  
*J. Electrochem. Soc.*, 127, p.324 (1980).

29. R.H. Wilson, J. Electrochem. Soc., 127, p.228 (1980).
30. R. Schumacher et al, J. Electrochem. Soc., 127, p.86 (1980).
31. W. Siripala and M. Tomkiewicz, J. Electrochem. Soc., 129, p.1240 (1982).
32. B. Parkinson et al, Electrochim. Acta, 25, p.521 (1980).
33. M. Miyake, H. Yoneyama and H. Tamura, Electrochim. Acta, 21, p.1065 (1976).
34. M. Tomkiewicz and J.M. Woodall, J. Electrochem. Soc., 124, p.1436 (1977).
35. A. Monnier and J. Augustynski, J. Electrochem. Soc., 127, p.1576 (1980).
36. Y. Matsumoto, T. Shimiza and E. Sato, Electrochim. Acta, 27, p.419 (1982).
37. A.J. Bard, Paper presented to the Spring Meeting The Electrochemical Society, Boston, U.S.A., (1979).
38. F. Mollers, H.Tolle and R. Memming, J. Electrochem. Soc., 121, p.1160 (1974).
39. K.L. Hardee and A.J. Bard, J. Electrochem. Soc., 122, p.739 (1975).
40. W. Gissler, P.L. Lensi and S. Pizzini, J. Appl. Electrochem., 6, p.9 (1976).
41. J. Keeney, D.H. Weinstein and G.M. Haas, Nature, 253, p.719 (1975).
42. P. Clechet et al, Electrochim. Acta., 24, p.457 (1979).
43. R.H. Wilson, J. Electrochem. Soc., 127, p.228 (1980).
44. P. Fleishauer and J.K. Allen, J.Phys. Chem., 82, p.432 (1978).

45. J.F. Juliao, F. Decker and M. Abramovich, J. Electrochem. Soc., 129, p.1240 (1982).
46. Y. Matsumoto et al, J. Electrochem. Soc., 127, p.2148 (1980).
47. K. Rajeshwar, J. Electrochem. Soc., 129, p.1003 (1982).
48. A.Heller and B. Miller, Electrochim.Acta, 25, p.29 (1980).
49. B. Noufi and J. Tench, J. Electrochem. Soc., 127, p. 189 (1980).
50. L.S. Yeh and N. Hackerman, J. Phys. Chem., 82,p.2719 (1978).
51. A.Heller, K.C. Chang and B. Miller, J. Electrochem. Soc., 124, p.697 (1977).
52. A. Fujishima, E. Sugiyama and K. Honda, Seisor Kenkya, 44, p.304, (1971).
53. A.B. Ellis, S.W. Kaiser and M.S. Wrighton, J. Am. Chem.Soc., 98:6 , p.1635 (1976).
54. J.M. Bolts et al, J. Am.Chem.Soc., 99:14, p.4826 (1977).
55. B. Miller et al, J. Electrochem.Soc., 124, p.1019 (1977).
56. J. Manassen, G. Hodes and D. Cohen, J. Electrochem. Soc., 124, p.532 (1977).
57. J. Manassen, G. Hodes and D. Cohen Nature, 261, p.403 (1976).
58. A.M. Buoncristiani, Paper presented to the Spring Meeting Electrochemical Society, Boston, U.S.A., (1979).

59. M.S. Wrighton et al, J. Am Chem.Soc., 98:10 ,  
p.2774 (1976).
60. J.G. Marvides et al, Appl. Phys. Lett., 28,  
p.241 (1976).
61. J. Kennedy and K.Frese, J. Electrochem. Soc.,  
125, p.709 (1978).
62. J. Kennedy and K. Frese, J. Electrochem. Soc.,  
125, p.723 (1978).
63. J. Curran and W. Gissler, J Electrochem Soc.,  
126, p. 56 (1979).
64. L.S.R. Yeh and N. Hackerman, J. Electrochem.  
Soc., 124, p.833 (1977).
65. S. Wilhelm et al, J. Electrochem. Soc., 126,  
p.419 (1979).
66. K.S. Yun et al, J. Electrochem. Soc., 127,  
p.85 (1980).
67. P.G.P. Ang and A.F. Sammells, Paper presented  
to Spring Meeting of the Electrochemical Society,  
Boston, U.S.A. (1979).
68. A.F. Sammells and P.G.P. Ang., J. Electrochem.  
Soc., 126, p.1831 (1979).
69. F.T. Liou, C.U. Yang and S.N. Levine, J. Electrochem.  
Soc., 129 , p.342 (1982).
70. P. Iwanski, J.S. Curran, W. Gissler and R. Memming,  
J. Electrochem. Soc., 128, p.2128 (1981).
71. J. Kennedy, M. Andermann and R. Shinar, J. Electrochem.  
Soc., 128, p.2371 (1981).
72. K.L. Hardee and A.J. Bard, J.Electrochem. Soc., 123  
p.1024 (1976).

73. K.L. Hardee and A.J. Bard, *J. Electrochem. Soc.*, 124, p.215 (1977).
74. J. Jorne. Paper presented to Spring Meeting of the Electrochemical Society, Boston, U.S.A. (1979).
75. W. Gissler and R. Memming, *J. Electrochem. Soc.*, 124, p.1710 (1977).
76. M.A. Butler, *J.App.Phys.*, 48, p.1914 (1977).
77. W. Kautek and F. Willig, *Electrochim Acta*, 26, p.1709 (1981).
78. H. Tributsch, *J. Electrochem. Soc.*, 125, p.1086 (1978).
79. Fu Ren et al, *J. Electrochem. Soc.*, 127,p.518 (1980).
80. Y. Nakato, A. Tsumura and H. Tsubomura, *J. Electrochem. Soc.*, 127, p.1502 (1980).
81. C. Vazquez-Lopez et al, *J. App. Phys.*,50, p.5391 (1979).
82. M.S. Wrighton et al, *J. Am.Chem.Soc.*, 98:1, p.44 (1976).
83. H. Tributsch and J.C. Bennett, *J. Electroanal Chem.*, 81, p.97 (1977).
84. S.M. Ahmed and H. Gerischer, *Electrochim. Acta*, 24, p.705 (1979).
85. D. Ginley and M. Butler, Paper presented to Spring Meeting of the Electrochemical Society, Boston, U.S.A., (1979).
86. J. O'M Bockris and K. Uosaki, *J. Electrochem. Soc.*, 124, p. 1348 (1977).



87. F. Williams and A. Nozik, *Nature*, 271, p.137 (1978).
88. H. Gerischer, *Sur. Sci.*, 18, p.97 (1969).
89. H. Reiss, *J. Electrochem. Soc.*, 125, p.937 (1978).
90. W.J. Albery and P.N. Bartlett, *J. Electrochem. Soc.*, 128, p.1492 (1981).
91. S.M. Wilhelm and N. Hackerman, *J. Electrochem. Soc.*, 128, p.1668 (1981).
92. R.M. Condea, *Electrochim. Acta*, 26, p.1797 (1981).
93. D. Caplan and M. Cohen, *Corr. Sci.*, 6, p.321 (1966).
94. N. Ramasubramanian, P.B. Sewell and M. Cohen, *J. Electrochem. Soc.*, 115, p.12 (1968).
95. C.J.R. Sheppard and H. Ahmed, *Corr. Sci.*, 16, p.819 (1976).
96. R.J. Hussey et al, *Oxid. of Metals*, 11, p.65 (1977).
97. P. Kofstad, *High Temperature Oxidation of Metals*, The Corrosion Monograph Series, J. Wiley and Sons Inc. (1977).
98. J.B. Goodenough, *Progress in Solid State Chemistry*, H.Reiss editor, Pergamon Press (Oxford), 5, p.145 (1971).
99. Technical note, *J. Electrochem. Soc.*, 111, p.376 (1964).
100. P. Delahay, *New Instrumental Methods in Electrochemistry*, Interscience, p.163 (1973).

101. H. Gerischer, *J. Electroanal. Chem.*, 82,  
p.133 (1977).
102. W.H. Strehlow and E.L. Cook, *J. Phys. Chem. Ref. Data*, 2, p.163 (1973).
103. A.T. Kuhn and R. Smailes, *Electrochemistry: the past thirty and the next thirty years*, ed. H. Bloom, F. Gutmann, Plenum Press, New York (1977).
104. U.S. patents 4,040,934 (1977), 3,963,593 (1976), 3,491,014 (1974).
105. W.N. Cathey, U.S. Bureau of mines, R1 8341 (1979).
106. W.T. Bryan, *Mater. Prof. Perf.*, 9(a), p.25 (1970).
107. G.F. Cammack and G.C. Wood, *Corr. Sci.*, 8, p.159 (1978).
108. R. Pretorius, *J. Electrochem. Soc.*, 128, p.107 (1981).
109. R. Bradley, G. Milnes and D. Munro, *Geochim. Cosmo. Acta*, 37, p.2379 (1973).
110. C. Greskovich and J. Schmalzried, *J. Phys. Chem. Solids*, 31, p.639 (1970).
111. Mme Lefebune - Mareau, *Bull. Soc. Roy. Sci. Liege*, 33, p.373 (1964).
112. N.A. Toropov and S.A. Babayan, *Zh. Neorgan. Khim.*, 11(1) p.15 (1966).
113. H. Kondo and S. Miyahara, *J. Phys. Soc. Japan*, 18, p.305 (1963).

114. D. Hamilton and C. Henderson, Mineral Mag., 36, p.832 (1968).
115. A.P. Kreshov et al, Zh. Obshch. Khim., 32, p.3864 (1962).
116. B.G. Sebeder and V.A. Levitski, Zh.Fiz.Khim., 36, p.460 (1962).
117. A. Burdese, F. Abbattiston and R. Samiani, Metallurgia Ital., 55, p.557 (1963).
118. A.L. Kondrashava et al, Zh. Prikl. Chim. (Leningrad), 45(10), p.2352.
119. N. Taylor, Z. Phys. Chem., 9, p.252 (1930).
120. A.E. Ringwood, Geochim. Cosmo.Acta, 26, p.457 (1962).
121. A.E. Ringwood, Nature, 187, p.1019 (1960).
122. A.E. Ringwood and P. Tarte, Nature, 193, p.971 (1962).
123. J. Hofmann and R. Gruehn, J. Crystal Growth, 37, p.155 (1977).
124. R. Bradley, A. Jamil and D. Monro, Paper presented to the Physical Chemistry and High Pressures symposium, London, p.147 (1962).
125. A. Chivikova et al, Bryul. Izobret, 1, p.22 (1962).
126. B. Lebedev and V.A. Levitsku, Zh. Fiz. Khim., 36, p.630 (1962).
127. T. Eguchi, Denki Kagaku, 29, p.19 (1961).
128. A.C.C. Tseung and J.R. Goldstein, J. of Material Science, 7, p.1383 (1972).

129. A.C.C. Tseung and S.C. Dhara, *Electrochim. Acta*, 19, p.845 (1974).
130. S.M. Jasem, Ph.D. Thesis 1978, The City University, London.
131. J. Giner and L. Suetete, *Nature*, 211, p.1291 (1961).
132. A.D.S. Tantram and A.C.C. Tseung, *Nature*, 221, p.167 (1969).
133. K.R. Williams, *An Introduction to Fuel Cells*, Elsevier, (1966).
134. M. Pourbaix , *Atlas d'Equilibres Electrochimique*, Gauthier - Villars, Paris,(1963).
135. M.C.M. Man, S. Jasem, K.L.K. Yeung and A.C.C. Tseung, Paper presented to Seminar on Hydrogen as an energy vector, its production, use and transportation, (1978).
136. R.S. Nicholson, *Anal. Chem.*, 37, p.1351 (1965).
137. R.N. Adams, *Electrochemistry at solid electrodes*, Marcel Dekker Inc., (1969).
138. D. Pletcher, *Advanced instrumental methods in electrode kinetics*, Southampton University, (1975).
139. J.S. Newman and C.W. Tobias, *J. Electrochem.Soc.*, 109, p.1183 (1962).
140. A.C.C. Tseung and P.R. Vassie, *Electrochim. Acta.*, 21, p.315 (1976).
141. B.S. Hobbs, P.R. Vassie and A.C.C. Tseung, *Electrochemical Engineering Syposium*, Institution of Chemical Engineers, ed. J.D. Thornton, 1, p.123 (1971).

142. S. Jasem and A.C.C. Tseung, Proc. Electrochem. Soc., 77-6, p.414 (1977).
143. C. Iwakura, K. Fukuda and H. Tamura, Electrochim. Acta., 21, p.501 (1976).
144. A.J. Krasilshchikov, Zh.Fiz. Khim., 37, p.531 (1963).
145. A. Damyanovic, A.T. Ward and M.O'Jeu, J. Electrochem. Soc., 121, p.1186 (1974).